Rolle der Histonmethylierung am H3 Lysin 9 in Apoptose und Seneszenz-bezogenen Zellschutz- Programmen in Myc-getriebenem Lymphom-Modell

DISSERTATION

zur Erlangung des akademischen Grades
doctor rerum naturalium
(Dr. rer. nat.)
im Fach Biologie

eingereicht an der
Mathematisch-Naturwissenschaftlichen
Fakultät I
Humboldt-Universität zu Berlin

von
Frau Dipl.-Biologin Vedrana Tabor
geboren am 08.05.1977 in Zagreb/Kroatien

Präsident der Humboldt-Universität zu Berlin:
Prof. Dr. Dr. h.c. Christoph Markisches

Dekan der Mathematisch-Naturwissenschaftlichen
Fakultät I:
Prof. Dr. Lutz-Helmut Schön

Gutachter:

1. Prof. Dr. Achim Leutz
2. Prof. Dr. Harald Saumweber
3. Prof. Dr. Thomas Sommer

eingereicht am: 17. Juli 2008
Tag der mündlichen Prüfung: 3. März 2009

Abstract

Maintenance of cellular failsafe pathways (apoptosis and senescence) is one of the hallmarks of life, as fine equilibrium between proliferation and growth arrest ensures that the cell can protect itself from the potentially dangerous mutations. Senescence is a mechanism distinguished by heterochromatin modifications leading to silencing of the genes responsible for the entry to the DNA synthesis [S] phase of the cell cycle. Involvement of epigenetic modifications in cancer development has been subject of a more intense research in the past few years. It was shown that the Rb-associated histone methyltransferase Suv39h1 is a critical mediator of senescence in a Ras-induced mouse lymphoma model. Additional mechanisms of the senescence regulation are currently being under investigation. In this thesis Eμ-myc transgenic mice, crossed to mice deficient for Suv39h1, were shown to succumb to the same type of B-cell lymphoma (similar to Burkitt's lymphoma in humans). Overexpression of Myc, as seen in human and mouse tumors will primarily induce an apoptotic response using p53 as a mediator of this response. In Eμ-myc, Suv39h1$^{-/-}$ mouse model deficiency in Suv39h1 has significantly shortened life expectancy, but it did not affect spontaneous apoptosis rates. This finding established Suv39h1 as a tumor suppressor in Myc-lymphomagenesis. Further, an additional mechanism of mediating oncogene-induced senescence involving cytokine signaling was identified and reported here. When intact Suv39h1 is present in the tumor, TGFβ is able to mediate oncogene-induced senescence *in vivo*. Finally, in the treatment studies it was shown that Suv39h1 deficient lymphomas have an impaired response to chemotherapy, caused by their inability to execute drug-induced senescence. This finding can be of use for the design of novel cancer therapies.

Zusammenfassung

Die Aufrechterhaltung der sogenannten failsafe Programme ist ein wichtiges Kennzeichen des zellulären Lebens, da das genaue Gleichgewicht zwischen Proliferation und Wachstumsarrest es sicherstellt, dass die Zelle sich selber vor potentiell gefährlichen Mutationen schützen kann. Apoptose und Seneszenz bewahren die Zellhomeostase und sind von aüsserster Bedeutung dafür, die Zelle vor maligner Transformation zu bewahren. Die Seneszens zeichnet sich dabei durch Veränderungen des Heterochromatins bei Genen aus, welche für den Eintritt in die DNA-Synthese-Phase des Zellzyklus verantwortlich sind. Insgesamt wurde die Bedeutung epigenetischer Modifikationen bei malignen Erkrankungen (hautsächlich fehlende oder zusätzliche DNA-Methylierung und Veränderungen der Histon-Modifikationen) in den letzten jahren immer deutlicher. So konnte gezeigt werden, dass die Rb-assoziierte Histon-Methyltransferase Suv39h1 ein entscheidender Vermittler der Seneszenz in Ras-induziertem Maus Lymphom-Modell ist. Andere Mechanismen, die verantwortlich sind für den Übergang von der anfänglichen Hyperproliferation zur Seneszenz *in vivo*, sind momentan Gegenstand der Forschung in zahlreichen Gruppen weltweit.

In dieser Arbeit wurde gezeigt, dass die transgenen Eμ-myc Maüse (ähnlich dem Burkitt's Lymphom im Menschen), wenn sie mit Suv39h1-defizienten Maüsen gekreuzt werden. Die Überexpression von Myc, wie sie in humanen und murinen Tumoren zu beobachten ist, induziert primär ein apoptotische Antwort mit dem zentralen Vermittler p53. Allerdings bewirkte die Suv39h1 Defizienz, obwohl sie die Lebenserwartung signifikant verkürzte, keine Veränderung der Apoptose-Rate in diesem Modell. Dieses Ergebnis demonstriert die Tumor-suprimierende Wirkung des Suv39h1 in Myc-getriebener Lymphomagenese. Weiterhin wurde in dieser Arbeit ein zusätzlicher Mechanismus zur Vermittlung Onkogen-induzierter Seneszenz unter Einbeziehung des Zytokin-Signaling identifiziert. Im Falle der Expression von intaktem Suv-39h1 in der Tumorzelle kann TGFβ die Onkogen-induzierte Seneszenz *in vivo* beeinflussen. Schliesslich ergaben die Untersuchungen, dass die Suv39h1-defizienten Lymphome über eine beeinträchtigte Therapie-Anwort verfügen, da sie keine Therapeutika-induzierte Seneszenz ausführen können. Insbesondere dieses Ergebnis könnte von grossem Wert bei der Entwicklung neuer Krebs-Therapien von Nutzen sein.

Za Dadu
[08.05.1998-08.05.2008]

"Njega su za sve spremali, izuzev za mene." Ilija Cvorovic aka Balkanski spijun

Contents

Chapter 1

Introduction

1.1 Aim and scope of the thesis

The maintenance of cellular failsafe pathways (e.g., apoptosis and senescence) is an essential prerequisite for most of the living creatures, since mutations in them potentially carry harmful consequences. It is crucial for the organism that failsafe pathways properly function and that they remain activated in response to different stress that cells are exposed to. When oncogenic signaling is imposed on cell, cell cycle "checkpoint" genes will force it to arrest and undergo apoptosis or senescence.

Part of the work presented in this thesis focuses on lymphoma development in animals with disrupted senescence machinery. Senescence is a permanent arrest in the first gap phase [G1] of the cell cycle. Senescence, like apoptosis, is established as a failsafe program responding to the different stress stimuli cell is exposed to: like oncogene activation, DNA damaging agents as well as agents that alter chromatin structure. Recent publications have shown that the oncogene-induced senescence is a barrier to the further tumor progression. However, signaling events mediating senescence are not yet fully identified, and a main part of this thesis work aimed at their identification. The second part of the work presented in this thesis focuses on elucidating a role of senescence in lymphoma therapy *in vivo* utilizing mouse model with specific genetic disruption of senescence machinery. Results obtained in this part could potentially be used as prognostic markers and consequently exploited for the better treatment design.

1.2 Introduction to thesis work

Mouse model used in this thesis comprises of two parts: Eμ-myc transgenic mice were crossed to Suv39h1 knockout mice in order to obtain animals developing lymphomas (driven by Myc over-expression) lacking gene that is known to mediate senescence by heterochromatin associated histone modifications (Suv39h1), to test for the Suv39h1 contribution to the tumor formation and the treatment. Therefore introduction is divided in three main parts. The first part of the introduction will describe senescence as a cellular failsafe mechanism, and its response to constant oncogenic stimuli, as well as key molecules implicated in mediating senescence response, lymphoma development and treatment. In the second part of the introduction most prominent histone modifications will be described. Last part of introduction will describe mouse models used in this thesis.

1.3 Cellular failsafe mechanisms in cancer

During many years tremendous efforts and resources have been employed, and some major breakthroughs have been made: cancer is classified as a complex genetic disease [HW00], promoting uncontrolled growth of cells which have lost their ability to execute apoptosis (programmed cell death) or senescence. In the course of its lifespan cell is facing the risk of malignant transformation. In order to prevent it cell can utilize one of failsafe programs available (apoptosis and senescence), and stop uncontrolled proliferation and consequent oncogenic transformation [Sch03](Figure 1.1).

The mechanism of apoptosis is well researched and understood, and in patients apoptosis is still considered the major response to treatment with the chemotherapeutic drugs [SL99]. However, when senescence is concerned we still do not have a full understanding of the components involved in its execution. Recently it became more obvious that the clearer understanding of the processes involved in senescence will be of tremendous benefit to the design of better and more straightforward treatment strategies.

1.3.1 Senescence

The phenomenon of replicative senescence was first recognized by Hayflick and Moorhead *in vitro*, observing that human diploid fibroblasts are displaying limited division potential. Later they revealed that division potential is dependent on the number of divisions a cell has undergone [HM61], [HAY65], [Sed98]. Excessive telomere shortening, leading to senescence is implicated

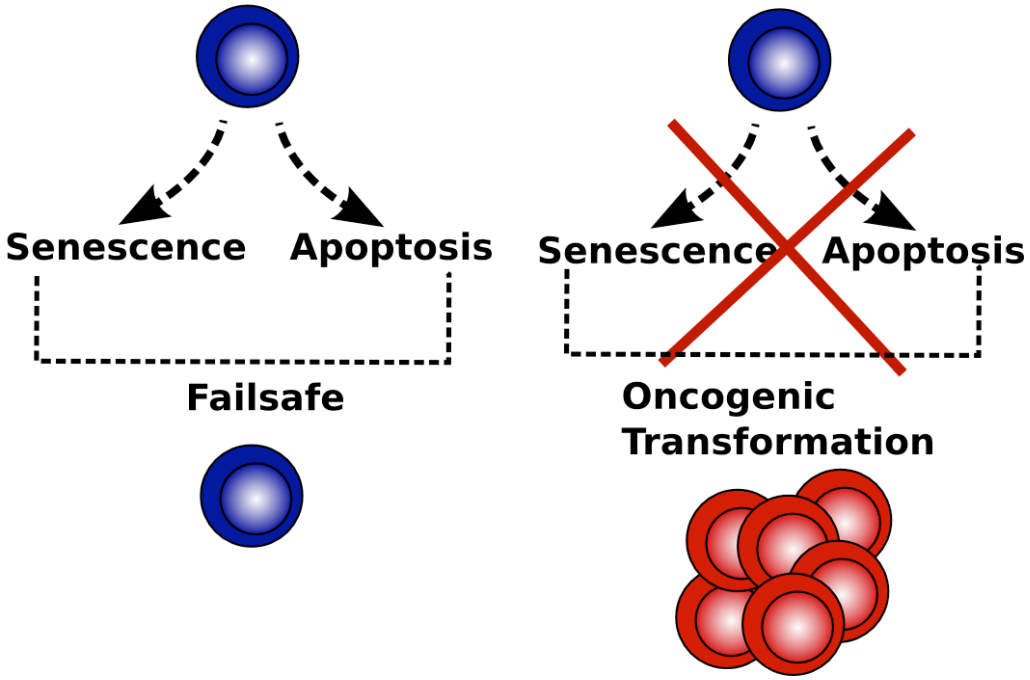

Figure 1.1: Oncogenic stress and cellular failsafe mechanisms. Apoptosis and senescence are two cellular failsafe mechanisms preventing oncogenic transformation. For the development of the full blown malignancy cells have to overcome these mechanisms.

in the loss of regenerative and proliferative potential in aging tissues, which contributes to the decrease in the tissue function [CddF07]. Premature senescence is characterised by a permanent arrest in the G1 phase of the cell cycle [HAY65], and this arrest can be provoked by diverse types of cellular stress, like oncogenic signaling, DNA damaging chemo-, radio-therapy, and lesions caused by reactive oxygen species and finally by a diverse range of cytokine signaling.

Characteristics of senescent cells

Senescent cells, unlike apoptotic cells, remain intact and viable for extended periods of time. Distinct morphological changes are following irreversible G1 growth arrest, cells become bigger and flattened, as well as displaying vacuole rich cytoplasm. Also, they show striking changes in expression of certain genes and proteins, some of which are cell cycle inhibitors and activators [JPS06],[CSS$^+$02],[MJL04],[SCW$^+$99],[TSPG06],[YKK$^+$04]. Amongst the most prominent changes are activation of the cyclin dependent kinase inhibitors (CDKI) p21^{Cip} and p16^{INK4a} [Cam01],[BLL$^+$05], upregulation of p53 [SLM$^+$97],[HSW$^+$93], p19^{Arf} [DIAC00],[KZR$^+$97] and promyelocytic-leukemia protein (PML)[FdSQ$^+$00],[PCS$^+$00]. Genes coding for proteins important for the cell cycle progression, like cyclin A, cyclin B and proliferating cell nuclear antigen (PCNA) are repressed in senescent cells [NNH$^+$03]-,[PC94],[SC90],[SDR$^+$91]. Genes encoding for secreted proteins like CXC motif ligand 6 and insulin like growth factor 2 associated protein (IGF2A) are also found to have deregulated expression in senescent cells when compared to the normal proliferating cells [JPS06],[CSS$^+$02],[MJL04],[SCW$^+$99]-,[TSPG06],[YKK$^+$04].

The oldest, and best known marker for a senescent cell is increased lyzosomal activity of the enzyme β-galactosidase, which is easily detectable by an assay using X-gal as substrate, at a non-physiological pH [5,5 for murine cells, and 6,0 for the human cells] and can be identified by the change of color (senescent cells display blue cytoplasmic staining) [DLB$^+$95]. Lack of DNA replication, as it occurs in senescent cells can be measured by incorporation of either BrdU (5-bromo-2'-deoxyuridine) or 3H-thymidine; however by this incorporation it is not possible to distinguish senescent (irreversibly arrested) from quiescent (reversibly arrested) cells. There are also cytological markers of senescence, visualizing senescence associated heterochromatic foci (SAHF) by binding of the DNA dye 4'6-diamidino-2-phenylindole (DAPI)[NNH$^+$03]. This can be accompanied with the presence of certain heterochromatin associated histone modifications (tri-methylation of lysine 9 residue on the histone H3, H3K9me3) and by heterochromatin proteins 1 (HP1). It is still a

matter of the debate that so far there is no truly validated molecular marker existing that would be able to identify senescent cells [Sed98].

Key molecules involved in regulation of cellular senescence

At the molecular level, the p53 and retinoblastoma (Rb) tumor suppressor pathways serve as critical cell cycle checkpoints that mediate both replicative and oncogene-induced senescence. The main function of the Rb gene is limiting cell proliferation by preventing entry into the DNA synthesis [S] phase of the cell cycle. When Rb protein is maintained in its hypophosphorylated (anti-proliferative) form by $p16^{INK4a}$, it is blocking E2f transcription factors from activating genes needed for DNA replication and nucleotide metabolism [GBBP07]. Progression into the S phase of the cell cycle is accelerated when Rb is phosphorylated, and its ability to block E2f is disrupted, that process is catalysed by cyclin D and E dependent kinases during the G1 phase of the cell cycle. Ras-induced senescent cells display Rb-mediated senescence associated heterochromatic foci (SAHF), these transcriptionally silenced heterochromatin regions map to E2f responsive promoters and have been shown to be an area with highly tri-methylated lysine 9 residues on the histone H3 (H3K9me3)[NNH$^+$03]. Tumor suppressor gene $p16^{INK4a}$, a critical mediator of G1/S phase transition, is also found overexpressed during replicative and premature senescence[Ser97],[SPE$^+$95]. It regulates senescence by inhibition of cyclin D-dependent kinases (CDK4 and 6) which are crucial for the entry in S phase of the cell cycle.

Further, the p53 protein is the most important sensor of stress in the cell. Under normal conditions p53 protein is rapidly degraded[Ore99]. When the cell is exposed to DNA damage or oncogenic signaling transcriptional activity of p53 increases, and a complex cascade that ends with elimination of damaged cells through apoptosis or senescence is triggered. Activity of p53 is regulated by posttranslational modifications (acetylation, phosphorylation, etc.), and transcriptionally by oncogenes, like Myc or Ras, as well as by the DNA damage (mediated *via* ATM/ATR pathway)[CHH$^+$00]. Genes that are activated by p53 include ones that encode the cyclin E and A-dependent kinase inhibitor $p21^{Cip}$, as well as many others implicated in apoptosis. The p53 protein directly activates its own negative regulator murine double minute 2 protein (MDM2), and in turn MDM2 induces ubiquitylation consequently leading to degradation of p53[JGO99]. Stabilization of p53 on the other hand is induced by $p19^{Arf}$, one of the main p53 regulators, by associating with MDM2, thereby blocking its ability to interact with the p53. $p19^{Arf}$ expression is reported to be increased in murine cells during the course of the cellular senescence[KZR$^+$97],[JKM$^+$99]. $p21^{Cip}$ is inhibiting activity of

cyclinD/CDK4, E/CDK2 and A/CDK2 complexes, which leads to the G1 arrest[HAW+93], $p21^{Cip}$ was also found to be expressed in human senescent cells[NNV+94], and was shown to be associated with the expression of wild-type p53 involved in G1-checkpoint control[eDTV+93].

In summary, it has become clear during the past few years that activation of both $p53/p19^{Arf}$ and the $pRb/p16^{INK4a}$ pathways is promoting growth cessation *via* senescence and apoptosis, underlining p53s importance as a key molecule in this process (Figure 1.2).

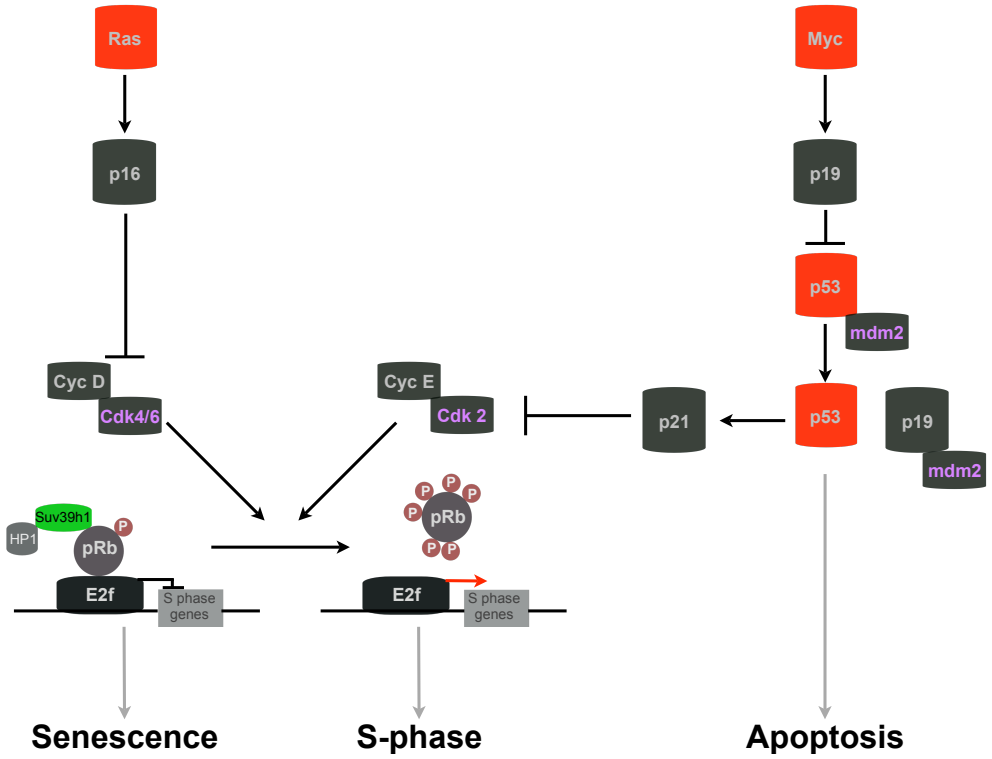

Figure 1.2: Cellular failsafe pathways activated in a response to oncogenic signaling. Oncogenic Ras signaling through $p16^{INK4a}$ and cyclin D-dependent complexes helps to cancel Rb suppression, liberating E2fs and stimulating S-phase entry. Oncogenic Myc signaling through $p19^{Arf}$ inhibits MDM2 and initiates p53 transcriptional response triggering either apoptosis or senescence. Induction of $p21^{Cip}$ by p53 inhibits cyclin E-Cdk2 and returns Rb to its hypophosphorylated (inhibitory) state. $p21^{Cip}$ action connects the Myc-$p19^{Arf}$-MDM2-p53 axis to Ras-$p16^{INK4a}$-Rb axis

Additional stimuli inducing senescence

DNA damage response (DDR) recently emerged as a biological tumorigenesis barrier evident in early stages of tumor development. It has been shown that in tumor specimens from human cancer patients there is a constitutive activation of DNA damage signaling, which is most prominent in the early pre-invasive stages of tumors [BHK$^+$05]. Further, markers of activated DDR are correlating to markers of cellular senescence in samples from human tumors, and data *in vitro* revealed that intact DDR machinery is a prerequisite of the oncogene-induced senescence [BRL$^+$06], [DMFC$^+$06]. It has been reported that accumulation of the reactive oxygen species (ROS) plays an important role in senescence induction as well[MGLF07]. Tumor microenvironment, especially oxygen tension, is also triggering premature senescence. It was reported that the proliferative lifespan of human diploid fibroblasts can be extended by changing their growth environment from hyperoxic conditions (when levels of oxygen exceeded 40%), to hypoxic conditions (3% oxygen) [CFR$^+$95]. It was shown that Ras protein can induce senescence *via* changes in intracellular levels of ROS [LFI$^+$99]. Cytokine induced reactive oxygen species [IKKM06] and potentially senescent growth arrest in a Ras setting could be related to TGFβ effects. TGFβ has at least two probable roles in carcinogenesis. In premalignant cells and cells in the early stages of the carcinogenesis TGFβ inhibits proliferation and may induce apoptosis or senescence [CBPC04]. Later, as the carcinogenesis process is more advanced cells lose their ability to respond to the previously inhibitory effects of TGFβ which most probably occurs *via* decreased expression of the TGFβ receptors or, as shown by repression of the TGFβ signaling by oncoproteins in hematological cancers [KMI$^+$98], [MMT$^+$01]. And at the advanced stages of cancer TGFβ promotes tumor progression [Ben04]. For example it was shown that in a response to TGFβ-1 signaling another cyclin-dependent kinase inhibitor (CDKI) p27^{Kip} mediates G1 cell cycle arrest [LEJ$^+$99], and it has been demonstrated that cytoplasmic promyelocytic leukemia protein (PML) plays an essential role in the modulation of TGFβ-1 signaling, whereas cells deficient for the PML displayed resistance towards TGFβ-1 induction of cellular senescence or apoptosis [LBP04].

Three recent reports show an important role of secreted proteins in enforcing the senescence response [KMV$^+$08], [AOB$^+$08], [WSZ$^+$08]. The work by Kuilman and co-workers provides a link between p15^{INK4b}, heterochromatin and the IL-6/ C/EBP pathway. It points to a coordinated function of IL-6 and C/EBP in upregulation of p15^{INK4b} expression, leading to the Rb activation and consequently oncogene-induced senescence[KMV$^+$08]. Work done by Acosta *et al* established a direct connection between DNA damage re-

sponse and chemokine signaling[AOB+08]. And finally, Wajpaeyee *et al* show negative feedback signaling response of insulin growth factor binding protein7 (IGFBP7) as an executor of antiproliferative effects in melanocytes containing activating mutations in the BRAF oncogene[WSZ+08](Figure 1.3).

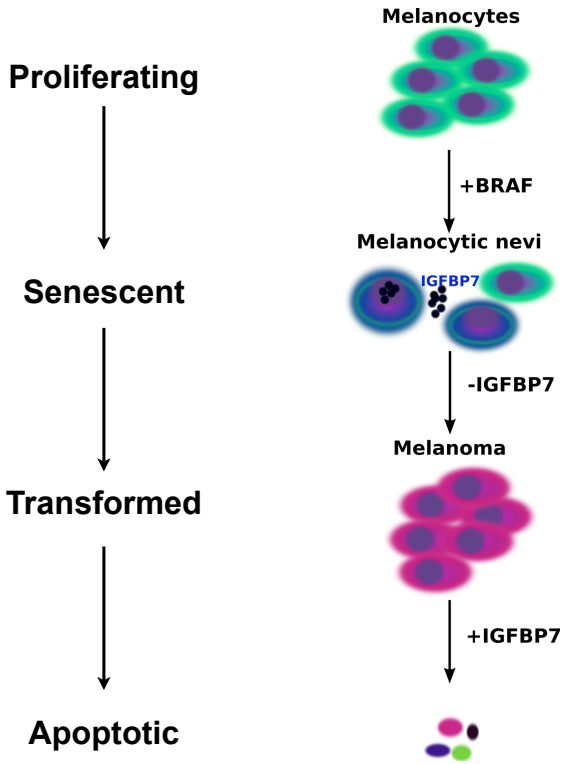

Figure 1.3: IGFBP7 and BRAF-induced senescence (adapted from Chien *et al* 2008). Early in melanoma progression, melanocytes acquire BRAF mutations that both stimulate proliferation and trigger senescence, partially *via* enhanced secretion of IGFBP7. Silencing of IGFBP7 enables BRAF expressing melanocytes to progress to melanoma stage. Melanoma cells remain sensitive to the induction of apoptosis by addition of IGFBP7.

c-Myc and its role in the oncogene-induced senescence

The Myc oncoprotein is a basic helix-loop-helix-leucine zipper transcription factor that coordinates cell growth and division by binding to specific DNA elements through dimerization with Max protein, and by this interaction it modulates transcription of a wide variety of genes [DDGK92]. Expression of the Myc gene is tightly coupled to the proliferation status of the cell. When

mitogen signals are added to cells Myc expression is rapidly increased, also Myc expression is enough to force quiescent cells into the cell cycle [Eil99]. To achieve its full oncogenic potential Myc cooperates with the deregulated function in certain pro-apoptotic and anti-apoptotic genes. Most prominent of those would certainly be loss of p53, closely followed by the overexpression of bcl-2 [EWR$^+$99].

Myc overexpression provokes genomic instability and sensitizes cells to apoptosis, which is executed *via* p19^{Arf}-MDM2-p53 pathway [ZER$^+$98]. Activation of Myc can be achieved *via* different mechanisms: chromosomal translocation, gene amplification, viral insertion, and by direct transcriptional effects [NTP99]. There have been reported a great variety of direct and indirect targets of Myc. Targets upregulated by Myc are for example: cyclin D2, cyclin E and CDK4, all of which are involved in G1/S transition. These activated cyclin/CDK complexes are able to inactivate the restriction point controlled by the Rb [BBK$^+$00]. In addition Myc successfully downregulates genes important for the negative regulation of the cell cycle (p21^{Cip}, p27^{Kip}, p15^{INK4b}) [SLM02], [MBP92], [YSW$^+$01]. Downregulation of p21^{Cip} occurs *via* interaction of Myc with Myc-interacting zinc finger-1 protein (Miz-1) [WCMA$^+$03], [HWB$^+$02] (Figure 1.4), in that way regulating p53 activity as well. By the same mechanism p15^{INK4b}, an important target of TGFβ is being repressed. However, p15^{INK4b} is responsive to signals from the SMAD machinery as well [YSW$^+$01], [SPK$^+$01].

1.3.2 Apoptosis

So far apoptosis is the most thoroughly studied cellular failsafe mechanism. It was first described by Kerr *et al* in 1972. Apoptosis is characterised by distinct morphological features: chromatin condensation followed by its fragmentation, membrane blebbing, and at the end phagocytosis of the cell fragments[MG95]. Biochemical features of apoptotic cell include internucleosomal cleavage of DNA, leading to an oligonucleosomal "ladder", and finally proteolytic cleavage of a great number of intracellular substrates. As a result of changes in the plasma membrane apoptotic cells are rapidly phagocytised before intracellular contents are released and without induction of the inflammatory response [MG95]. Apoptosis is a tightly regulated proces, mainly driven by the caspase cascade [TL98]. Apoptosis is triggered by growth factor depletion, hypoxia and radiation, as well as DNA damage, telomere malfunction and inappropriate proliferative signals produced by oncogenic mutations [KZRVU$^+$97]. The majority of the anticancer agents identified to date mediate their cytotoxic effects *via* apoptosis. Since p53 is the first tumor suppressor gene linked to apoptosis [WBL99], a particular

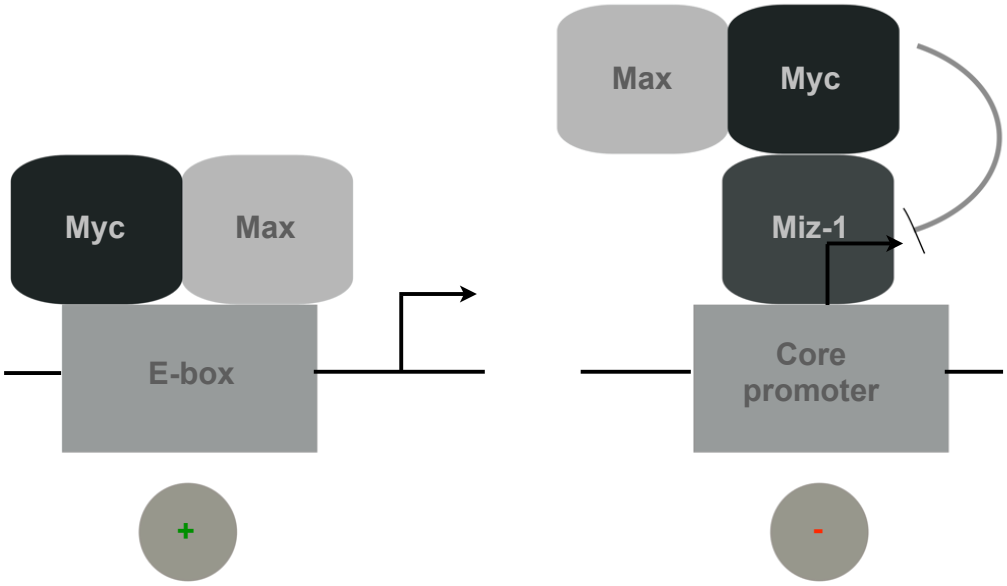

Figure 1.4: Mechanism of transcriptional repression by c-Myc (adapted from Eilers *et al* 2003). c-Myc binds to specific DNA sequences (E-boxes) through heterodimerization with Max, activating transcription of several target genes. Myc transcriptionally represses several target genes *via* interaction with Miz-1.

degree of chemosensitivity in a certain tumor can be directly connected to its p53 status [SL99].

1.3.3 Lymphoma development and treatment

The term "cancer" embodies hundreds of forms of a disease arising as a result of genetic and epigenetic changes, and all of the tissues and organs carry a risk to develop tumor during the lifetime. To become malignant the cell must lose or gain certain attributes, such as an ability to produce and convey signals sufficient for its growth, sustained angiogenesis, ability to evade failsafe programs, unlimited replicative potential, and ability to methastasise [HW00].

Normally mitogenic oncogenes, like Ras and Myc provoke checkpoint-mediated failsafe programs, e.g. senescence [EWG+92] or apoptosis [Lan95]. However, when acting together Myc and Ras were able to transform normal rodent cells, and evoke proliferation by cancelling each others failsafe programs [She96] (Figure 1.5). Transforming potential of Myc and Ras together and their ability to cancel each others failsafe programs showed that with the disrupted apoptosis and senescence cells will progress to the stage of fully blown malignancy.

Key molecules involved in lymphoma development

Defects in tumor suppressor genes or activation of proto-oncogenes are frequently found in human malignancies. Retinoblastoma (Rb) gene mutations are occurring widely in human cancers [VLL00]. Almost all of the human tumors have certain dysregulation of p53 activity [VH06]. Compared to other tumor suppressors p53 is most frequently involved in the pathogenesis of B-cell non-Hodgkin lymphomas [BTO+95].

Alterations in the expression of c-Myc oncogene are found in the pathogenesis of several human malignancies, including Burkitt's lymphomas [KK85]. For example inactivation of p53 occurs following c-Myc translocation in Burkitt's lymphomas [BTO+95]. Burkitt's lymphomas are characterized in more than 80% of the cases by chromosomal translocation occurring between c-Myc gene on chromosome 8, and one of the Ig (immunoglobulin) genes on either of chromosomes 2, 14 and 22 [AHP+85]. This chromosomal translocations are also typical for the human B and T cell acute lymphocitic leukemias (ALL) [MBP92]. The Eμ-myc transgene is derived from a translocation found in a murine plasmacytoma, juxtaposing the enhancers of the immunoglobulin heavy chain to the proximal region of the c-Myc gene [AHP+85]. In Eμ-myc transgenic mice p53 loss has been shown

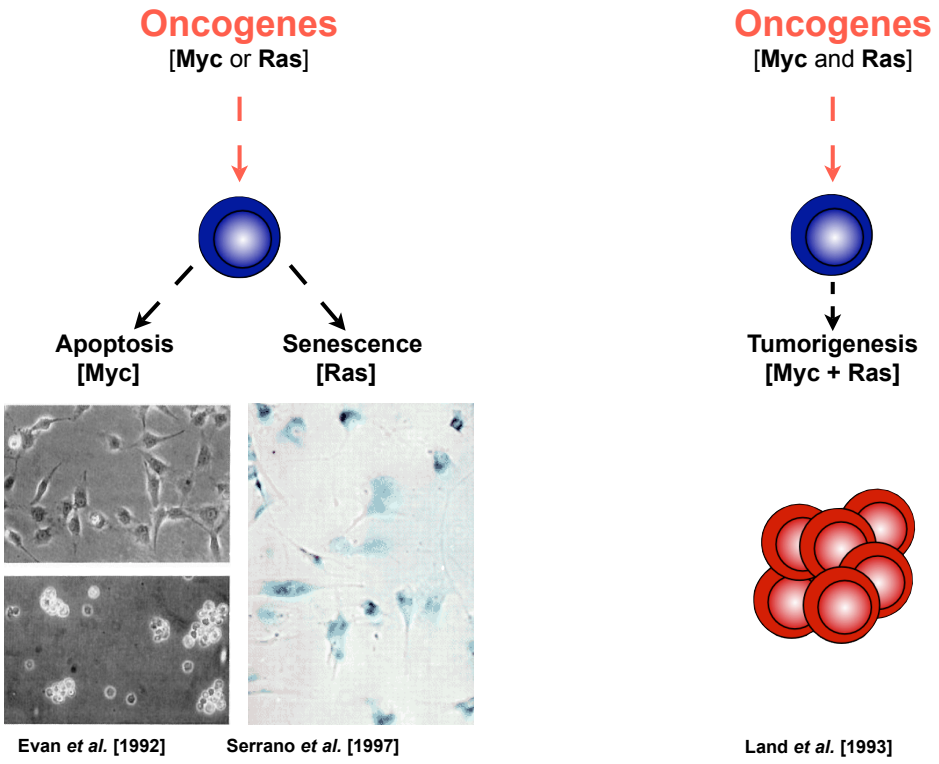

Figure 1.5: Oncogenic transformation. Each Ras and Myc are inducing the cellular failsafe machinery. However, when together they are cancelling each others failsafe programs and this leads to oncogenic transformation.

to reduce tumor latency [BTO+95]. Chromosomal translocations, involving bcl-2 gene are characteristic for follicular lymphomas, there immunoglobulin heavy chain enhancer is juxtaposed to the bcl-2 gene, resulting in high expression of bcl-2 [NCLW+88]. Bcl-2 overexpression is associated with a poor treatment prognosis, resulting from resistance to chemotherapy and radiation treatment [WBL99].

Histone modifications and lymphoma development

Deregulation in the balance of epigenetic modifications may lead to alterations in gene expression and can result in cellular transformation, which would lead to the full blown malignancy. As observed in the Ras-induced lymphoma model disruption of histone methyltransferase leads to significantly shortened tumor latencies, showing that deregulation in epigenetic regulator impacts on tumor formation latencies [BLL+05].

Tumor treatment

Search for the therapeutics that would inhibit oncogenic Myc provided insights in potency of Myc as an anti-cancer target. It is known that in the different tissues induction of oncogenic Myc will lead to the full-blown malignancy [PKE02], [FB99]. When Myc activity is blocked it will in most of the cases lead to tumor regression [JB04]. So far all of the therapy strategies were based on targeting regulatory steps (from transcription to translation), or to inhibit protein-protein interactions necessary for Myc action (e.g., targeting Myc-Max interaction). All of the above mentioned approaches utilize apoptosis as a response to therapy. A study by te Poele *et al* showed for the first time a correlation between the senescent response and chemotherapeutic treatment in clinical cancer. They also detected spontaneous senescence occurring in a low number of tumor cases [tPOJ+02]. In Eμ-myc mouse lymphoma model, both senescence and apoptosis were contributing to the *in vivo* response to chemotherapy [SL02]. When apoptosis was blocked in Eμ-myc lymphomas senescence became the principal tumor response to chemotherapy. Recent work done by two independent groups [MBSE06], [XZM+07] showed how reactivation of intact p53 in different models of aggressively growing cancer leads to a near-complete regression, exposing senescence as a primary mechanism of tumor regression.

1.4 Histone modifications

Changes in histone modifications can regulate gene expression, and are defined by the term "epigenetics". This term refers to all of the modifications in chromatin, but not including alterations in the DNA sequence [Kou07]. As opposing opinion to the DNA dogma (DNA-RNA-protein transfer of information) the "Histone code" model was proposed at the begining of this century [SA00], explaining that acess to certain genome regions is regulated *via* histone modifications, which are involved in changing the higher order of chromatin structures, and by this are able to regulate transcriptional states[WP96]. This model has changed the view on the regulation of the processes involved in tumor formation. Histones are small basic proteins consisting of a globular domain and a more flexible and charged NH2 terminus (called "histone tail") protruding from the nucleosome. The basic, multiple repeating unit of the chromatin is consisting of histone octamere (comprised of pair of each of the histones H2A, H2B, H3 and H4) arround which the DNA is wrapped in two almost full circles, and an linker histone (H1) connecting each of the histone octameres[Kor74],[KT74],[LMR$^+$97],[ABW$^+$91]. The epigenetic changes, which can ultimately cause differences in the transcription of the various genes, can be accomplished *via* hypo- or hyper- DNA methylation or by a diverse range of the histone modifications[FT04].

In the last couple of years intensive research pointed in the direction of lysine methylation of histone residues as an important factor in gene silencing[LJ02],[LOJ03],[BK04]. Local hypermethylation of tumor suppressor genes is promoting oncogenesis[LPA$^+$04], and also global hypomethylation enhances oncogene expression, and contribute to the genomic instability[JB02]. Phosphorylation of serine and threonine histone residues is mediating transcriptional gene activation, as well as apoptosis. This phosphorylation is executed by histone specific kinases (e.g., Rsk-2, Aurora B, ATM, ATR, DNA-PK)[DS99].

Histones undergo post-translational modifications which alter their interaction with both DNA and proteins[Ito07]. The tails of histones H3 and H4 can be covalently modified at several places. These modifications are reversible, which makes the chromatin structure dynamic, it can rapidly switch from non-accessible to accessible[CASC00]. Covalent modifications of histone tails include: acetylation of lysine residues, methylation of lysine and arginine residues, phosphorylation of serine and threonine residues, ADP-ribosylation of glutamic acids and ubiquitinylation and sumoylation of lysine residues[RE02]. Histone methylation, which can occur on the lysine or arginine residues and its exclusive dependency on the site where it occurs, may lead to the transcriptional activation or repression. Euchro-

matic structures are mostly characteristic for the "on" transcriptional states, where histones are hyperacetylated, and histone H3 is methylated on three main lysine residues (K4, K36 and K79)[JA01]. Heterochromatic structures are characteristic for the "off"-transcriptional states, mostly present in the non-dividing, arrested cells. In these structures histone H3 displays trimethylation on three main lysine residues (K9, K20 and K27), and histone H4 on the single lysine residue (K20)[SA00],[Tur00]. Histone acetylation, as well as hyperacetylation in general correlates with transcriptional activity. This process is executed by histone acetyltransferase (HAT) enzymes, and can be reversed by histone deacetylase (HDAC) enzymes[HMT$^+$06]. Some histone modifications function as molecular switches, disabling or enabling occurrence of an additional covalent mark. If histone H3 is subjected to phosphorylation on the serine 10 residue, governed by Aurora kinase, it facilitates acetilation on lysines 9 and 14 and methylation on lysine 4, but methylation of lysine 9 residue is not any more possible. This modification is involved in both transcription and cell division, and is present on metaphase chromosomes. The same residue becomes de-phosphorylated as soon as the cell exits mitosis. This is a very dynamic process, and well organized interplay between phosphorylation of serine 10 residue and methylation of lysine 9 residue of the histone H3 and is crucial for the maintenance of healthy growing cell[Wat93].

1.4.1 Suv39h1 histone methyltransferase

As previously mentioned histone methylation is executed by histone methyltransferases (HMT), some of which are: Suv39h1, Set9 and Ezh2. Histone methyltransferases can mono-, di- or tri- methylate lysine residues, and mono- or di-methylate arginine residues. Depending on the methylation state and the residue methylated biological responses will differ[PK71].

Genes of the Su(var) [suppressor of variegation] group encode numerous histone deacetylases (HDAC) and protein phosphatases, as well heterochromatin associated proteins, one of which is Su(var)3-9, that was identified in D. melanogaster and S. pombe[WSTR89],[RS92]. In H. sapiens and M. musculus SUV39H1 and Suv39h1, were identified respectively[REO$^+$00]. These proteins were shown to execute HMT functions, methylating histone H3 at lysine residue 9 (H3K9). By methylating this lysine residue Suv39h1 is creating a docking site for the HP1γ, a heterochromatin protein involved in a formation of a higher order chromatin (heterochromatin), therefore leading to the gene silencing (Figure 1.6 and Table 1.1). It was shown that Suv39h proteins are essential for the epigenetic regulation in the mammalian development[POS$^+$01].

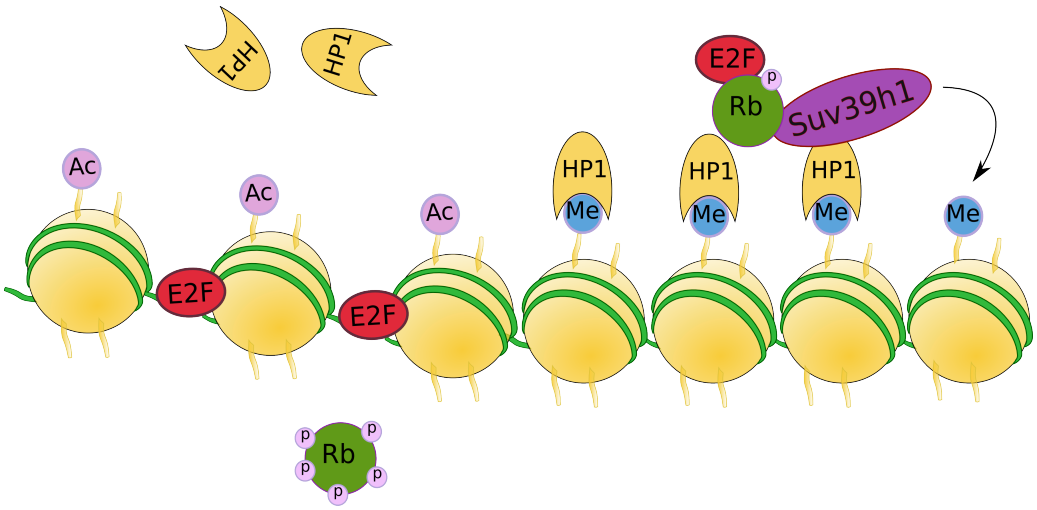

Figure 1.6: Suv39h1 promotes chromatin silencing. Suv39h1 methylates lysine 9 residue on histone H3; this creates a docking site for heterochromatin proteins like HP1 that bind to the tri-methylated lysine 9 mark (H3K9) as well as to Suv39h1/Rb complex. This leads to the stabilization of the heterochromatic region. At the same time acetylation of lysine 9 leads to the relaxed chromatin structure, and enable E2f to dock on a promoter of the S-phase genes.

Table 1.1: Chromatin states

Active chromatin	Silenced chromatin
H3K9Ac	H3K9me3
H3S10P	HP1 docked on H3K9me3
Hyperphosphorylated Rb	Hypophosphorylated Rb
E2f on promoters of the S-phase genes	E2f bound to Rb

SUV39H family members are highly conserved from yeast to humans by their structure and function. The proteins consist of two highly conserved chromatin regulatory motifs, one is located at the N-terminus, and is known as "chromo" domain, and the second is located on the C- terminus and is known as the SET [SUV39H SU(VAR)3-9; E(Z); TRX] domain (Figure 1.7). SET domain properties are not straightforward, because only some of the SET domain containing proteins are reported to have histone methyltransferase activity, where SUV39H family belongs[FCHC00],[JLDR98]. During the mouse embryogenesis, as well as in adult mice Suv39h1 is expressed in various tissues. Suv39h1/Suv39h2 double knockout mouse embryo fibroblasts (MEF) show changed patterns of the methylated lysine 9 residue from the pericentric heterochromatic regions, pointing out the role of Suv39h1 and Suv39h2 as safeguards of the pericentric chromatin regions[OSP$^+$00], [POS$^+$01].

Among the many Suv39h1 interacting proteins Rb is of particular interest. Suv39h1 interacts with the Rb protein on the euchromatic portions of the genome. It was demonstrated that Rb is crucial for directing methylation of the histone H3. Suv39h1 is binding to Rb in a complex with HP1γ, which predominantly localizes to euchromatic regions, and contains a chromodomain capable of recognizing methylated lysine 9 on histone H3[BZP$^+$01],[LOR$^+$01]. This is pointing out that the Suv39h1-HP1γ complex is not only in charge of methylating pericentric regions of heterochromatin leading to silencing, but also has a role in repressing genes in the euchromatic region, which are connected to Rb[NSB$^+$01](Figure 1.8).

1.5 Mouse models

The following mice were used: Eμ-myc transgenic mice[AHP$^+$85], Suv39h1 knock-out mice[POS$^+$01], p53 knock-out mice[JRW$^+$94], p19^{Arf} knock-out mice[KZR$^+$97] and p16^{INK4a} knock-in mice[KQM$^+$01].

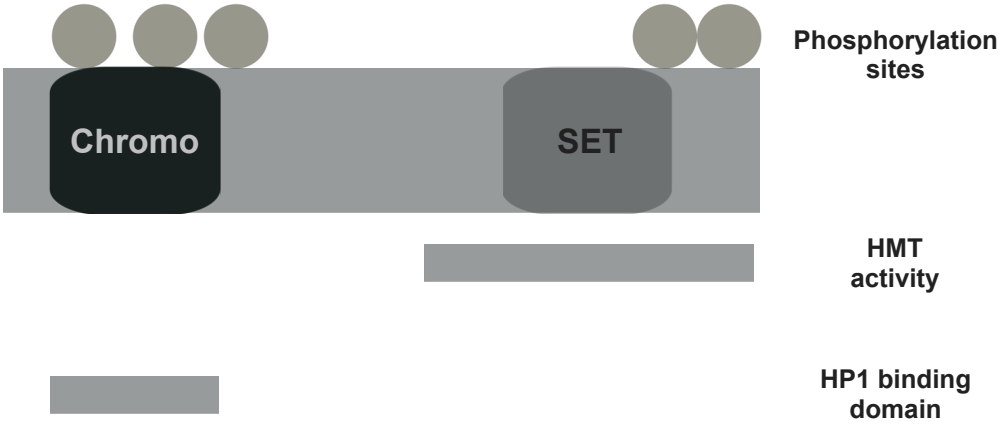

Figure 1.7: Suv39h1 structure. The Suv39h1 protein consists of two highly conserved elements: SET domain and chromodomain. SET domain confers HMTase activity of Suv39h1, while the chromodomain serves as a binding site for HP1 proteins.

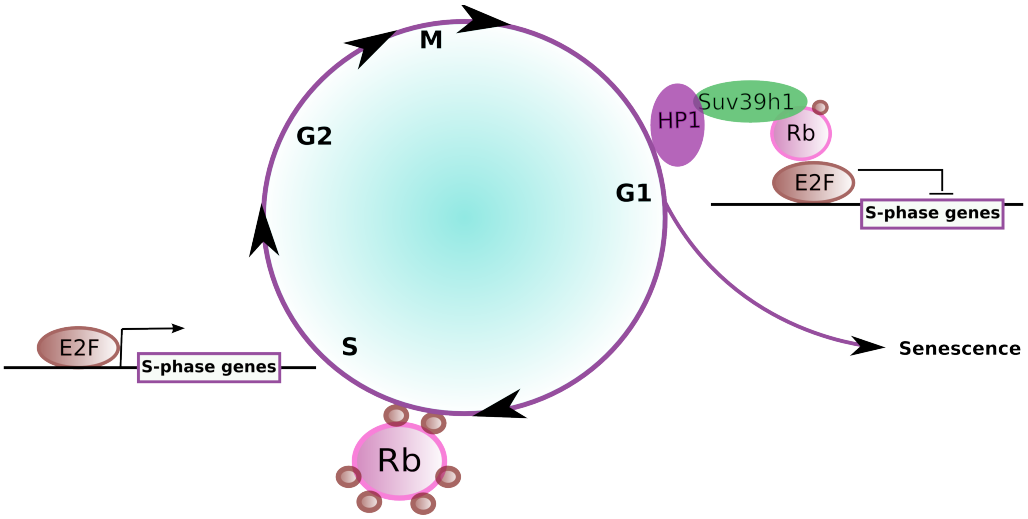

Figure 1.8: Suv39h1 as a putative executor of cellular senescence. Suv39h1 interacts with Rb, when it is hypophosphorylated and E2f-bound. This association is a consequence of tri-methylated lysine 9 residue on hisvtone H3 and is preventing the transcription of the genes important for the progression to the S-phase of the cell cycle.

1.5.1 Eμ-myc transgenic model

The Eμ-myc transgene is derived from a translocation originally found in the mouse plasmocytoma. It was engineered in a way that the immunoglobulin heavy chain enhancer (Eμ) was juxtaposed to the proximal region of the c-Myc gene [AHP+85]. This Eμ-myc transgene is mediating constitutive overexpression of the c-Myc oncogene in predominantly the B cell lineage. Mice carrying this transgene succumb to pre-B cell lymphomas resembling human non-Hodgkin lymphomas. These lymphomas are monoclonal[AHP+85],-[ASA87],[LHCA86]. Eμ-myc animals are a very attractive model for the treatment studies *in vivo*[SWBR+00], one of the advantages of working with this mouse model is that tumor burden can be easily monitored by palpation of the peripheral lymph nodes, therefore making lymphomas detectable before mice succumb to the disease[SL02] (Figure 1.9). Also, it was previously shown in this model that p53, as well as the INK4a/Arf mutations have a distinct effect not only on tumorigenesis, but also on the therapy outcome by partially disabeling apoptosis[SL02].

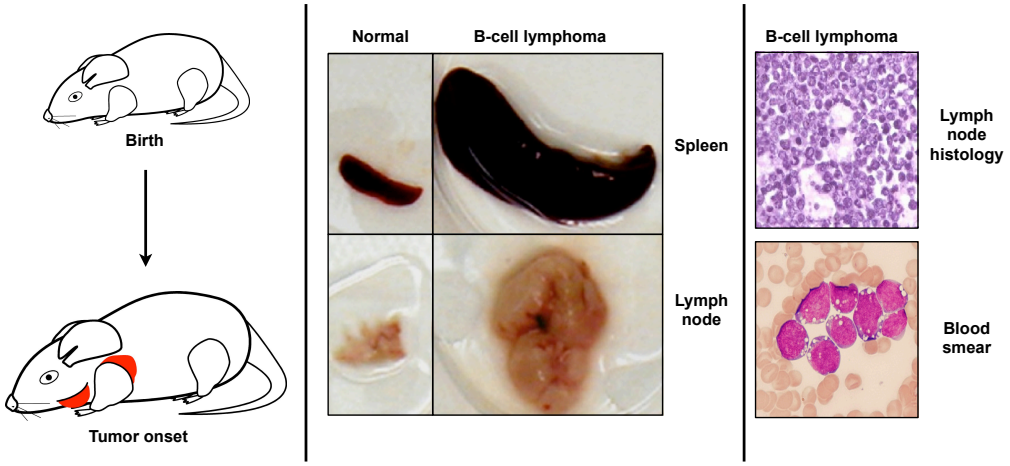

Figure 1.9: Eμ-myc mouse model. Left: The Eμ-myc mouse model is a well tractable lymphoma model, since the onset of the disease can be monitored by palpation of the peripheral lymph nodes (depicted in red). Middle: Mice with B-cell lymphomas have significantly enlarged spleens and lymph nodes. Right: Lymph nodes in patients with B-cell lymphomas display typical "starry sky" morphology, as a result of macrophage infiltrations arround apoptotic cells. Their blood smears display severely increased numbers of blastic cells.

1.5.2 Suv39h1 knock-out model

Peters *et al* generated mice deficient either for Suv39h1 or Suv39h2. Single knock-out animals are born at Mendelian ratios, displayed normal viability and fertility, and without any overt phenotype[POS$^+$01]. The murine Suv39h1 locus on the X-chromosome was disrupted by homologous recombination replacing the N-terminal chromo domain with a Neo-cassette. By intercrossing mice deficient for both Suv39h1 and Suv39h2 it was shown that deficiency in both genes leads to chromosomal instabilities and severely impaired viability. Despite viability Suv39h1 and Suv39h2 double knockout mice are born only at sub-mendelian ratios, due to an increased rate of prenatal lethality[POS$^+$01]. In a EμN-Ras model Suv39h1$^{-/-}$ or Suv39h1$^{+/-}$ mice are prone to B-cell lymphoma, and the remaining Suv39h1 allele of Suv39h1$^{+/-}$ animals is inactivated in tumors[BLL$^+$05].

1.5.3 Other mouse models used in this thesis

p19^{Arf} and p16/p19^{INK4aArf} knock-out and p16^{INK4a} knock-in model were used in this thesis work as well. Since the main scope of this thesis does not reside on the p53, p19^{Arf}, INK4a/Arf and p16^{INK4a} models, they were merely used as controls in certain experiments performed, and therefore I am limiting myself from further introduction. A detailed description of the above mentioned mice can be found in the following publications: Jacks *et al*, Current Biology 1994(for p53 knock-out mouse[JRW$^+$94]); Krimpenfort *et al*, Nature 2001 (for p16^{INK4a} knock-in mouse[KQM$^+$01]) and Kamijo *et al*, Cell 1997 (for p19^{Arf} knock-out mouse[KZR$^+$97]).

In summary, This thesis provides insights in oncogene-induced senescence evoked by a constant Myc-signaling, requiring an intact epigenetic machinery to achieve permanent arrest in the first gap [G1] phase of the cell cycle, a mechanism that has previously been described for Ras-induced senescence. This signaling involves retinoblastoma (Rb) tumor suppressor as a central mediator of heterochromatin formation, and consequent silencing of the genes necessary for the entry into the DNA synthesis [S] phase of the cell cycle. Rb is able to exert its silencing functions only when histone H3 is adequately tri-methylated by a histone methyltransferase Suv39h1. Further, the extent of cells entering this permanent arrest depends on the intact DNA damage signaling machinery, as well as on the extent of cytokine signaling. The tumor suppressor protein p53 resides in the centre of the DNA damage signaling cascade, and only intact p53 will ensure that both apoptosis and senescence are executed, making it a critical cell cycle checkpoint. Further, recently emerging mechanism is the cytokine mediated induction of senes-

cence as a response to oncogene signaling, but currently only little is known about this phenomenon. Recent reports unveiled senescence as a program promising great tumor therapy potential. Hence, long term treatment responses in a Burkitt's like B-cell lymphoma model that additionally carries specific genetic disruption targeting senescence machinery were investigated in this thesis.

Chapter 2

Materials and Methods

2.1 Materials

2.1.1 Antibodies

All of the primary and secondary antibodies used are listed in table 2.1 and table 2.2.

2.1.2 Bacteria Strains

E.coli DH5α-Genotype: F-j80dlcZDM15D(lacZYA-argF)U169 deoR, recA1 endA1 hsdR17 rk-mk+phoA supE44l- thi-1 gyrA96 relA1

2.1.3 Bacteria Media

All of the bacteria media used are listed in table 2.3 and table 2.4

Table 2.1: Primary Antibodies

Name	Number	Supplier
Anti-α tubulin(T-5168)	B-5-1-2	Sigma
Anti-CDK4 (DSC156)	2906	Cell Signaling
Anti- c-Myc	N-262	Santa Cruz
Anti-Histone H3 Lysine 9 tri-methylation	8898	Abcam
Anti-human pRb	G3-245	BD Pharmingen
Anti-HP1γ	42s2	Upstate
Anti-Ki67 antigen	TEC-3	DAKO
Anti-p16INK4a	M-156	Santa Cruz
Anti-p21 Cip1	C-19	Santa Cruz
Anti-p27 Kip1	2552	Cell Signaling
CyclinA	CY-A1	Sigma
CyclinE (HE12)	4129	Cell Signaling
Anti-p53	CM5	Novocastra
Anti-phospho p53 (Ser15)	9284	Cell Signaling
Anti-phospho Histone H3 (Ser10)	9701	Cell Signaling
CD11b	550282	BD Pharmingen
FITC conjugated CD 90.2	553003	BD Pharmingen
FITC conjugated CD 5	553020	BD Pharmingen
FITC conjugated sIgM	553437	BD Pharmingen
R-PE conjugated CD 19	557399	BD Pharmingen
R-PE conjugated CD 45R (B220)	553090	BD Pharmingen

Table 2.2: Secondary Antibodies

Name	Number	Supplier
Anti-rabbit IgG (donkey)	NA934	Amersham
Anti-mouse IgG (sheep)	NXA931	Amersham
Alexa Fluor 488 goat anti-mouse	A21121	Invitrogen
Alexa Fluor 488 donkey anti-rat	A21208	Invitrogen
Alexa Fluor 594 donkey anti-rabbit	A212027	Invitrogen
Alexa Fluor 594 goat anti-mouse	A11005	Invitrogen

Table 2.3: Bacteria Media 1

LB-Medium (Luria-Bertani)	quantity (g) in 1 l [pH 7.2-7.5]
Trypton	10
Yeast Extract	5
NaCl	10

Table 2.4: Bacteria Media 2

LB-Medium (Luria-Bertani)+Ampicilin	quantity (g) in 1 l [pH 7.2-7.5]
Ampicilin	100mg/ml
Trypton	10
Yeast Extract	5
NaCl	10

2.1.4 Buffers and Solutions

Table 2.5: Red Blood Cells Lysis Buffer

ACK buffer	quantity (g) in 1 l [pH 7.2-7.5]
NH_4Cl	10
Yeast Extract	5
NaCl	10

Table 2.6: Blocking Buffer

Blocking agent	Solvent
5% dry milk	1xTBS-T
5% BSA	1xTBS-T

Table 2.7: $CaCl_2$

$CaCl_2$ (g)	H_2O (l)
5,88	0,02

Table 2.8: Chloroquine [100mM]

Chloroquine-diphosphate (g)	H_2O (l)
0,516	0,01

Table 2.9: DEPC water

DEPC (%)	H_2O (l)
0,1	1

Table 2.10: DNA lysis buffer

name	quantity
Tris-HCl, pH 8,5	100 mM
EDTA	5 mM
SDS	0,2%
NaCl	200 mM

Table 2.11: Fixative solutions

Assay	fixative	solvent
IHC	2% paraformaldehyde	1xPBS
SAβ-galactosidase	2% paraform-, 0,25% glutar -aldehyde	PBS-Mg

Table 2.12: 2x Hepes Buffered Saline [HBS]

components	concentration in 0,1 l [pH 7.05]
NaCl	280 mM
KCl	10 mM
Na_2HPO_4 x $2H_2O$	1,5 mM
Dextrose	12 mM
HEPES	50 mM

Table 2.13: 0,5M Hepes

components	quantity (g)
HEPES	11,9

Table 2.14: Loading Buffer

type	components	quantity/concentration
6x-DNA	Bromphenol-blue	0,25%
loading	Xylene-cyanol	0,26%
buffer	Glycerol	30%
5x-protein	Tris-HCl [pH 6,8]	0,1 M
loading	Glycerol	30%
buffer	SDS	4%
	Mercaptoethanol	1μM
	Bromphenol-blue	0,2%

Table 2.15: Lysis Buffer: Proteins

components	quantity/concentration in 0,05l
Tris-base [pH 7.6]	50mM
NaCl	150mM
NP-40	1%
Na-deoxycholate	0,25%
Na-orthovanadate	1mM
NaF	10mM
PMSF	1mM

Table 2.16: Potassium cyanide (KC)

components	quantity(mg) in 0,025l
$K_3Fe(CN)_6$	20
$K_4Fe(CN)_6$ x $3h_2O$	1,050

Table 2.17: Phosphate Buffered Saline [PBS]

components	quantity (mM) in 1 l [pH 7,4]
NaCl	137
KCl	2.7
Na_2HPO_4	10
KH_2PO_4	2

Table 2.18: PBS/$MgCl_2$

components	quantity (mM) in 1 x PBS[pH 5,5]
$MgCl_2$	1

Table 2.19: Plasmid Mini Preparation Solutions

solution	components	quantity (mM)
I	Glucose	50
	Tris [pH 8,0)	25
	EDTA [pH 8,0]	10
II	NaOH	0,2 N
	SDS	0,5 %
III	KAc	5M
	CH_3COOH	15%

Table 2.20: 10 x Protein Running Buffer

components	quantity (g) in 1l [pH 8,3]
Tris-base	30
Glycin	144
SDS	10

Table 2.21: 50 x TAE

components	quantity in 1l
Tris-base	242 g
Glacial CH_3COOH	57,1 ml
EDTA [pH 8,0]	50 mM

Table 2.22: 10 x TBS

components	quantity in 1l
Tris [pH 8,0]	0,1M
NaCl	300 ml

Table 2.23: 1 x TBS-Tween [TBS-T]

components	quantity in 1l of 1 x TBS
Tween-20	0,2%

Table 2.24: TE-buffer

components	quantity (mM) in 1l [pH 7,5]
EDTA	0,1
Tris	10

Table 2.25: T-PBS

components	quantity in 1x PBS
Triton X-100	0,2 %

Table 2.26: 1 M Tris-HCl pH6,8

components	quantity(g) in 0,1l [pH 6,8]
Tris-base	12

Table 2.27: 1 M Tris-HCl pH8,8

components	quantity(g) in 0,1l [pH 8,8]
Tris-base	18

Table 2.28: Washing Buffer, Protein

components	quantity in 1l TBS-T
Dry milk	0,5 %

Table 2.29: 40x X-Gal Solution

components	quantity (mg) in 1ml of DMFO
X-gal	40

Table 2.30: X-Gal Staining Solution

components	quantity
X-gal solution	1x
KC solution	1x
PBS/$MgCl_2$	9,25 ml

2.1.5 Chemicals and Reagents

Table 2.31: Chemicals I

Name	Number	Supplier
Acetone	8002	J.T.Baker
Acrilamide-bis 30%	10688	Serva
Adriamycin	D1515	Sigma
Agar-Agar	5210.2	ROTH
Agarose	11404	Serva
Albumin Fraktion V	8076.2	ROTH
Ammoniumperoxisulfat (APS)	9592.3	ROTH
Ampicilin, sodium salt	K029.1	ROTH
5-Bromo-2Õ deoxy uridine	B5002	Sigma
Bromphenol blue	018069	Eurobio
Calcium chloride ($CaCl_2$)	5239.1	ROTH
Chloroform	1.02431.1000	Merck
Chloroquine-diphosphate	C6628	Sigma
DAPI	D9542	Sigma
DEPC (Diethyl pyrocarbonate)	D5758	Sigma
DMF (Dimethylformamide)	T921.1	ROTH
DMSO (Dimethylsulfoxid)	1.02952.1000	Merck
DTT	018742	Eurobio
EDTA (Ethylenediaminetetraacetate)	8043.2	ROTH
Ethanol, absolute	P075.1	ROTH
Ethidium-bromide powder	E8751	Sigma
FBS (Fetal bovine serum)	40Q7441K	Biochrom
5-Fluoro-2«-deoxyuridine	F0503	Sigma
5-Fluorouracil	F6627	Sigma
Formaldehyde	P733.2	ROTH

Table 2.32: Chemicals II

Name	Number	Supplier
Glacial acetic acid	971803	Merck
Glucose	6887.1	ROTH
a-D(+) Glucose (Dextrose)	6887.1	ROTH
Glutaraldehyde	4995.1	ROTH
Glycerine	4043.1	ROTH
Glycine	23390	Serva
Hydrocloric acid, HCl	1.00317.1000	Merck
HEPES	9105.3	ROTH
Interleukin 7, recombinant	RDI-207	RDI
1 kb ladder	N3232	NEB
L-Glutamine	K0283	Biochrom
Magnesium chlorid [$MgCl_2x6H_2O$]	2189.2	ROTH
β- Mercaptoethanol	4227.1	ROTH
Methanol	5370	J.T.Baker
Milk powder	T145.2	ROTH
$MgCl_2$	2189.2	ROTH
Nonident 40 (NP-40)	74385	Fluka
dNTP	K0391	ROTH
PBS Dulbecco	0699H	Biochrom
pBR mix 328	902.1	ROTH
PCR buffer	4379876	ABI
Penicillin-streptomycin	A22139120	Biochrom
Paraformaldehyde	P6184	Sigma
PMSF (Phenylmethylsulfonylfluoride)	P7626	Sigma
Polybrene (Hexademethrinebromide)	H9268	Sigma
Potassium bicarbonate [$KHCO_3$]	P-9144	Sigma
Potassium ferricyanide [$K_3Fe(CN)_6$]	P3667	Sigma
Potassium ferrocyanide [$K_4Fe(CN)_6$ x 3 H_2O]	P9387	Sigma
Potassiumchloride (KCl)	319309	Sigma
Potassiumacetate (KAc)	4986.1	ROTH
2-propanol	I9030	Sigma
Propidium iodide	P4170	Sigma
Protease inhibitors	11873580001	Roche

Table 2.33: Chemicals III

Name	Number	Supplier
Puromycin	540222	Calbiohem
ROTI- prestained	T852.1	ROTH
RotiQuant, Bradford reagent	0038.2	ROTH
SDS	2326.2	ROTH
Sodiumchloride (NaCl)	1.06400.5000	Merck
Sodium citrat [$C_6H_5Na_3O_7$ x 2 H_2O]	3580.1	ROTH
Sodium-desoxycholate	D6750	Sigma
Sodiumfluoride (NaF)	S1504	Sigma
Sodiumhydroxide (NaOH)	6771.1	ROTH
Sodiumorthovanadate	S 6508	Sigma
Sodium pyrophosphate [$Na_4P_2O_7$ x 10 H_2O]	S6422	Sigma
Taq polymerase	N8080171	ABI
Tris(hydroxymethyl) aminomethane	1.08382.0500	Merck
TEMED (Tetramethylethylenediamine)	T7024	Sigma
TGF-β	100-B-001	R&D Sys
Triton-X 100	1.08603.1000	Merck
TRIZOL	15536-026	Invitrogen
Trypan-blue	T6146	Sigma
Trypsin-EDTA	L 2153	Biochrom
Trypton/Pepton	8952.3	ROTH
Tween 20	9127.1	ROTH
Vecta-Shield, mounting medium	H-1400	Vector
X-Gal	2315.3	ROTH
Xylene-cyanol	018074	Eurobio
Xylol	9713.1	ROTH
Yeast extract	2363.3	ROTH

2.1.6 Cells

Table 2.34: Cell Lines

Cell Line	Description
NIH 3T3	Adherent mouse embryonic fibroblast cell line; ATCC number:CRL-1658
Phoenix Eco j^-	Adherent human embryonic kidney cell line 293T, adenovirus transformed and stably transfected with plasmids encoding the MML virus sequence (gag, pol, env). www.stanford.edu/group/nolan.html

Table 2.35: Primary Cells

Primary Cell	Description
B-Lymphoma cells	Primary murine Myc-driven lymphoma cells, isolated from the lymph-nodes of animals with the different genetic background. Grown in suspension, requiring feeder cells.
FLC	Primary murine fetal liver cells, isolated from the E15.5 mice. Grown in suspension, requiring feeder cells.
MEF	Primary murine embrionic fibroblasts, isolated from E12.5 mice. Adherent cells.

2.1.7 Cell Culture Media

Table 2.36: DMEM

medium	components
DMEM	Dulbecco's modified Eagle medium
	Glucose 4500 mg/l
	L-Glutamine
	Pyruvate

Table 2.37: IMDM

medium	components
IMDM	Iscove's modified Eagle medium
	L-Glutamine
	HEPES 25 mM

Table 2.38: Adherent Cell Culture Medium(ACCM)

medium	components
ACCM	DMEM
	10 % FCS
	Penicilin-Streptomycin (100 U / ml)

Table 2.39: B-Cell Medium(BCM)

medium	components
BCM	DMEM+IMDM 1:1
	20 % FCS
	Penicilin-Streptomycin (100 U/ ml)
	4 mM L-Glutamine
	25 mM β- Mercaptoethanol

Table 2.40: Freezing Medium(FM)

medium	components
FM	90 % FCS
	10 % DMSO

2.1.8 Mouse Strains

Table 2.41: Mouse Strains

Mouse strain (modification)	Description
C57BL/6 (Eμ-Myc transgenic)	Adams *et al*, Cell 1985 WEHI, Melbourne, Australia
C57BL/6 (Suv 39h1 knock-out)	Peters *et al*, Cell 2001 IMP, Vienna, Austria
C57BL/6 (p 53 knock-out)	Jacks *et al*, Current Biology 1994 Whitehead institute, Cambridge, USA
C57BL/6 (p 16 knock-in)	Krimpenfort *et al*, Nature 2001 NKI, Amsterdam, The Netherlands
C57BL/6 (p 19 knock-out)	Kamijo *et al*, Cell 1997 Howard Hughes Medical Institute, Memphis, USA

2.1.9 Enzymes

Table 2.42: Enzymes

Name	Supplier
BamH I	NEB
Bgl II	NEB
Cla I	NEB
Hind III	NEB
EcoR I	NEB
Xho I	NEB
Xba I	NEB
Proteinase K	Merck
Rnase A	Fluka
RNAsin RNAse Inhibitor	Invitrogen
Superscript REverse Transcriptase II	Invitrogen

2.1.10 Expression Vectors

Used plasmids are ecotrophic vectors based on the Moloney Murine Leukemia Virus (MMLV) and taken for retroviral transduction of rodent cells.

The Murine Stem Cell Virus (MSCV) vector contains the packaging sequence, the gene of interest in the multiple cloning site (MSC) driven by a Phosphoglycerate kinase (PKG) promoter and a selectable marker (antibiotic resistance) or Green Fluorescent protein (GFP) between the 5' and 3' LTR. (Figure 2.1).

Table 2.43: Expression Vectors

Vector	Insert
MSCV-bcl2-IRES-GFP	murine bcl2 fcs
MSCV-IRES-GFP	-
MSCV-bcl2-puro	murine bcl2 fcs
MSCV-puro	-
pBabe-MycER-puro	human c-myc fused to human estrogen receptor

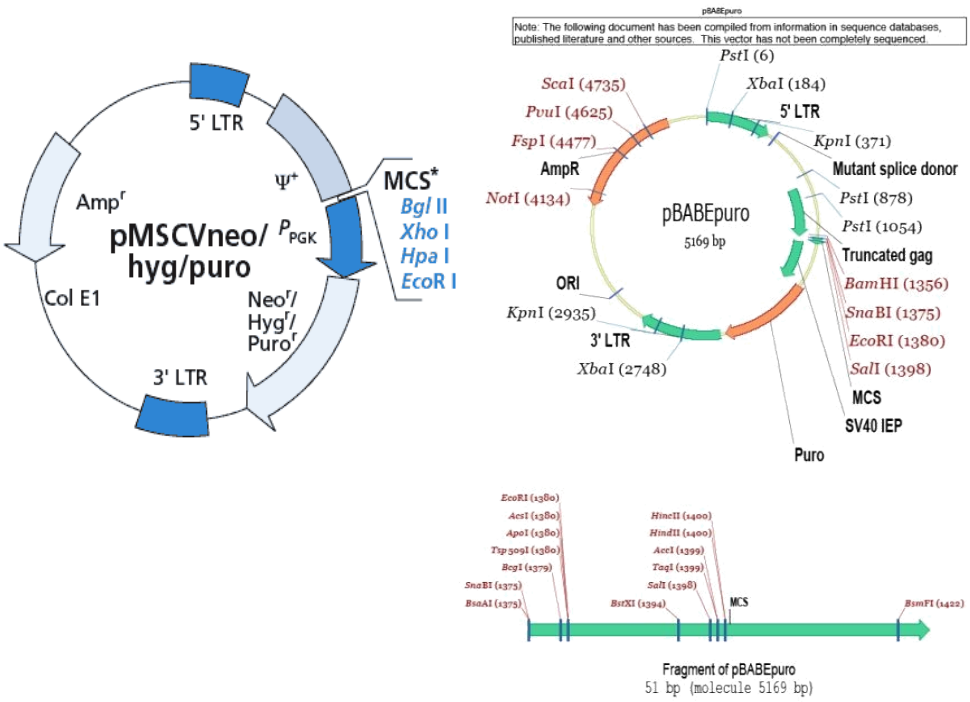

Figure 2.1: Plasmid maps, adapted from clonotech.org and addgene.org

2.1.11 Kits

Table 2.44: Commercial Kits

Name	Number	Supplier
Cell Proliferation Kit	RPN 20	Amersham
In situ cell death detection kit	111684809910	Roche
Leukostat kit	CS430-A4	Fischer Diagnostics
Quantikine	MB100B	R& D systems
Reverse transcription kit	11917-010	Invitrogen
RNeasy Mini Kit	74104	Qiagen
Supersignal West Pico	18561357-36	Pierce

2.1.12 Plastic-ware and other dispensable materials

Table 2.45: Plastic and Dispensable Materials

Name	Number	Supplier
Cell culture dishes, various sizes	-	TPP
Centrifuge tubes, various sizes	-	Falcon
Cryotubes	PK-100	Simport Plastics
Einmal-Kuevetten	8129	ROTH
Frosted slides 76x26 mm	S9105	Engelbrecht
Hybond ECL	RPN303D	Amersham
Immersion oil	56822	Fluka
Microlance tm3 25Gx1″, Nr18	REF300400	BD
Neubauer cell-counter chamber	0640030	Superior Marienfeld
Nylon mesh (35 μm)	17-35/22	Sefar
Omnifix 2 ml luer lock	REF4617029V	BRAUN
Omnifix 10 ml luer lock	REF4617100V	BRAUN
Pasteur Pipettes 230 mm, glass	VWRI1822	VWR International
Polystirene tubes (5 ml)	352005	Falcon
Syringe filter sterile 0.45 μm	P667.1	ROTH
Syringe filter sterile 0.22 μm	P666.1	ROTH
Scalpel, disposable	No23	Feather
Serological pipetes, various sizes	-	Falcon
Syringe 1 ml luer	REF300013	BD Plastik
Whatman paper	Z132403	Schleicher Schuell
X-omat tm LS 18x24	8688681	KODAK

2.1.13 Machines

Table 2.46: Machines

Name	Supplier
Bio Photometer, 8.5 mm	Eppendorf
Block termostat 100	Kleinfield Labortechnik
Centrifuge, 5415D	Eppendorf
Centrifuge, Rotina 35R	Hettich
Cytospin inserts, 1670	Hettich
Cytospin plastics, 1688	Hettich
Electrophoresis Power Supply, E802	Consort
FACS Calibur	Becton Dickinson
Fluorescence microscope, Axioplan	Zeiss
Flow Hood Typ UVF 6.18S	BDK
Megafuge 1.0R	Haraeus
Microscope, Televal 31	Zeiss
Micro-wave	Bauknecht
PTC-1	MJ Research, Inc
Shaker Heidolph	UNIMAX 1010
Steri-cult 200 incubator	Labtect
TRANSBLOT SD	BIORAD
UV detection system, Biometra T13	Biometra
Vortex-Genie	ROTH
Western-blot Chamber	C.S.B. Scientific CO

All materials/ machines not listed in detail are standard lab equipment.

2.1.14 Oligonucleotides

Table 2.47: Genotyping PCR Primers

Name	Sequence	Product size
Eμmyc	5'-CAGCTGGCGTAATAGCGAAGAG-3'	transgene
	5'-CTGTGACTGGTGAGTACTCAACC-3'	830 bp
Suv39h1	5'-GTTGATGCTTCCTGGTGTGTAGG-3'	wt 417 bp
	5'-TTTGAGGGGACGACGACAGTATG-3'	ko 588 bp
	5'-AACAGATGTGGGGTTGGTGGAG-3'	
p53	5'-TATACTCAGAGCCGGCCT-3'	wt 450 bp
	5'-ACAGCGTGGTGGTACCTTAT-3'	ko 600 bp
	5'-TCCTCGTGCTTTACGGTATC-3'	

Table 2.48: RT-PCR Primers I

Name	Sequence	Product size
Activin-A	5'-AGGACCTGTACCCAACAAC-3' 5'-ACATCTGCTGGAAGGTGGAC-3'	195 bp
cEBP/β	5'-CAAGCTGAGCGACGAGTACA-3' 5'-CAGCTGCTCCACCTTCTTCT-3'	157 bp
Culin 2	5'-TGGCAGTTCTTCTTGCCTTT-3' 5'-GTGGCGTATCCTTCTGCATT-3'	243 bp
Cyclin A1	5'-GAGAGGGAAATTGCAGCTTG-3' 5'-TCAGTCCTGATGCACACTCC-3'	240 bp
Cyclin D1	5'-AGTGCGTGCAGAAGGAGATT-3' 5'-CACAACTTCTCGGCAGTCAA-3'	238 bp
Fgf 1	5'-GGACACCGAAGGGCTTTTAT-3' 5'-ACAGCTCCCGTTCTTCTTGA-3'	151 bp
Foxo3a	5'-GGGAGTTTGGTCAATCAGA-3' 5'-GCCTGAGAGAGAGTCCGAGA-3'	193 bp
H2aX	5'-TACCTCACTGCCGAGATCCT-3' 5'-GCTCTTCTTGGGCAGCAG-3'	192 bp
HP1β	5'-AGCGCAAAGCTGATTCTGAT-3' 5'-GAATGCCACGTTAGCCTTTC-3'	265 bp
HP1γ	5'-GAGATGCTGCTGACAAACCA-3' 5'-GCTCCTCGTAGAAGGCAATG-3'	189 bp
Jumonji 2B	5'-AAGGCTGAGGAGGAGAGGAG-3' 5'-CCCTGTGAAGGTAGCAGCTC-3'	215 bp
Lsp 1	5'-CCTGAACCGCTCCATTAAAA-3' 5'-AGTGGCCACGAACTTGTACC-3'	358 bp

Table 2.49: RT-PCR Primers II

Name	Sequence	Product size
Myst 4	5'-ATGGGAGGCAGTATCTGTGG-3' 5'-TGCATAGGAGGTCACAGCAG-3'	465 bp
Mei	5'-CCTGTTAATTGGGCTCCAGA-3' 5'-TTCACGTGAGAGGACACAGC-3'	262 bp
p15	5'-TTACCAGACCTGTGCACGAC-3' 5'-GCAGATACCTCGCAATGTCA-3'	159 bp
p16	5'-TCAACTACGGTGCAGATTCG-3' 5'-TCGCACGATGTCTTGATGTC-3'	194 b
p19	5'-GTCGCAGGTTCTTGGTCACT-3' 5'-CGAATCTGCACCGTAGTTGA-3'	246 bp
p21	5'-GTACTTCCTCTGCCCTGCTG-3' 5'-TCTGCGCTTGGAGTGATAGA-3'	173 bp
p27	5'-CAGAATCATAAGCCCCTGGA-3' 5'-TCTGACGAGTCAGGCATTTG-3'	224 bp
PAI-1	5'-AGTCTTTCCGACCAAGAGCA-3' 5'-ATCACTTGCCCCATGAAGAG-3'	209 bp
PAN-1	5'-TCCAGAGAATGTTGCTGCAC-3' 5'-AGAGGGCAGCTTTTCACAAA-3'	190 bp
PCNA	5'-TTGGAATCCCAGAACAGGAG-3' 5'-CAGTGGAGTGGCTTTTGTGA-3'	287 bp
PPGB	5'-ACAGCCCCTTCCAACTACCT-3' 5'-GAGCGAATCCACAAACCACT-3'	243 bp
SMAD 2	5'-GGAACCTGCATTCTGGTGTT-3' 5'-ACGTTGGAGAGCAAGCCTAA-3'	150 bp

Table 2.50: RT-PCR Primers III

Name	Sequence	Product size
SMAD 3	5'-CTGGGCCTACTGTCCAATGT-3' 5'-GCAGCAAATTCCTGGTTGTT-3'	239 bp
SMAD 4	5'-AGCTCCAGCCATCAGTCTGT-3' 5'-GCAGGACTTCATCCAAGAGC-3'	188 bp
Suv39h1	5'-CGAGTTCTTAAGCAGTTCCAC-3' 5'-TGCAGGTTGGGATCACAACTATGG-3'	743 bp
Taf4b	5'-TGGTTGCCCTAAGACAGCTT-3' 5'-TCTCAGGCTGAAGGGACACT-3'	366 bp
TGF-β1	5'-ATACGCCTGAGTGGCTGTCT-3' 5'-TTCTCTGTGGAGCTGAAGCA-3'	301 bp
TGF-β2	5'-CCTTCGCCCTCTTTACATTG-3' 5'-TTCGATCTTGGGCGTATTTC-3'	250 bp
TGF-β3	5'-GCATCCACTGTCCATGTCAC-3' 5'-GCGGAAGCAGTAATTGGTGT-3'	257 bp
βIGH3	5'-TGACAAGGTCATTTCCACCA-3' 5'-GTGGCCAGGATGTCTTTGTT-3'	384 bp
TBP	5'-AACAGCCTTCCACCTTATGC-3' 5'-CATGTTCTGGATCTTGAAGTC-3'	681 bp

Primers were designed using the Primer3 program, Whitehead Istitute, Massachusetts Institute for Technology.

2.2 Methods

2.2.1 Mice

Breeding and maintenance

Mice recieved a standard laboratory diet and drinking water *ad libitum*, and were bred and maintained under specific pathogen free (SPF) conditions at the Animal Facility of Campus Virchow Hospital, Charite Universitätsmedizin Berlin. All experiments with live animals were performed according to the regulations of the institutional animal care.

Tumor onset monitoring

Mice were monitored for the onset of the disease every 3 days by palpation of the peripheral: prescapular and cervical lymph nodes (LN). "Well palpable" lymphoma reflects LN enlargements of 5mm or more.

Statistical comparison of Kaplan-Meier curves is based on the log-rank test. For comparisons of means and standard deviations ("s.d." denoting a significant P-value of < 0.05) the unpaired t-test was applied. All error bars represent the s.d.

Peripheral blood smears

Table 2.51: Materials Used-BS

Blood smears-Materials Used
Glass slides
Scalpel
Leukostat^{TM} kit

Blood samples were obtained by tail artery bleeding, one drop of blood was smeared onto the glass slide and stained as follows:

Slides were submerged into the Leukostat^{TM} fixative solution, briefly dried, then submerged in Leukostat^{TM} Solution I for 1 minute. Remaining Solution I was removed from the slide and slide was submerged into the Leukostat^{TM} Solution II for 30 seconds. Post staining slides were washed in H_2O and dried for 5-10 minutes, afterwards they were examined under the microscope.

Table 2.52: Materials Used-DNA extr

DNA Extraction - Materials Used
Lysis Buffer
Proteinase K [20mg/ ml]
Ethanol
Isopropanol
TE buffer

DNA isolation and PCR-based determination of genotype

0.5 cm of mouse tail was cut off and incubated in 450 μl lysis buffer and 50 μl Proteinase K in a Eppendorf tube at 55^{O}C for at least 2 hours. Post incubation resulting product was spun down at maximum speed for 20 minutes to pellet down the undigested left-overs. Supernatant was transfered into a new tube, already containing 500 μl isopropanol, contents inside the tube was mixed by inverting it several times. At this point DNA formed visible precipitate, and can be "fished out" by pipet tips and briefly washed in 75% ethanol. Post washing DNA was briefly dried and transferred to a new tube containing 200 μl 0.1 TE buffer.

Table 2.53: Materials Used-genotyping

Determination of Genotype- Materials Used
DNA (0.5 μg/ml)
PCR buffer
$MgCl_2$
dNTP
Taq polimerase
Primer mix
PCR products
6x DNA loading buffer
1kb ladder
pBr marker
Agarose
TAE
Ethidiumbromide

Mice were genotyped for following modifications: Myc transgene, Suv39h1 knock-out, p53 knock-out, p16 knock-in, Arf knock-out.

PCR reactions were prepared according to the following protocol:

Table 2.54: Materials Used-PCR

PCR Reaction- Materials Used
10x PCR buffer (including 15mM $MgCl_2$)
dNTP 10 mM
Taq polymerase [5U/ml]
Primer mix 1mM

Mastermix was prepared in a volume of 24 μl per 2μl of DNA sample and PCR reaction was run on the cell cycler as follows:

Table 2.55: PCR Reactions

Genotype tested	temperature (^{O}C)	time (minutes)	number of cycles
Eμ-myc	94	5	1
	94 , 64 , 72	1,1,1	32
	72	5	1
Suv39h1	94	5	1
	94 , 55.9 , 72	0.5 , 0.5 , 0.5	35
	72	10	1
p53	94	5	1
	94 , 62 , 72	0.5 , 1, 1	34
	72	5	1
p 16	94	5	1
	94 , 62 , 72	0.5 , 1, 1	34
	72	5	1
Arf	94	5	1
	94 , 62 , 72	0.5 , 1, 1	34
	72	5	1

Agarose gels were prepared according to the following procedure: agarose was dissolved in 1x TAE at the desired concentration and boiled in a microwave until the agarose was completely melted.The agarose solution was cooled down to about 50^{O}C and ethidiumbrodmide was added to the final concentration of 0.2 μg/ml.

Gel chamber was filled with 1x TAE and 10 μl aliquots of the PCR samples, including the corresponding amount of loading buffer were loaded into the wells. After samples were loaded, electrophoresis was run at 120 V until the desired resolution of DNA fragments was achieved. In order to determine DNA size of the fragments, standard marker was used. DNA products was visualized by UV-light, and documented by taking a photomicrograph.

Lymphoma processing

Table 2.56: Materials Used-lymphoma

Lymphoma Processing- Materials Used
LN of the lymphoma bearing mice
Ethanol
PBS
Mouse dissection tools
Frosted glass slides
Nylon mesh
ACK buffer
Formaldehyde

Post CO_2 sacrification animal was bathed in ethanol, and fixed onto the dissection board. Mouse was opened as follows: skin along the ventral midline from the groin to the chin was carefully cut not to damage the muscle wall underneath.

Incision was made above the knee on both sides of the animal and skin was reflected back. Pre-scapular, cervical and back leg LN were measured and excised with scalpel, and placed in a dish containing sterile PBS.

Transparent peritoneal wall was cut carefully, body cavity was opened up and reflected back to have access to the structures underneath.

Mesentheric LN was excised and measured, and other internal organs (liver and spleen) were measured and observed for signs of pathological infiltrations and or any abnormalities.

After removing the diaphragm on the bottom of the breast, the sternum was opened by lifting it up with forceps and cutting along each side up to the girdle to have access to the thoracic organs.

Thymus size was examined and peripheral blood smear was obtained by intracardial aspiration. LN were either fixed in 4% Formalin, snap frozen in liquid nitrogen or prepared as a single cell suspension.

LN in 1x PBS were minced between two frosted glass slides. Mixture was filtered through a sterile 35 μm nylon mesh membrane and centrifuged at 1200 rpm for 5 minutes (4^OC). To lose the reminder of the red blood cells, pellet was resuspended in 3 ml of ACK lysis buffer and incubated at RT for 5 minutes. Before centrifugation (1200 rpm, 5 min, 4^OC), 27 ml of B cell medium were added for neutralization. Cells were either plated as a single cell suspension on a feeder layer or frozen down in liquid nitrogen. The same procedure applies if preparing spleen or thymus single cell suspensions.

Lymphoma reconstitution and treatment in vivo

Table 2.57: Materials Used-reconstitution and treatment

Lymphoma Reconstitution, Treatment- Materials Used
Primary, non cultured lymphoma cells
Bcl2-transduced lymphomas
PBS
Syringe
Needle
Mouse restrainer
Cyclophosphamide (CTX)

Non-cultured or bcl2 transduced lymphoma samples were transplanted in a pair of genetically matched, wild-type 6-10 week of age female mice by tail vein injection. Prior to the transplantation mice were heated for 5 minutes for the better visualisation of the tail vein. Total of 200 μl of cell suspension ($5x10^6$ viable lymphoma cells in PBS) was transplanted per mouse.

Recipient mice were palpated for tumor formation every 3 days, and when tumors became well palpable a single dose (300 mg/kg of body weight) of cyclophosphamide (CTX) was administered intraperitoneally, and mice were further monitored by palpation of the peripheral LN for treatment response.

Animal treatment *in vivo*

Animals were exposed to either: 0.4 mg/ml of caffeine in drinking water starting at birth; 0.5% w/v solution of N-Acetylcysteine in drinking water starting at birth; or 60 mg/L of lisinopril in drinking water starting at three weeks of age.

Mice were monitored for time to tumor onset latencies, and lymph nodes were used for the subsequent analysis.

2.2.2 Bacterial Transformation

An aliquot of DH5α competent bacteria was thawn on ice for 5 minutes, then 100 ng of the desired plasmid was added. Mixture was left on the ice for 10 minutes, then it was transferred to 42^{O}C for 90 seconds. After that mixture was returned to ice for 5 minutes, then 500 μl of LB medium was added, and left for 30 minutes at 37^{O}C, gently shaking. Mixture was centrifuged, and 350 μl of the supernatant was removed, while bacteria were resuspended in the rest of it, and plated on the LB-Amp agar plates.

Bacteria were allowed to form colonies overnight in 37^{O}C.

2.2.3 BrdU incorporation

Table 2.58: Materials Used-BrdU

BrdU incorporation- Materials Used
BrdU[10mg/ml]/FU[1mg/ml] labeling solution
4% paraformaldehyde in PBS
Xylene
Ethanol
Permeabilization buffer
Blocking solution
TBST
Syringes
2N HCl
Cell proliferation kit
anti-BrdU primary antibody
Secondary antibody
Lymphoma cells

24 hours prior to CO_2 euthanasia, 10 μl labeling solution/g body weight was intraperitoneally injected. Lymphoma cells and lymph nodes were harvested at the end of labeling. For BrdU detection in situ whole lymph nodes were either fixed for 24 hours in 4% neutral buffered formalin, and later in PBS for the long-term storage or alternatively lymph nodes were cryopreserved. Formalin fixed lymph nodes were paraffin embedded and subsequently slides were made from samples. Deparaffinization was done as follows: 2x 5 minutes in Xylene, 2x5 minutes in decreasing ethanol series (95-70%), and 2x 5 minutes in PBS. For BrdU detection in suspension lymphoma cells were fixed for 15 min in 1 ml of 4% paraformaldehyde. Cells were permeabilized in TBS-TritonX100 for 5 minutes at RT, and washed in TBST. DNA was denatured with 2N HCl for 5 minutes at RT. Afterwards cells were neutralized with 0.1M Sodium Borate for 5 minutes at RT, and blocked with 5% bovine serum albumin. First antibody was incubated for 60 minutes, and the secondary one for 30 minutes. For tissue sections DAB substrate was added according to the manufacturers instruction, and sections were evaluated under the light microscopy. Cell suspensions were incubated with the DNA staining solution for 30 minutes at RT and evaluated by flow cytometry.

2.2.4 Cell Culture

Adherent cell culture

NIH3T3 fibroblasts and Phoenix eco cells were used in various experiments.

Table 2.59: Materials Used-adherent cells

Adherent Cell Culture- Materials Used
DMEM medium
PBS
Trypsin

NIH 3T3 fibroblasts or Phoenix cells were seeded 50% confluent in DMEM medium and cultivated under standard conditions (37^{O}C, 21% O_2, 5% CO_2, 95% humidity) until they reached confluency. Cells were split by removing the medium and washing with 1x PBS. Cells were deatached by adding 1ml of trypsin at 37^{O}C for 5 minutes. After resuspending the cells in culture medium, cells were re-seeded in the desired density onto new cell culture plates containing 10 ml of the fresh medium.

Table 2.60: Materials Used-feeder cells

Feeder Cell Preparation- Materials Used
NIH 3T3
DMEM medium
B-cell medium
PBS
Trypsin
Trypan blue

NIH 3T3 fibroblasts were seeded in DMEM medium and allowed to reach 70% confluency, cells were irradiated with 20Gy. 12 hours post irradiation cells were split according to standard procedures and resuspend in fresh B cell medium. Cell number and viability was assessed by by trypan blue exclusion. $10^4/cm^2$ of cells was seeded in a B-cell medium,and cultured under standard conditions (37^{O}C, 21% O_2, 5% CO_2, 95% humidity). 24 hours later feeder layers were ready to use. Feeder layers were not used more than 10 days after the irradiation, when first flattened or vacuole enrichment was observed.

Fetal liver cells

FLCs were used for the direct transplantation experiments, with minimal (1-2 hours) or no culturing at all.

Table 2.61: Materials Used-FLC

Fetal Liver Cells- Materials Used
PBS
Frosted slides
BCM

Breeder cages were set up to produce the genotype of interest. Females were checked for pregnancy by vaginal plugging. Animals were sacrifised at gestation day 14,5-15,5 by CO_2 sacrification. Abdominal cavity was opened and uterus was resected. Placenta was cut out and placed in a 10 cm^2 plate containing PBS. Maternal part of placenta was removed and embryos were released into the PBS. Yolk sac was dissected. Head of the embryo was saved for the further genotyping.

Liver was well visible and was isolated from the abdomen by scalpel section. Liver was minced between the frosted slides and as a single cell suspension was used for the transplantations.

DNA isolation was equal to the tail material and the follow up genotyping PCR was as previously described.

Lymphoma cell culture

Table 2.62: Materials Used-lymphoma culture

Lymphoma Cell Culture- Materials Used
Lymphoma cells
Feeder cells (irradiated NIH 3T3)
Conditioned B-cell medium (incubating on feeder cells)
PBS
Trypsin
Trypan blue

For primary lymphoma cell culture, single cell suspension of mouse lymphoma was seeded (about 5 x 10^6 total) onto the feeder plate containing 10 ml of conditioned B cell media. Cells were cultured under the standard conditions (37^OC, 21% O_2, 5% CO_2, 95% humidity).

When density of lymphoma population reached 5 x 10^6 cells/ ml, cells were passaged. Also, even if cells did not reach high confluence, but the medium changed colour from its normal red to acidic orange yellow cells were passaged.

Passaging of primary lymphoma cells was done in either of 2 ways, mostly depending on the quality of the feeder layer:

I by reseeding on same feeder layer

II by seeding on a fresh feeder layer

10 ml of B-cell medium containing lymphoma was centrifuged for 5 minutes at 1200 rpm, at 4^OC, 8ml of the medium was removed and remaining 2 ml of B-cell medium with lymphoma cells inside was pasaged into new plates containing feeder layer with 8 ml of conditioned B-cell medium.

Passaging of the cells, depending on their doubling speed, was done every 3-5 days.

Mouse embryo fibroblast (MEF) culture

Table 2.63: Materials Used-MEF

Mouse Embryo Fibroblast Cell Culture- Materials Used
0,05% TRYPSIN-EDTA
PBS
DMEM

Breeder cages were set up to produce the genotype of interest. Females were checked for pregnancy by vaginal plugging. Animals were sacrifised at gestation day 11,5-12 by CO_2 sacrification.

Abdominal cavity was opened and uterus was resected. Placenta was cut out and placed in a 10 cm^2 plate containing PBS. Maternal part of placenta was removed and embryos were released into the PBS. Yolk sac was dissected, afterwards, all the red structures, representing early stages of the internal organs and vessels were also resected. Head of the embryo was saved for the further genotyping.

Leftover embryo was transferred to a 10 cm^2 plate with trypsin inside. Embryo was then disrupted with a scalpel and a 18G needle/syringe. After cutting and mincing and multiple aspirations plate was incubated for 20 minutes at 37^OC. Trypsin- cell suspension was resuspended by pipetting, and suspension was placed in 10 cm^2 plates, medium was added up to 10 ml. Medium was changed the next day.

DNA isolation was equal to the tail material and the follow up genotyping PCR was as previously described.

MEFs were usually passaged every 2 days, when reached confluent. Passage 1 MEFs were used for the further experiments.

Cryopreserving and thawing of cells

Table 2.64: Materials Used-cryopreserving

Cryopreserving of Cells- Materials Used
Cells (all types)
DMEM
B-cell medium
Freezing medium
PBS
Trypsin
Cryo-tubes

Cryopresrving

Adherent cells:

Media was removed from the plate. Cells were washed with PBS, detached with 1ml Trypsin and resuspend in DMEM medium, and centrifuged (1200 rpm, 5 min, RT).

Cells grown in suspension:

Cells were directly harvested from the culture plate and centrifuged (1200 rpm, 5 min, RT).

After centrifugation supernatant was removed and pellet was resuspend in ice-cold freezing medium. Cells were frozen in the density of $2x10^6$ cells/ml, and transferred immediately onto dry ice (-20^OC) ice and after 1 hour transferred to the liquid nitrogen for a long term storage.

Table 2.65: Materials Used-thawing

Thawing of Cells- Materials Used
Frozen cells (all types)
DMEM
B-cell medium
Feeder layer
PBS

Cells were thawn at 37^{O}C for no more than 2 minutes, and dropwise transferred to 10 ml of the respective medium. After centrifugation (1200 rpm, 5 min, 4^{O}C), supernatant was removed and pellet was resuspend in 1 ml of the respective medium. Cells were seeded in an appropriate cell number on culture dishes or on feeder cells, depending on the cell type.

Flow cytometric analysis

A flow cytometric analysis was used to characterize viable/ senescent/ dead (SSC/FSC scan or Annexin V/PI staining) cell populations, measure efficiency of retroviral transduction (when GFP was used as a selectable marker) was performed with Becton-Dickinson FACScan using 488-nm laser (emission wavelengths are FL1: 515-545 nm, FL2:564-606 nm and FL3: 650 nm). Data were analyzed using CELLQUEST software (Becton-Dickinson), and approximately 10 000 cellular events were counted.

Detection of senescent cells. 500,000 of each freshly prepared lymphoma

Table 2.66: Materials Used-Flow cytometry-senescence

Flow cytometry for senescence- Materials Used
Lymphoma cells
PBS

was washed and resuspended in PBS and immediately measured by forward/ side scatter on flow cytometer. Senescent cell population is bigger and more granular, shifting in both light scatter parameters from normally viable cells and creating a distinct subpopulation.

AnnexinV/PI protocol : cells were resuspended in 1mg/ml freshly prepared dilution of Annexin V and incubated for 10 minutes at RT in the dark. Solution of PI was added to the cells (to a final concentration of 1mg/ ml) prior to the analysis on flow cytometer.

Table 2.67: Materials Used-Flow cytometry-apoptosis

Flow cytometry for AnnV/PI- Materials Used
Lymphoma cells, treated or untreated with ADR
PBS
AnnexinV
Propidium Iodide (PI)

2.2.5 Immunofluorescence

Table 2.68: Materials Used-IF

Immunofluorescence- Materials Used
LN (parrafin embeded or snap frozen)
Primary lymphoma cells
Primary spleenocytes
PBS
T-PBS
Xylol
Ethanol
Fixative solution
Blocking solution
Primary antibodies
Secondary antibodies
Mounting medium

Tissue protocol

Tissues sections (8 μm thick) were processed as follows:

Paraffin embeded sections: Slides with the paraffin embeded sections were heated at 55^{O}C for 30 minutes, and afterwards submerged into xylol for 5 minutes, repeating this step 2 times. Following, cells were re-hydrated in the reducing gradients of ethanol (starting at absolute ethanol, finishing at 70% ethanol). Slides were kept for 5 minutes in each of the ethanol concentrations. Post ethanol slides were submerged into PBS. Sections were permeabilized in T-PBS for 30 minutes at room temperature(RT), then incubated in the primary antibody over-night at 4^{O}C. Slides were washed three times in PBS and subsequently incubated in corresponding secondary antibody for 60 minutes (RT) in dark. Final washing was in T-PBS (3x 15 min), and slides were mounted and fluorescence was detected under the microscope immediately.

Frozen tissues:

Tissues were fixed in 1-2 % Paraformaldehyde/Glutaraldehyde mix for 10 minutes (4^{O}C), slides were washed in PBS/ $MgCl_2$ and stained for the β-galactosidase activity for 6-8 hours.

Cell protocol:

Cells were either thawn or harvested at the appropriate time point from the culture or the tumor-bearing animal, centrifuged (1200 rpm, 5 min, 4^{O}C) and washed PBS. Cell number and viability was assessed by trypan blue exclusion. 500μl were transferred to a slot of the cytospin plastic and centrifuged at 700 rpm for 8 minutes (15^{O}C). Supernatant was carefully removed by aspiration and cells were fixed by a freshly prepared fixation solution. After incubation (15 minutes, RT), slides were washed three times in PBS and permeabilized in T-PBS for 30 minutes (RT). Cells were incubated in the first antibody over-night at 4^{O}C. Slides were washed three times in PBS and subsequently incubated in corresponding secondary antibody for 60 minutes (RT) in the dark. Cells were washed in T-PBS (3x 15 min), and slides were mounted and fluorescence was detected under the microscope immediately. Alternatively cells were fixed in the 1-2% Paraformaldehyde/Glutaraldehyde mix for 10 minutes (4^{O}C), then washed in PBS/$MgCl_2$ and stained for the β-galactosidase activity for 6-8 hours.

2.2.6 Immunophenotyping

Table 2.69: Materials Used-IPh

Immunophenotyping- Materials Used
Primary lymphoma cells
Primary spleenocytes
Primary thymocytes
PBS
FITC or PE-conjugated antibodies
Flow cytometer

10^6 primary lymphoma cells as well as the spleenocytes and thymocytes (antibody-controls) were centrifuged (1200 rpm, 5 min, 4^{O}C) and washed in PBS. Antibodies were diluted in 100 μl PBS, and cell pellet was resuspend in the staining mixture, and incubated for 30 minutes on ice in the dark. Post staining cells were thoroughly washed in PBS, filtered through a 35 μm nylon mesh and transferred on ice for immediate analysis by Flow cytometry.

2.2.7 Mitotic Trap

Table 2.70: Materials Used-mitotic trap

Mitotic trap- Materials Used
Lymphoma cells
Nocodazole
H3S10P antibody
4% paraformaldehyde
TBS-TritonX-100
PBS
Flow cytometer

Eμ-myc and Eμ-myc, Suv39h1$^{-/-}$ cells were freshly isolated and subjected to 100μM of Nocodazole for 0, 3, 6 and 9 hours. After the exposure cells were immediately fixed in 4% formaline (15 minutes, RT), permeabilized in TBS-tritonX-100 (10 minutes, RT) and stained for the phosphorylated serine 10 residue on the Histone H3 (H3S10P; 1 hour, RT), washed two times with PBS and stained for secondary, fluorescent conjugated antibody (1 hour at RT), and analyzed by flow cytometry.

2.2.8 Reactive oxygen species quantification

Table 2.71: Materials Used-ROS

ROS quantification- Materials Used
Lymphoma cells
DCF
PBS
Flow cytometer

Eμ-myc lymphoma cells from untreated and N-Acetylcysteine treated mice were quantified for the reactive oxygen species (ROS) by exposure to the 2'7'- dichlorofluorescein (DCF), and flow cytometric analysis. DCF positive cells were visualised by immunofluorescence.

2.2.9 Retroviral Transduction

Phoenix cells transfection

Phoenix cells were grown in a 10 cm^2 plate to a maximal density of 70%. 20μg retroviral plasmid DNA, 15μg helper plasmid DNA and 62.5μl $CaCl_2$

Table 2.72: Materials Used-retroviral Transduction

Retroviral Transduction- Materials Used
Phoenix cells (low passage)
Primary lymphoma cells
NIH 3T3
MEF
B-cell medium
Feeder layer
PBS
Retroviral plasmid DNA
Ecotropic plasmid helper DNA
H_2O
$CaCl_2$
HBS
Glass pasteur pipettes
Chloroquine
Polybrene
Puromycin
Blasticidin
Hygromycin
FLOW equipment

were mixed and adjusted with sterile water to 500μl. 500μl of HBS was added dropwise under constant agitation (air bubbles). Precipitate became visible within 5 minutes at RT. Meanwhile, old medium of Phoenix cells was exchanged for 9 ml of conditioned B-cell medium containing 25 mM Chloroquine and the precipitate (1 ml) was added dropwise. Cells were cultured under the standard conditions (37^{O}C, 21% O_2, 5% CO_2, 95% humidity).

Retroviral transduction

12 hours post phoenix cells transfection medium including the precipitate was removed. Cells were washed carefully with 1x PBS and 3 ml of conditioned B cell medium or a fresh DMEM (depending on the desired cell type to be transduced) was added to collect the first virus supernatant in the next 24 hours, post collection virus supernatant was filtered through a 0.45 μm filter. Adherent cells:

Media was removed from the plate. Cells were washed with PBS, and covered with 3 ml of the medium containing virus supernatant including polybrene.

Cells grown in suspension:

Viable and well growing cell population was pelleted by centrifugation (1200 rpm, 5 min, RT) and resuspended in the virus supernatant including polybrene.

New medium (3 ml) was added to the Phoenix cells for the next round of transduction. After 8-12 hours of incubation, the second virus supernatant was harvested and added according to the upper mentioned procedure to the adherent or lymphoma culture with the first supernatant.

Cells were then spinoculated (1500 rpm, 10 min, 32^{O}) and grown for the next 8-12 hours. New medium (3 ml) was added to the Phoenix cells for the next round of transduction.

The third and forth virus supernatant was collected after 8-12 hours, and proceeded according to the first two prior described rounds of transduction.

12 hours post last transduction, medium was removed from the cells, and replaced with the new conditioned B-cell medium or DMEM, according to the cell type.

Cells were grown for an additional 24 hours in order to express the gene of interest. For cells transduced with GFP (green fluorescent protein)-plasmids, percentage of positive cells was determined by Flow cytometry, while for cells transduced with an antibiotic marker (puromycin, hygromycin or blasticidin), the cell population was selected with puromycin or blasticidin (for 3-4 days) and hygromycin (5 days) until non-transduced cells were no more viable.

2.2.10 RNA

Isolation

For RT-PCR:

Total RNA from the mouse lymph nodes was isolated with TRIZOL (Invitrogen) according to the manufacturers protocol. 10^6 cells were pelleted by centrifugation in centrifuge at 12,000g, 10 minutes at 4^OC. It was followed by lysing in 1 ml of TRIZOL reagent. Upon adding of Trizol samples were incubated for 5 minutes (RT), which permited complete dissociation of nucleoprotein complexes. 200 μl of chloroform were added to each sample. tubes were shaken vigorously by hand for 15 seconds and incubated for 3 minutes (RT). Afterwards samples were centrifuged at 12,000 x g for 15 minutes at 4^OC. Following centrifugation, the mixture separated into a lower red, phenol-chloroform phase, an interphase, and a colorless upper aqueous phase. RNA remains exclusively in the aqueous phase.

Aqueous phase was transferred to a fresh tube, and RNA was precipitated by mixing with 500 μl of isopropyl alcohol. Samples were incubated at RT for 10 minutes and centrifuged at 12,000 x g for 10 minutes at 2 to 8^OC. Supernate was removed and RNA pellet was washed once with 1 ml of 75% ethanol. Sample was mixed by vortexing and centrifuged at 7,500 x g for 5 minutes at 4^OC. RNA pellet was briefly air-dried (5-10 minutes). RNA was dissolved in RNase-free water(DEPC-mqH_2O) and incubated for 10 minutes at 55^OC.

For microarray and semi-quantitative-RT-PCR:

Prior to lysing 5x10^6 cells were washed once in PBS, then lysed in 2 ml of RLT buffer, and immediately homogenized by passing 10 times through 18 gauge needle with syringe. 2ml of 70% ethanol was added and mixed thoroughly.Samples were transfered to RNeasy Midi column in 15ml tube, and centrifuged at 3000 x g for 5 minutes; flow-through was discarded and 4ml of buffer RW1 was added onto the column. Columns were centrifuged at 3000 x g for 5 minutes; flow-through was discarded, 10 μl of DNAse I stock solution together with 70 μl of RDD buffer was added to the membrane, and incubated at RT for 15 minutes, 800 μl of the buffer RW1 was added and columns were eluted by centrifuging at 300 x g for 5 minutes, afterwards flow-through was discarded. Following this, 2.5ml of buffer RPE was added onto the column, and centrifuged at 3000 x g for 2 minutes; flow-through was discarded. Again, 2.5ml of buffer RPE was added,and samples were centrifuged at 3000 x g for 5 minutes; flow-through was discarded. RNeasy Midi column was transferred to clean 15ml tube, and 150 μl of RNAse free H_20 was added, and incubated for 1 minute at RT. RNA was eluted by

centrifuging at 3000 x g for 3 minutes. At the end 260/280 O.D was measured. And 1 μg of the samples was run on the denaturising gel to visualise RNA 28 S and 18 S bands, while 5S band was not visible due to the Rneasy column cleanup.

2 μl of the total RNA was used for the cDNA synthesis.

cDNA synthesis

Table 2.73: Materials Used-cDNA synthesis

cDNA synthesis- Materials Used
RNA extracted from lymphoma or spleenic B-cells
Random hexamere (500 ng)
DEPC-mqH_2O
5x first strand buffer
0.1 M DTT dNTP mix (10 mM each)
1 U RNasin (RNAse inhibitor enzyme)
200 U Superscript Reverse Transcriptase II [SSRT-II]

2 μg of RNA and 1μl of random hexamere primer were mixed and volume was adjusted to 10 μl with DEPC H_2O. In order to destroy secondary RNA structures samples were incubated for 10 minutes at 70^OC, and subsequently stored on 4 ^OC. For each sample following cDNA synthesis mix was prepared: 4 μl of the first strand buffer, 1μl of DTT, 1.5μl of dNTP and 1.5μl of RNAsin. Mix was added to each sample and incubated for two minutes on 42 ^OC, and then 2 μl of SSRT-II was added to each sample and incubated for further 58 minutes. Reaction was stopped by incubating samples on 70 ^OC for 15 minutes; samples were stored at 4 ^OC for the short term storage (up to one day) or -20 ^OC for the long term storage.

2.2.11 Short Term (24 hours) Cytotoxicity Assay

Table 2.74: Materials Used-cytotoxicity Assay

Short term cytotoxicity assay- Materials Used
Lymphoma cells
Adriamycin
Trypan blue solution (diluted in PBS)
Neubauer counting chamber

Eμ-myc; Eμ-myc, Suv39h1$^{-/-}$ and Eμ-myc p53 $^{-/-}$ cells were seeded onto feeder layers at a density of 250 000 cells/ cm^2. 12 hours later cells were exposed to 0, 0.001, 0.005, 0.01, 0.05 and 0.1μg/ml adriamycin (ADR), and after 24 hours percentage of surviving cells was generated using trypan blue dye exclusion method (at least 200 cells, both dead and alive) were counted per each sample.

2.2.12 TGFβ ELISA

Table 2.75: Materials Used-TGF β ELISA

TGF β ELISA- Materials Used
Lymphoma cells
PBS
Quantikine commercial TGFβ ELISA kit

Eμ-myc and Eμ-myc, Suv39h1$^{-/-}$ cells were seeded onto feeder layers at a density of 250 000 cells/ cm2 for 5 days. Supernatant was collected and processed according to the manufacturers (Quantikine) instructions. Eμ-myc and Eμ-myc, Suv39h1$^{-/-}$ lymph nodes were resected, weighed, placed in 200 μl PBS and the tissue was disrupted by ultrasonic homogenisator. Supernatant was collected and processed according to the manufacturers (Quantikine) instructions.

2.2.13 TGFβ treatment

Table 2.76: Materials Used-TGFβ treatment

TGFβ treatment- Materials Used
Lymphoma cells
TGFβ-1
Trypan blue solution (diluted in PBS)
Neubauer counting chamber

Lyophilized purified human TGFβ-1 was prepared according to manufacturers instructions. Eμ-myc and Eμ-myc, Suv39h1$^{-/-}$ cells were seeded onto feeder layers at a density of 250 000 cells/ cm2. One day later cells were exposed for 24 hours (for the RNA isolation), or alternatively for 5 days to 0, 10, 100 and 1000 pM TGFβ Post treatment percentage of surviving cells was generated using trypan blue dye exclusion method (at least 200 cells, both dead and alive) were counted per each sample. Eμ-myc/bcl2; Eμ-myc, Suv39h1$^{-/-}$/bcl2; Eμ-myc, p53 $^{-/-}$/bcl2 and Eμ-myc, Arf$^{-/-}$/bcl2 cells were seeded onto feeder layers at a density of 250 000 cells/ cm^2. One day later cells were exposed for 5 days to 0, 10, 100 and 1000 pM TGFβ. Post treatment percentage of surviving cells was generated using trypan blue dye exclusion method (at least 200 cells, both dead and alive) were counted per each sample. Wild type and Suv39h1 mouse embryo fibroblasts were stably retrovirally transduced with pBabe-MycER-puro plasmid and selected for the puromycin resistant clones. Post selection cells were treated with 100 pM TGFβ.

2.2.14 Trypan blue dye exclusion method

Cell viability estimates were obtained by briefly mixing lymphoma cells with trypan-blue dye (30μl of lymphoma cell suspension with 30μl of trypan-blue reagent) and placed on Neubauer hemacytometer, observed under the

Table 2.77: Materials Used-dye exclusion method

Trypan blue dye exclusion method- Materials Used
Lymphoma cells
Trypan blue solution (diluted in PBS)
Neubauer counting chamber

microscope and counted. Counting for each lymphoma population was done in triplicate.

2.2.15 Western blot

Preparation of SDS-PAGE gel: glass plates were cleaned well with ethanol before they were set in the casting apparatus.

Gel mixture was vortexed and casted between the fixed and closed glass plates. 2-propanol was added on top of the casted gel in order to prevent evaporation. Upon polimerization 2-propanol was removed from the gel.

Mixture was vortexed and casted between the fixed and closed glass plates, on top of the separating gel, comb was inserted. After polymerization comb was removed, slots were rinsed with mqH_2O and the gel was inserted into the gel running apparatus.

Protein isolation (whole cell protein extracts): cells were once washed in 1x PBS and centrifuged at 1200 rpm for 5 minutes (RT). Cell pellet was resuspend in protein lysis buffer (vol=3x volume of cell pellet) and incubated 40 minutes on ice. To separate cell debris from proteins, lysates were centrifuged (14.000 rpm, 20 minutes, 4^OC) and supernatant containing the proteins was transferred to a new tube. Protein concentration was determined by a standard Bradford assay and aliquots were kept at -80^OC for the long term storage. Protein measurement (Bradford«s protein micro-assay). A ready-to-use Bradford solution was prepared by diluting Bradford reagent 1:4 with H_2O using 1 ml per cuvette and sample. A BSA standard curve was set up in the following concentrations: no BSA, 1, 2, 4, 6, 8 and 10 mg BSA including each 1 μl of the protein lysate (corresponding to the volume of the protein lysate that is measured afterwards). To create a standard curve, the absorbance of the individual BSA-samples were determined in a photometer at a wavelength of 595 nm against the mock control. Standard curve appeared in a linear regression (R2 values close to 1.0). For the individual protein lysates, each 1 ml was pipetted to 1 ml of the pre-diluted Bradford solution and measured in accordance to the standard curve. Preparation of the protein samples: protein samples were thawed on ice. Volume for the desired protein concentration was calculated and the respective amount of

Table 2.78: Materials Used-Western blot

Western blot- Materials Used
Lymphoma cells
MEFs
Protease inhibitors
Protein lysis buffer
RotiQuant
BSA
Tris-HCl [pH 6.7]
Tris-HCl [pH 8.8]
Acrylamide-bis
SDS
TEMED
2-propanol
Methanol
Running buffer
Roti-prestained marker
Hybond ECL
Whatman paper
TBS-T
Blocking solution
Primary antibodies
Secondary antibodies
Supersignal West pico
Kodak X-O-mat films LS

loading buffer (sample buffer) was added before the samples were boiled for 10 minutes at 95^{O}C. Running the gel: gel apparatus was filled with 1x running buffer. 100 μg of boiled protein samples were loaded into the slots using 15μl of a molecular weight standard (Rotimark Prestained) as a marker. Gel was started at a voltage of 60 V until dye front reached the front of the separating gel. Gel was run at a voltage of 150 V until dye front was close to the bottom. After disassembling the gel apparatus, stacking gel was carefully removed and separating gel was immediately used for further blotting. Semi-dry blotting procedure: a Hybond ECL blot membrane and six pieces of Whatman paper were cut in the size of the gel and semi-dry blotting chamber was cleaned. Membrane was activated with methanol for a few seconds, rinsed with H_2O and soaked in transfer buffer. A semi-dry blotting "sandwich" was set up in the following order: 3 Whatman papers, Activated blot membrane, Gel, 3 Whatman papers. Air bubbles were removed and the "sandwich" was

Table 2.79: Materials Used-separating gel

Separating- Materials Used
mqH_2O
30% Acrylamide
Tris pH 8,8
SDS
APS
TEMED

Table 2.80: Materials Used-stacking gel

Separating- Materials Used
mqH_2O
30% Acrylamide
Tris pH 6,7
SDS
APS
TEMED

blotted for 60-180 minutes and 0.8 mA each cm^2 gel. Afterwards, blotting apparatus was disassembled membrane was labelled. Antibody incubation: labelled membrane was blocked for 30 minutes at RT in blocking solution under gentle agitation. Meanwhile, the first antibody was diluted in an appropriate concentration. Membrane was incubated either 4 hours (RT) or over night (4^OC) under gentle agitation. Afterwards, membrane was washed 3x 5 minutes in washing buffer. Subsequently, membrane was incubated for 60 minutes in the corresponding secondary antibody (RT) under gentle agitation followed by three washing steps (3 x 15 minutes). Two components of the ECL detection kit were diluted 1:1 in the dark and transferred onto the wet membrane. After 5 minutes, membrane was wrapped in a transparent cover and put into a cassette. Membrane was exposed to an X-O-Mat LS film for 5-30 minutes, depending on the individual antibodies and the amount of protein.

Chapter 3

Results

3.1 Tumor development

3.1.1 Animal models used and main breeding setting

To assess the role of Suv39h1 in Myc-driven lymphomagenesis male Eμ-myc mice were bred to female Suv39h1 $^{+/-}$ and Suv39h1$^{-/-}$ mice (Figure 3.1). Both of the mouse strains were bred in a C57BL/6 background. Approximately 3 weeks after birth offspring was separated and genotyped using standard protocol procedures described in the method section. Since Suv39h1 locus is X-linked, Suv39h1 heterozygous mice can only be Suv39h1$^{+/-}$ female mice. Mice deficient for a functional Suv39h1 can be Suv39h1 $^{-/y}$ (male) or Suv39h1 $^{-/-}$ (female). Cohorts of mice were monitored for tumors every three days by palpation of the peripheral lymph nodes, starting at approximately three weeks post birth. Also, animals were observed for any sign of sickness, like severe weight loss and hyperventilation. When scored as palpable (P) or well palpable (PP) in two consecutive times animal was sacrificed and lymph nodes, spleen, liver and thymus were extracted. Cells from lymph nodes and spleen were isolated as described in the method section. From each animal one lymph node was fixed in the 4% formaldehyde for immunohistochemistry assays on paraffin embedded sections, and one lymph node was immediately frozen in liquid nitrogen for subsequent enzymatic assays. Other isolated organs were fixed in 4% formaldehyde. Isolated lymphoma cells, as well as the lymph nodes were used for all the subsequent experiments. All of the animal experiments described in this thesis were in accordance with animal welfare protocols.

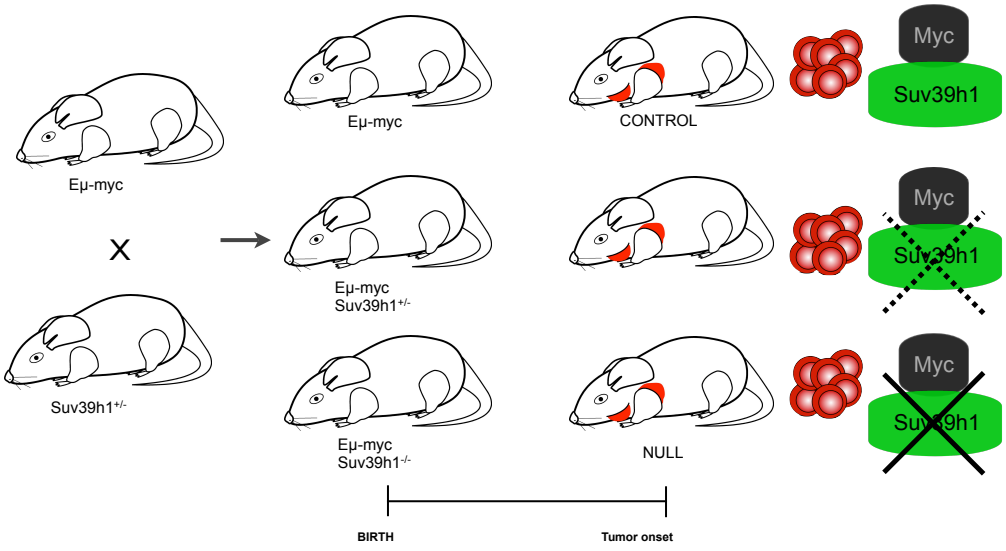

Figure 3.1: Breeding outline. Eμ-myc mice were bred to mice bearing targeted genetic lesions in the Suv39h1 locus. Mice were monitored for tumor latencies by palpation of peripheral lymph nodes every 3 days. When animal developed a tumor (depicted as pre scapular and cervical lymph node in red) scored palpable (P) or well palpable (PP) in two consecutive palpations (3 days apart each) it was sacrificed and lymphoma cells were isolated and used in subsequent experiments.

3.1.2 Phenotypic characteristics of Myc-driven lymphomas with different Suv39h1 status

Histology and hematology of Myc-driven lymphomas

Histological examinations at terminal stages of disease in both Suv39h1 proficient and deficient Eμ-myc animals showed lymphoma exhibiting the same grade of aggressiveness. Hematoxylin and eosin (HE) staining in lymphoid as well as non-lymphoid organs revealed that in both cohorts dissemination of lymphoma is not overtly different (Figure 3.2: done in collaboration with C. Loddenkemper *et al*).

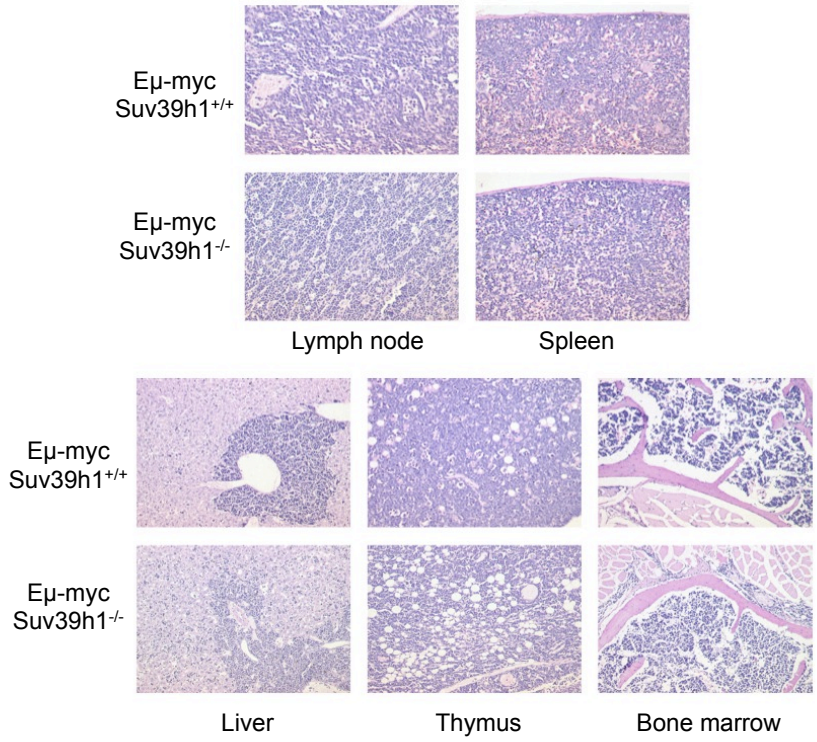

Figure 3.2: Histopathology of Myc- driven lymphomas does not differ between Suv39h1 proficient and deficient lymphomas. Hematoxylin and eosin (HE) staining of representative organs affected by Myc-driven lymphoma revealed no overt differences in lymphoma infiltration rates between Suv39h1 proficient and deficient animals (n=3 for each genotype done in collaboration with C. Loddenkemper *et al*).

Further hematological examination, by testing blood smears of mice at the stage of terminal disease revealed lymphatic cell infiltration, occuring

frequently in Myc overexpressing lymphomas, with equal distribution in both genotypes (Figure 3.3).

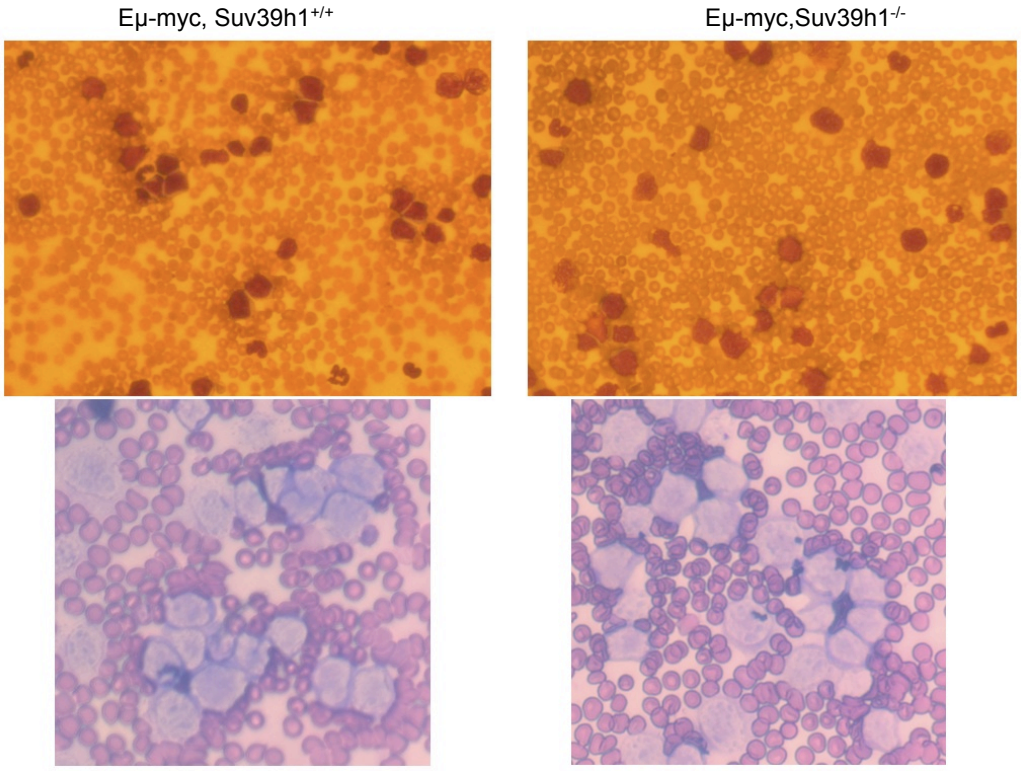

Figure 3.3: Mice of both genotypes show equal extent of immature lymphoblast cell infiltration. Peripheral blood samples obtained from both Suv39h1 proficient and deficient animals were stained according to Wright's staining protocol. Staining revealed drastic increase in the immature lymphoblastic cell population (dark purple cells) in both genotypes (note: in healthy mice number of lymphoblastic cells per vision field should not exceed 1). Inlay: magnified image of blood smear (lymphoblastic cell population is belonging to larger and light blue cells).

Concluding from the histological and hematological examinations no overt differences were found in the lymphoid infiltrations of Eμ-myc tumor bearing animals in Suv39h1 proficient and deficient lymphomas, indicating similar phenotype of invasiveness.

Immunophenotypical characteristics of Myc-driven lymphomas

Myc transgenic animals develop B-cell lymphomas without any differentiation block, therefore in order to test for the lineage comitment as well as for the differentiation status in lymphomas deficient for Suv39h1 gene freshly prepared single cell suspensions from lymph node tissues were stained for B cell immunological markers (CD45R [B220] surface IgM [sIgM] and CD19), as well as for a T-cell marker (CD90.2 [Thy1.2]) and a marker for myeloid cells (CD11b [Mac-1]). Wild-type lymph node, thymus, spleen and periferal blood were used as controls for B-cell, T-cell, B- and T-cell mixed population and myeloid marker respectively. Viable fraction of lymphoma cells could be diferentiated from dead cells and cellular debris having lower forward/ side scatter parameters, on the basis of foward/ side scatter analysis viable population of lymphoma cells was further plotted in a dot-plot according to the parameters set by controls (Figure 3.4 shows representative pictures, experiment was conducted on 10 different lymphomas from each genotype).

Analysis revealed that both groups are commited to the B cell lineage (as seen by positivity for B-cell markers CD45R and CD19, and negativity for the T-cell marker CD 90.2). Further by assesing differentiation attributes it is shown that lymphomas of both backgrounds are equally distributed between pre-B cell (early; sIgM negative) and immature- B cells (late; sIgM positive) B cell lymphomas (Eμ-myc were 45,45% sIgM positive; Eμ-myc Suv39h1$^{-/-}$ were 40% sIgM positive). Only one Eμ-myc lymphoma case had both sIgM positive and sIgM negative B-cells. Additionally, lymphomas tested using a myeloid marker (CD11b) show indistinguishable phenotype in both genotypes (<5% CD11b positive cells in both of the genotypes).

Results shown above confirm that there are no immunophenotypical difference in the two tested genotypes. They are belonging to B-cell lymphomas with no visible maturation defect.

Level of c-Myc expression in Myc-driven lymphomagenesis

The expression of c-Myc, as well as Myc's target CDK4 was tested in cells extracted from lymph nodes of animals at terminal stages of disease. Proteins extracted from the whole cell lysates of lymph nodes (4 different animals each genotype) were tested in a Western blot analysis for c-Myc and CDK4 expression levels (Figure 3.5).

Results show that loss of Suv39h1 does not alter level of Myc expression, nor it blocks Myc-induced signaling as seen by no impact on the expression of Myc's target CDK4.

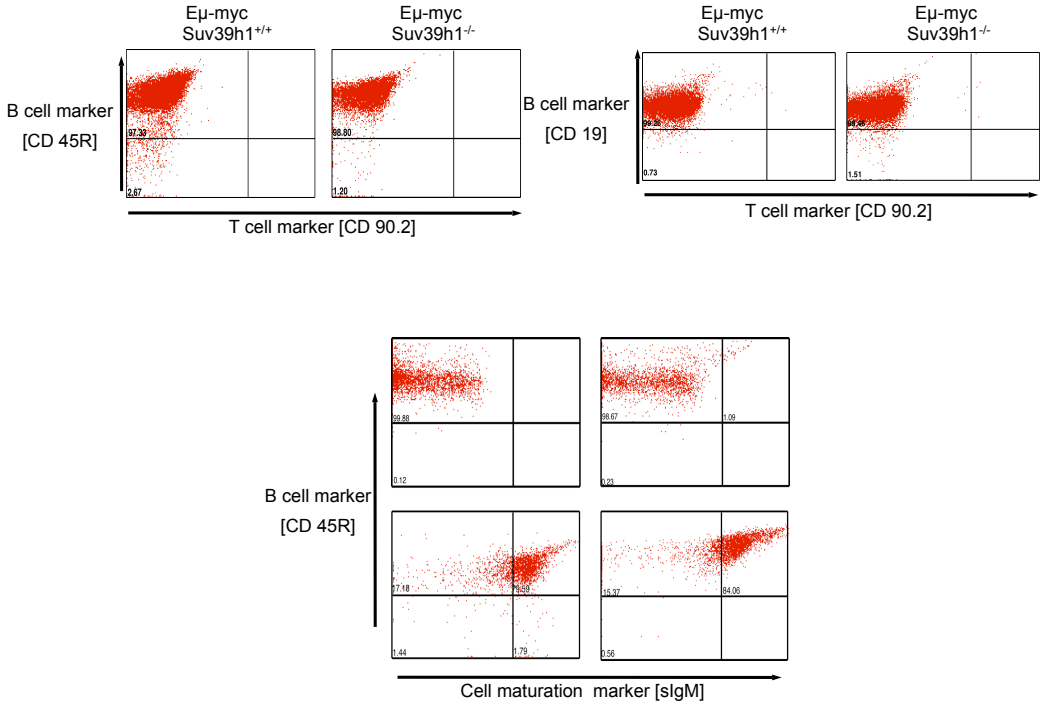

Figure 3.4: Suv39h1 proficient and deficient Myc-driven lymphomas display similar immunological phenotype. Immunophenotypic analysis of lymphoma cells extracted from lymph nodes of animals belonging to Eμ-myc and Eμ-myc, Suv39h1$^{-/-}$ or$^{-/y}$ revealed no overt differences. Two-color flow cytometry of lymphoma populations for B-cell markers (CD45R-PE [Phycoerythrin excitation laser 488nm, peak emission 575 nm, detected in FL2 channel] and CD19-PE) and T-cell marker (CD90.2-FITC [Fluorescein-Isothiocyanat-excitation laser 488nm, peak emission 518 nm, detected in FL1 channel]) revealed that both lymphoma groups are committed to the B-cell lineage. Two-color flow cytometry of lymphoma populations for B-cell marker (CD45R-PE) and a B-cell differentiation marker (sIgM-FITC) revealed that both of the lymphoma groups belong to the same stages of B-cell development. Flow cytometry for the myeloid marker (CD11b) revealed similar distribution in both lymphoma genotypes [Wild-type thymus was used as a positive control for the CD90.2 staining, wild-type lymph nodes were used as a positive control for the CD45R and CD19 stainings, wild-type spleen was used as a positive control for both CD90 and CD45R staining and peripheral blood from wild-type mice was used as a positive marker for CD11b staining].

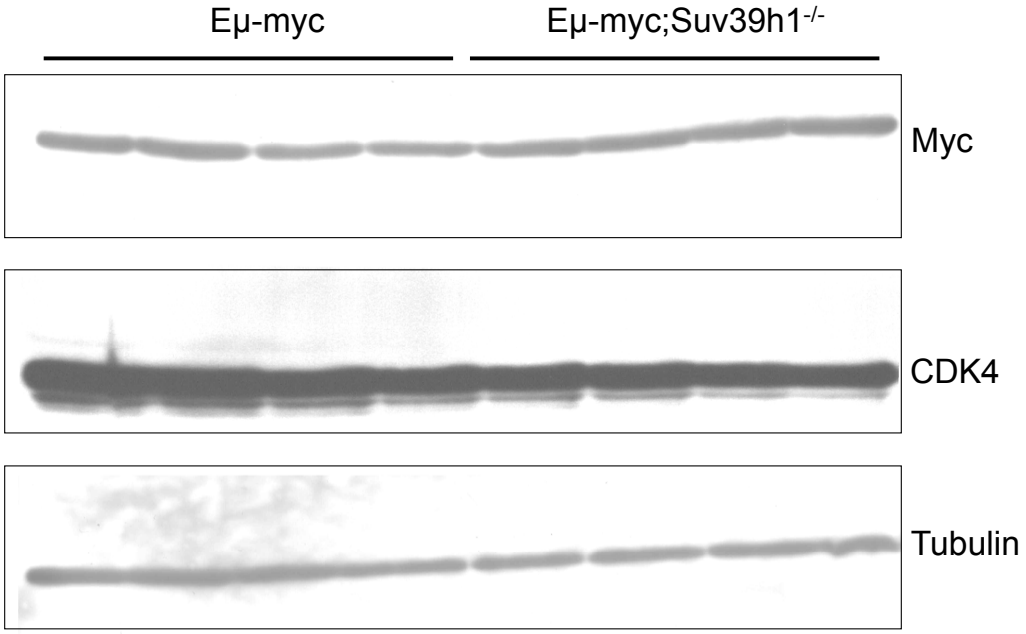

Figure 3.5: Myc is equally expressed in lymphoma belonging to both Suv-39h1 proficient and deficient group of Eμ-myc transgenic mice. Western blot analysis of lymphoma cells extracted from lymph nodes of animals with intact and disrupted Suv39h1 gene. TOP: c-Myc expression, MIDDLE: CDK4 expression and BOTTOM: Tubulin expression (used as a loading control) in Eμ-myc (n=4) and Eμ-myc, Suv39h1$^{-/-}$ (n=4).

Impact of Suv39h1 loss on Myc-driven lymphomagenesis

The offspring from cross of Eμ-myc and Suv39h1 knock-out mice was monitored for tumor latencies. As shown in here, Suv39h1 loss has a significant impact on acceleration of the Myc-driven lymphomagenesis.

Eμ-myc mice, with no additional targeted genetic lesions (referred to as controls, n=93) succumbed to lymphoma with a median age of 144 days, while mice lacking one (Eμ-myc, Suv39h1$^{+/-}$; n=41) or both Suv39h1 alleles (Eμ-myc, Suv39h1$^{-/-}$; n=31) developed lymphomas at a median age of 54 and 57 days respectively (P <0,0001). Interestingly, lymphomas developing in Eμ-myc, Suv39h1$^{+/-}$ and Eμ-myc, Suv39h1$^{-/-}$ animals share virtually indistinguishable tumor latencies (P=0,4634). Kaplan-Meier "Time-to-tumor-onset" latencies plot is shown in figure 3.6.

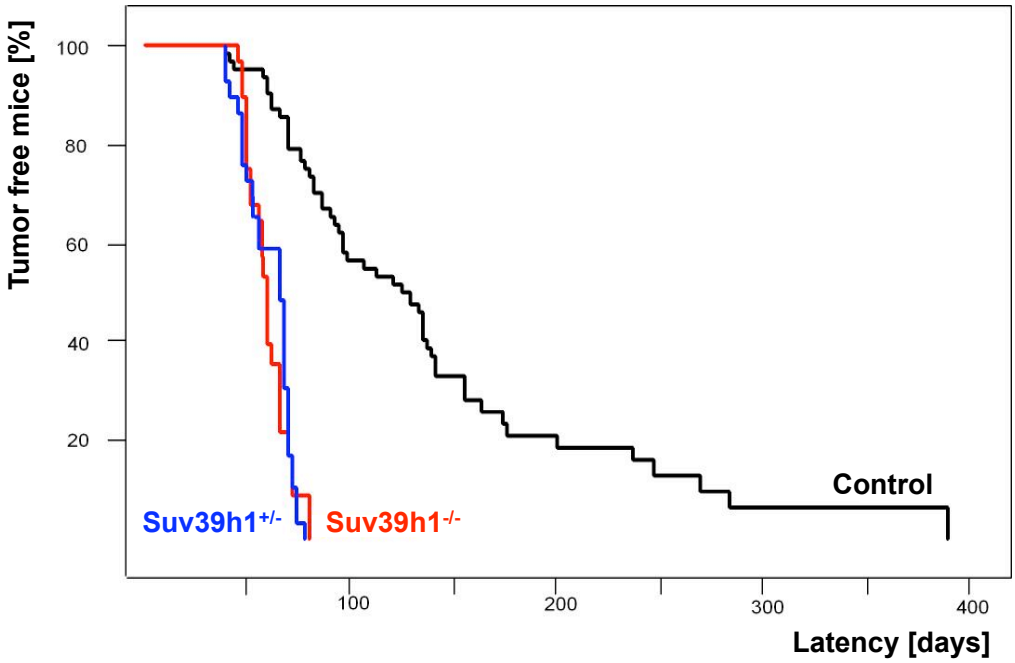

Figure 3.6: Defects in Suv39h1 accelerate Myc-lymphomagenesis. Kaplan--Meier "Time-to-tumor-onset" latencies of Eμ-myc (n=93, black line); Eμ--myc, Suv39h1 $^{-/-}$ (Suv39h1 $^{-/-}$ and $^{-/y}$, n=31; red line); Eμ-myc, Suv39h1 $^{+/-}$ (n=41, blue line).

Results shown here reveal that loss of gene implicated in epigenetic silencing, and mediating Ras-induced senescence provides growth advantages

for lymphomas arising in environment with overexpressed Myc. As Myc is primarily utilizing apoptosis as a program to terminate malignant cell outgrowth, this finding provided an interesting addition to the network of Myc's action. Results of *in vivo* Myc lymphomagenesis shown in here had 2 major points: Suv39h1 plays an important role in Myc-driven lymphoma formation; additionally lymphomas arising in Suv39h1$^{+/-}$ background follow the same latency pattern as Suv39h1$^{-/-}$ lymphomas, and both of the findings provided to be of importance for the further research.

In Suv39h1$^{+/-}$ setting Myc-lymphomas are composed of cells which have randomly inactivated intact Suv39h1

Parallel to the observation that Suv39h1 deficiency accelerates Myc driven lymphoma formation, it was also found that Suv39h1$^{-/-}$ and Suv 39h1$^{+/-}$ animals share identical tumor latency (Figure 3.6). This finding could be explained through deregulation in several mechanisms: either intact Suv39h1 is necessary for full Suv39h1 function, similar to many haploinsufficiency models. However the important difference in this model is that one of Suv39h1 alleles will be inactivated via random X-chromosomal inactivation, normally occuring in cells. In this respect it is only possible that Myc expressing cells acquire additional growth advantages when Suv39h1 is absent. Hence, when Myc is overexpressed in cells which have inactivated allele with the intact Suv39h1 they will accumulate faster than cells still containing intact Suv39h1, as seen in tumors developed in Suv39h1$^{+/-}$ mice. In order to test this hypothesis Suv39h1 mRNA expression levels of Suv39h1$^{+/+}$, Suv39h1$^{+/-}$ and Suv39h1 $^{-/-}$ lymphomas were evaluated by an RT-PCR approach. In all of the tested cases (5/5 for Suv39h1$^{+/-}$) there was no detectable Suv39h1 transcript, showing invariable loss of the Suv39h1 expression occuring in Eμ-myc Suv39h1$^{+/-}$ lymphomas (Figure 3.7).

Loss of Suv39h1 in a course of Myc-driven lymphomagenesis provides growth advantage for tumor cells, as seen by shortened tumor latencies in figure 3.6. Additionally, as shown in figure 3.6 and figure 3.7 favourable environment for the faster development of Myc-driven lymphoma will be one without expression of Suv39h1, directly pointing out to an *in vivo* tumor suppressive role of Suv39h1.

Proliferation of cells in Myc-driven lymphomagenesis

In accordance with results shown previously revealing the tumor suppressive potential of Suv39h1 (as seen by the shortened tumor latencies when Suv39h1 is disrupted), the contribution of Suv39h1 loss to proliferation rates was

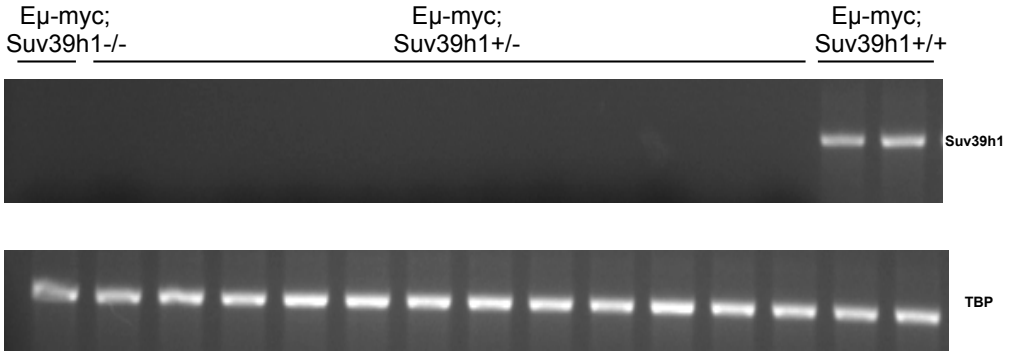

Figure 3.7: Myc-driven lymphomas develop in a setting where remaining Suv39h1 allele was inactivated via random X-chromosomal inactivation. RT-PCR analysis. TOP: Suv39h1 mRNA status in Myc driven lymphomas was assessed in Suv39h1$^{-/-}$ (n=1); Suv39h1$^{+/-}$ (n=5); Suv39h1$^{+/+}$ (n=2). BOTTOM: TBP (TATA-box binding protein) mRNA status was used as a loading control.

tested.

For that purpose the cell cycle marker Ki67 *in situ* (Ki67 antigen is a cell cycle related nuclear protein expressed by proliferating cells in all phases of the active cell cycle [S, G2, M, G1]; done in collaboration with C. Lodenkemper *et al*) was employed on lymph nodes from manifest lymphomas. This staining was also employed on a single cell lymphoma population by immunofluorescence and flow cytometric analysis (as a negative control in the flow-cytometry assay G1 arrested NIH 3T3 cells were used, figure 3.8).

As shown by the staining there is a larger fraction of Ki67 positive cells in Eμ-myc, Suv39h1$^{-/-}$ lymphomas (89,4 $\pm$ 5,2%) when compared to the Eμ-myc lymphomas (76,4 $\pm$ 7,7%; P=0,0096). Difference observed here could provide an explanation to shortened tumor latencies found in mice bearing defects in Suv39h1 gene. Maintaining approximately 15% more of cells actively participating in the cell cycle would ensure Suv39h1 deficient animals develop tumors significantly faster then Suv39h1 proficient animals.

Approach alternative to Ki67 *in situ* staining is incorporation of 5-bromo-2'- deoxyuridine (BrdU a synthetic thymidine analogue that incorporates into the newly synthesised DNA strands of actively proliferating cells) in tumor bearing mice. BrdU was used together with 5-fluoro1H-pyrimidine-2,4-dione (FU, blocker of thymidine synthase) incorporation *in vivo* protocol (for more detail please see method section 2.2.3) in order to analyze the proliferative capacity of lymphoma cells. Lymphoma bearing mice of Suv39h1 proficient

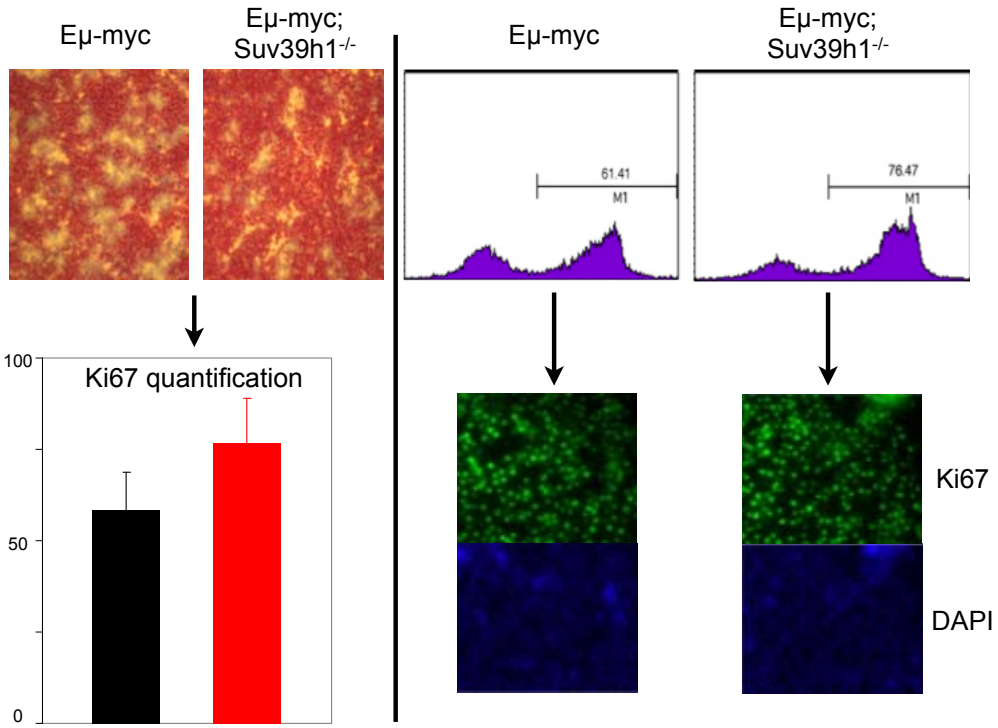

Figure 3.8: Suv39h1 $^{-/-}$ lymphomas display more cells in cycle. LEFT: Assesment (done in collaboration with C. Lodenkemper *et al*) and quantification of Ki67 stainings *in situ* in Eμ-myc (n=9), Eμ-myc Suv39h1$^{-/-}$ (n=7) lymphomas. RIGHT: Flow cytometric analysis based on Ki67 assessment in Eμ-myc (n=18) and Eμ-myc Suv39h1$^{-/-}$ (n=11), and subsequent immunofluorescent Ki67 analysis of lymphoma cells in Eμ-myc (n=18) and Eμ-myc Suv39h1$^{-/-}$ (n=11) [20 Gy γ-irradiated 3T3 cells were used as a Ki67-negative control for the flow cytometric analysis and immunofluorescence staining].

and deficient background were injected intraperitoneally with a single dose of BrdU/FU mixture and sacrificed after 24 hours. Lymph nodes and single cell extracts were subjected to further analysis. BrdU positivity was assesed in a whole lymphoma single cell suspension by flow cytometry analysis (Figure 3.9).

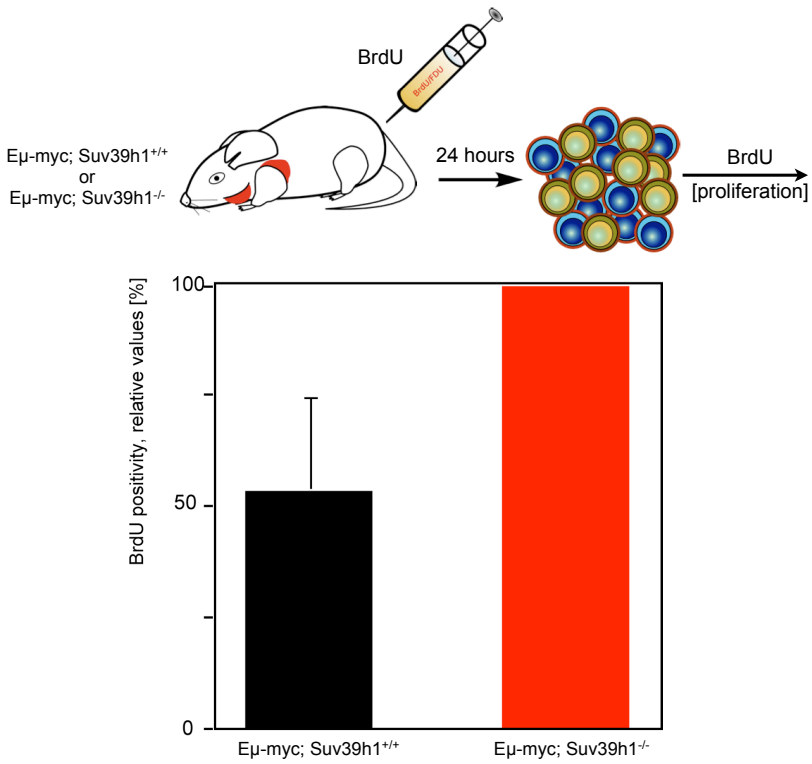

Figure 3.9: Suv39h1 deficient mice display more cells in cycle *in vivo*. TOP: Eμ-myc (n=3); Eμ-myc Suv39h1$^{-/-}$ (n=3) lymphoma bearing mice were injected intraperitonealy with 100 mg/kg of body weight BrdU and 10 mg/kg of body weight FU mixture and sacrificed after 24 hours. Lymphoma cells were isolated and subjected to the analysis of BrdU incorporation. BOTTOM: quantification of BrdU incorporation *in vivo* by flow cytometry analysis, plotted as relative to values for Suv39h1$^{-/-}$ lymphomas.

Results obtained here show that a higher fraction of Suv39h1 deficient cells incorporated BrdU when compared to control lymphomas. However 24 hour exposure to BrdU prevented us to interpret this result as a speed of the cell cycle assessment.

Further, the possibility of hyperproliferation as a cause of shortened latencies in Suv39h1 deficient Myc lymphomas was tested.

To determine the speed of cell cycle in both genotypes staining with a specific mitotic marker histone H3 phosphorylated on serine 10 residue (H3S10P) was used. Immunofluorescent staining *in situ* was done on the lymph node sections from Suv39h1 proficient and deficient lymphomas (n=3 for each; figure 3.10 upper panel done in collaboration with C. Lodenkemper *et al*). Although in the *in situ* staining there is apparently more cells staining positive for H3S10P marker in Suv39h1 deficient lymphomas, it was reasoned that this might be a consequence of the overal difference in number of cells in cycle between Suv39h1 deficient and control lymphomas.

To further investigate the possibility of a different cell cycle speed as a cause of difference observed in the overall number of cells in cycle a "mitotic trap" protocol using the drug Nocodazole (NOC) was employed. Nocodazole is a known anti-neoplastic agent, which exerts its effects by depolymerizing microtubules, therefore causing an arrest in mytosis [M] phase of the cell cycle (cells are arrested in prometaphase). Freshly explanted lymphoma cells were treated with NOC in the concentration 100 ng/ml of media for the period of 0, 3, 6 and 9 hours. Cells were collected at the indicated time periods, stained for the H3S10P and subjected to the flow cytometric analysis [here is shown 0-6 hours change] (Figure 3.10, bottom panel).

This result shows, that although initially there are more cells in cycle observed in Suv39h1 deficient lymphomas, cells from both genotypes are proliferating with the same average speed through the cell cycle *in vitro* (values for the "mitotic trap" experiment from figure 3.10 are for Eμ-myc 8,92 $\pm$ 6,04% and Eμ-myc, Suv39h1$^{-/-}$ 7,53 $\pm$ 4,19%; P=0,247).

To further test if the observation from the previous experiment could be explained on a molecular basis of possibly deregulated cyclin-CDK signaling, which would impair proliferative capacity of cells, protein levels of cyclin A, which is required for the S phase progression, and cyclin E, which is playing a role in G1/S transition were assessed by Western blot (Figure 3.11).

Differences observed on a molecular level with upregulated E2F target cyclin A and cdk2 binding partner cyclin E reflect the findings that Suv39h1 deficient lymphomas have more cells actively participating in the progression through the cell cycle, enabeling them to develop fully grown tumor with shorter onset latencies.

Impact of p53 loss on Suv39h1 status in Eμ-myc lymphomas

According to previously published research it is known that p53 has an important role in Eμ-myc lymphomagenesis *in vivo*, and that in the setting when Myc is overexpressed tumor cells are developing in an environment where expression of the remaining p53 wild-type allele in p53$^{+/-}$ setting is

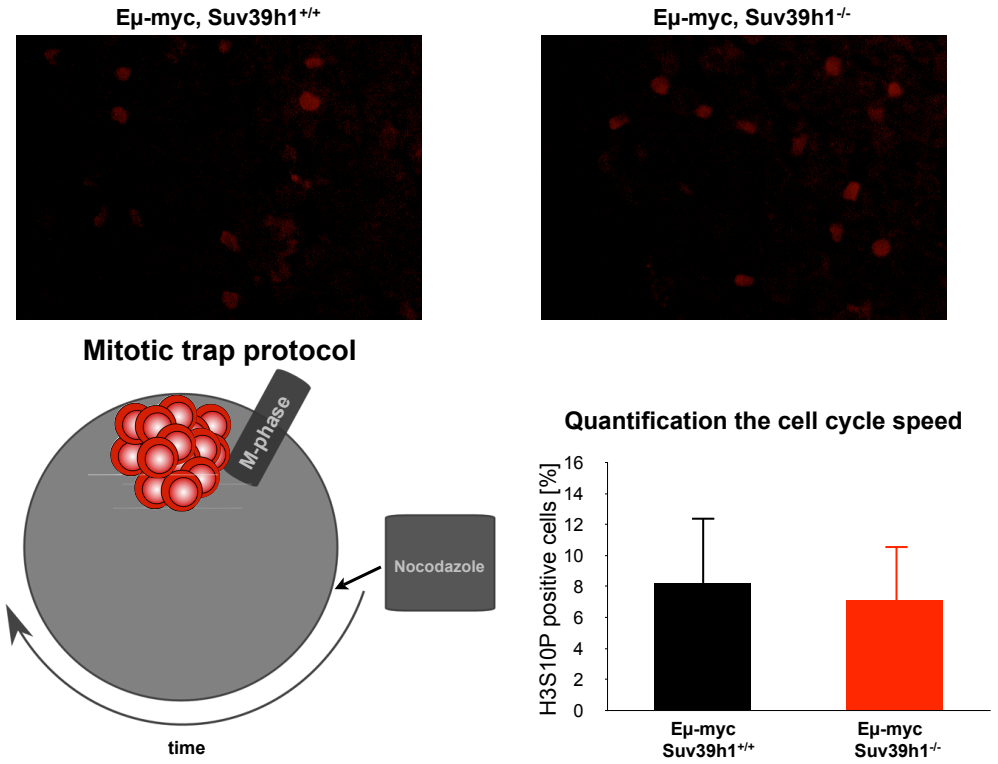

Figure 3.10: Histone H3 Serine 10 phosphorylation. TOP: Immunofluorescent histone H3 serine 10 phosphorylation (H3S10P) staining *in situ* on Eμ-myc (n=3) and Eμ-myc, Suv39h1$^{-/-}$ (n=3) lymphomas. BOTTOM. Left: Freshly explanted lymphoma cells were treated with Nocodazole (NOC) and tested for H3S10P in 3, 6 and 9 hours periods. Right: Histogram bar represents difference in Eμ-myc (black, n=6) and Eμ-myc, Suv39h1$^{-/-}$ (red; n=5) between time points 0 and 6 hours of NOC treatment.

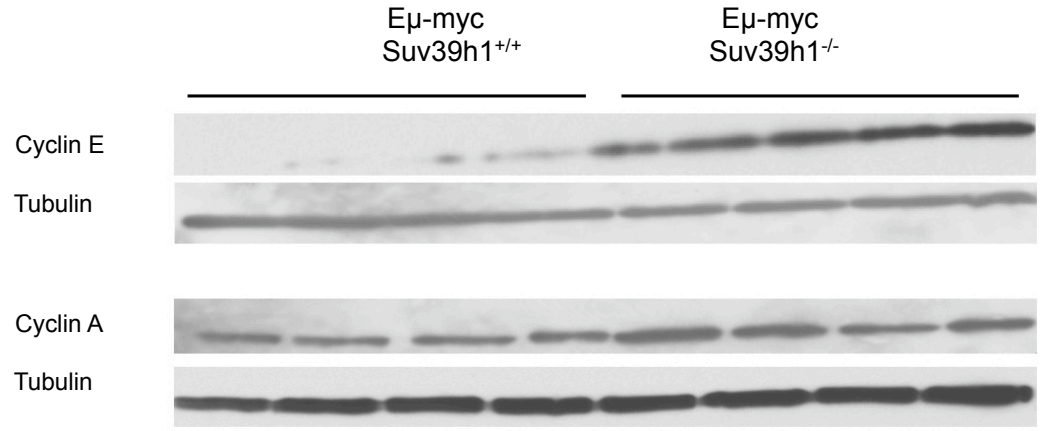

Figure 3.11: Suv39h1 deficient lymphomas show upregulation in cyclin E and A protein expression as seen by western blot analysis of lymphoma cells extracted from lymph nodes of animals with intact and disrupted Suv39h1. TOP: Cyclin E status with respective tubulin as a loading control. BOTTOM: Cyclin A status with respective tubulin as a loading control in Eμ-myc (n=4) and Eμ-myc, Suv39h1$^{-/-}$ (n=4).

lost. This is a consequence of the loss of heterozygosity (LOH), and results in the shortened tumor latencies.

Here was investigated whether loss of Suv39h1, as observed in Eμ-myc, Suv39h1$^{+/-}$ could potentially prevent p53$^{+/-}$ loss of heterozygosity. For this purpose Eμ-myc mice were crossed to Suv39h1$^{+/-}$, p53$^{+/-}$ mice. Mice were monitored for tumor latencies by palpation of peripheral lymph nodes every three days, and latencies were plotted as a Kaplan- Meier "Time-to-tumor onset" plot (Figure 3.12).

As expected, all of the animals succumbed to lymphoma, as seen in the tumor onset latencies plot. Time to tumor onset in Eμ-myc p53$^{+/-}$ Suv39h1 $^{+/-}$ (n=9) was 27 days and in Eμ-myc, p53$^{+/-}$, Suv39h1 $^{-/-}$ (n=5) was 32 days (when compared to either Eμ-myc, Suv39h1$^{+/-}$ or Eμ-myc, Suv39h1 $^{-/-}$; P <0,005).

Further, all lymphomas arising in p53 $^{+/-}$ background were tested for the potential loss of the remaining p53 allele (loss of heterozygosity), often observed in Eμ-myc p53$^{+/-}$ lymphoma setting. In addition loss of the Suv39h1 expression was tested in the same setting (Figure 3.13).

These results indicate that Myc tumors with disrupted Suv39h1 primarily select against the remaining p53 allele, as all of the p53$^{+/-}$ animals (9/9 cases tested) have lost their remaining wild-type allele. Concluding from

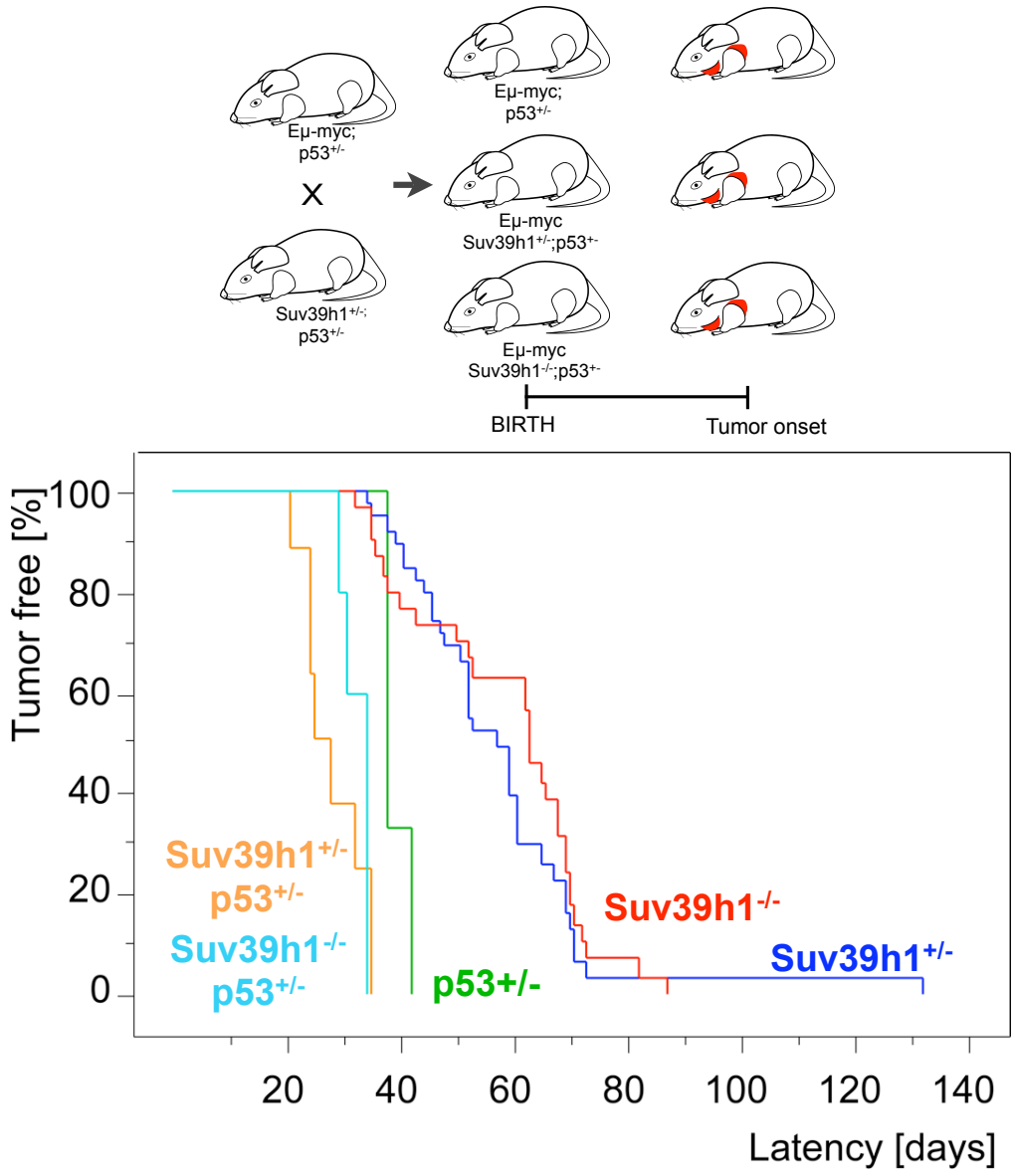

Figure 3.12: Defects in Suv39h1 and p53 accelerate Myc-driven lymphomagenesis: TOP: Breeding outline. Eμ-myc mice were crossed to mice bearing targeted genetic lesions in the Suv39h1 and the p53 locus. Tumor latencies were recorded and tumor cells were isolated and submitted to the analysis of p53 and Suv39h1 transcript. BOTTOM: Kaplan-Meier "Time-to-tumor-onset" latencies: Eμ-myc, Suv39h1$^{-/-}$ (n=31; red line); Eμ-myc, Suv39h1 $^{+/-}$ (n=41; blue line); Eμ-myc, p53$^{+/-}$ (n=3; green line); Eμ-myc, Suv39h1$^{+/-}$, p53 $^{+/-}$ (n=9; orange line); Eμ-myc, Suv39h1$^{-/-}$, p53 $^{+/-}$ (n=5; light blue line).

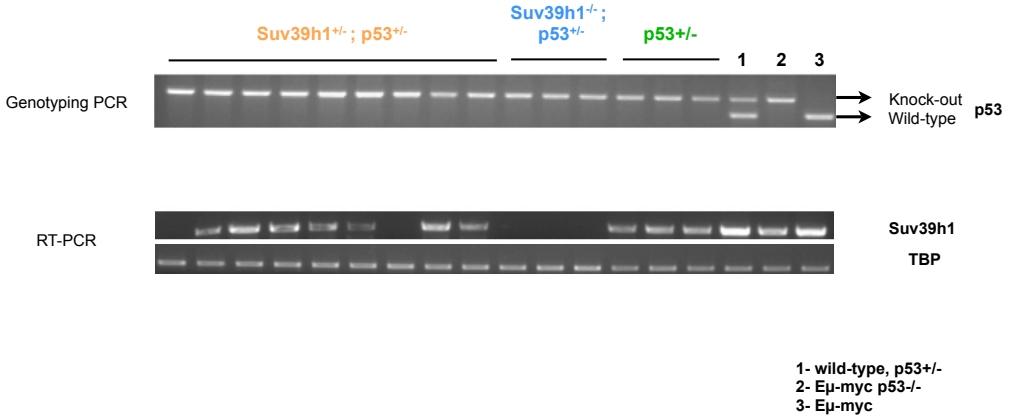

Figure 3.13: Lymphoma cells primarily select against p53 during Myc-lymphomagenesis. p53 status was tested in allele-specific PCR to detect mutant (upper band) or wild-type (lower band) p53 allele in Suv39h1$^{+/-}$, p53$^{+/-}$ lymphomas (n=9), Suv39h1$^{-/-}$, p53 $^{+/-}$ lymphomas (n=3), Suv39h1$^{+/+}$, p53$^{+/-}$ lymphomas (n=3); as a control p53$^{+/-}$ (1), p53$^{-/-}$ (2), Eμ-myc (3) and Eμ-myc, Suv39h1$^{+/-}$ (4) animals were used. In addition, Suv39h1 mRNA levels were tested for the lymphomas developed in the same animals, with TBP as a loading control.

these results p53 loss of heterozygosity is set as an early event in Myc driven lymphomagenesis, and it provides enough survival advantages to protect from further loss of Suv39h1 (observed in 7/9 cases tested). This results are well in line with p53's central role in apoptosis and senescence.

3.1.3 Defects of failsafe machinery in Suv39h1 deficient lymphomas

Impact of Suv39h1 loss on apoptotic machinery

Apoptosis is a hallmark of Myc-driven lymphomagenesis, and a significant proliferative advantage has been observed when tumors are deficient for p53, since deficiency in p53 is leaving them apoptotically incompetent. Therefore when it was revealed that Suv39h1 deficiency accelerates Myc-driven lymphomagenesis, as well as that Suv39h1 loss is dispensable in the p53 deficient setting, possible defects in apoptotic machinery of Suv39h1 deficient lymphomas were tested.

Spontaneous apoptosis rates of lymphomas arising in both Suv39h1 proficient and deficient animals were assessed. When observing Hematoxin and Eosin (HE) staining (done in collaboration with C. Loddenkemper *et al*) a "starry sky" phenotype becomes visible [macrophage infiltrations around apoptotic cells, which is a typical feature of human Burkitt's lymphomas]. In TUNEL staining *in situ* (terminal deoxynucleotidyl transferase dUTP nick end labeling; marking fragmented DNA typical for apoptotic cells) no overt differences in spontaneous apoptosis rates between two lymphoma groups were detected(Eμ-myc 11,168 $\pm$ 2,56%; Eμ-myc, Suv39h1$^{-/-}$ 13,863 $\pm$ 4,418%; P=0,2117; Figure 3.14).

Results in the figure 3.14 clearly show that there is no detectable difference in the spontaneous apoptosis rates as a response to Suv39h1 loss in Myc lymphoma model *in vivo*. Therefore differences in tumor latencies did not arise due to the defects in apoptosis.

This finding indicated a possibility of defects in senescence machinery in Suv39h1$^{-/-}$ lymphomas.

Impact of Suv39h1 loss on senescence machinery

Observation from previous experiments revealed that control lymphomas have overall less cells in cycle when compared to the Suv39h1 deficient lymphomas, however both genotypes share an almost identical speed of cell cycle.

To directly evaluate oncogene induced senescence as a potential mechanism contributing to the prolonged time of tumor formation in Eμ-myc

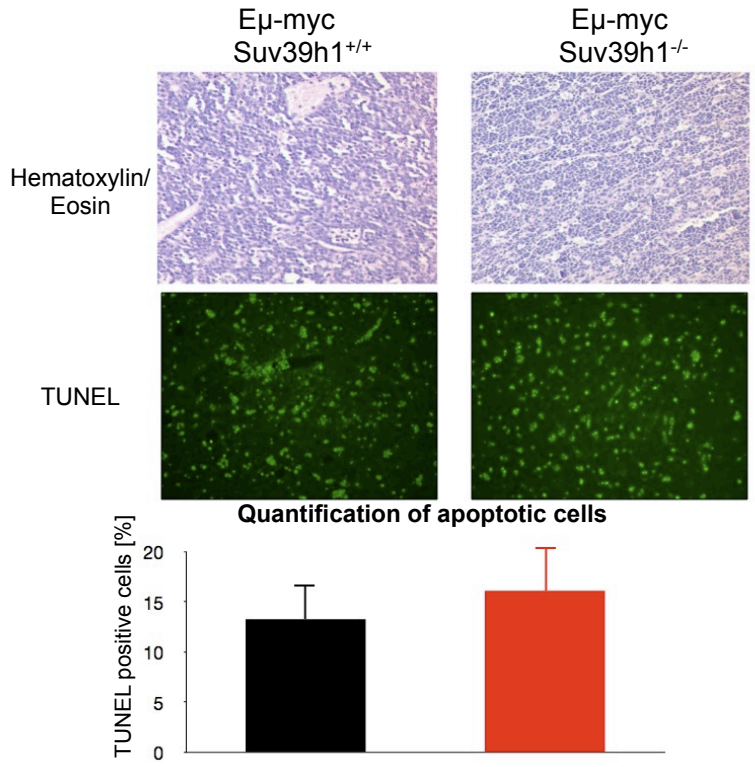

Figure 3.14: Ability to undergo spontaneous apoptosis does not depend on Suv39h1 status in Eμ-myc lymphomas. LEFT: Hematoxilyn and Eosin staining of Eμ-myc (n=3) and Eμ-myc, Suv39h1$^{-/-}$ (n=3) lymph nodes with "starry sky" phenotype (typical for Burkitt's lymphomas, done in collaboration with C. Lodenkemper *et al*). RIGHT Top: TUNEL *in situ* staining of Eμ-myc (n=3) and Eμ-myc, Suv39h1$^{-/-}$ (n=3) lymph nodes. Bottom: quantification of TUNEL staining *in situ*.

mice senescence-reminiscent characteristics of lymphoma cells were assessed by flow cytometric light scatter analysis. Single cell preparations of Eμ-myc lymphomas (n=5) when compared to Eμ-myc Suv39h1$^{-/-}$ lymphomas (n=4) demonstrated that a fraction of cells is displaying typical morphological alterations present in senescent cells (enlargment and granularity), while Suv39h1$^{-/-}$ were lacking cells with those attributes (Figure 3.15). Further, cells tested for typical senescence marker H3K9me3 (tri-methylated lysine 9 residue on histone H3) revealed positive staining only in Eμ-myc lymphomas (20,537 $\pm$ 3,148%), while in Eμ-myc Suv39h1$^{-/-}$ lymphomas no positive staining was observed (5,29 $\pm$ 2,857%; P=0,0004).

This experiment indicates that Suv39h1 deficient lymphomas show no detectable sign of a senescent phenotype as enlarged cells with granule rich cytoplasm, or positive marks for tri-methylated histone H3 lysine 9 residue, while in control lymphomas those marks are present in a fraction of whole lymphoma. Shown in here, Eμ-myc lymphomas with intact Suv39h1 retain the possibility of executing sporadic oncogene-induced senescence, and this could explain the initial difference observed in tumor latencies.

Senescence *in vivo* at the stage of terminal illness was tested in lymphoma tissue by 2 senescent markers: senescence associated β-galactosidase (SA β-gal) reactivity *in situ* and tri-methylated lisine 9 residue on histone H3 (H3K9me3; figure 3.16).

While Eμ-myc lymphoma cells sporadically display senescent phenotype, as seen by SA β-gal (14,319 $\pm$ 6,005%) and H3K9me3 (9,683 $\pm$ 3,683%) staining, Eμ-myc Suv39h1$^{-/-}$ lymphomas are lacking positive cells when stained for both markers (0,809 $\pm$ 0,12% for SA-β-gal and 2,023 $\pm$ 1,409% for H3K9me3 marker; P <0,0001 for both stainings).

Another potential senescence maker commonly used is HP1γ. HP1 proteins are components of heterochromatinization machinery, they are recruited upon Suv39h1 tri-methylation of lysine 9 residue on the histone H3, and dock to tri-methylated lysine 9 residue on histone H3, spreading higher order chromatin (Figure 3.17).

Immunofluoresecent staining of HP1γ showed that HP1γ positive cells recapitulate the distribution of SA β-galactosidase staining as well as H3K9me3 positivity (Eμ-myc 14,172 $\pm$ 4,998%; Eμ-myc Suv39h1$^{-/-}$ 3,118 $\pm$ 1,286%; P=0,004). Although HP1 proteins are abundantly present in cells, they can most likely be visualized only when in clusters, as seen in figure 3.17, which occurs when they accumulate through binding to tri-methylated lisine 9 residue.

These experiments demonstrate that Suv39h1 resides in a signaling pathway activated during Myc lymphomagenesis in order to prevent malignant transformation by mediating senescence.

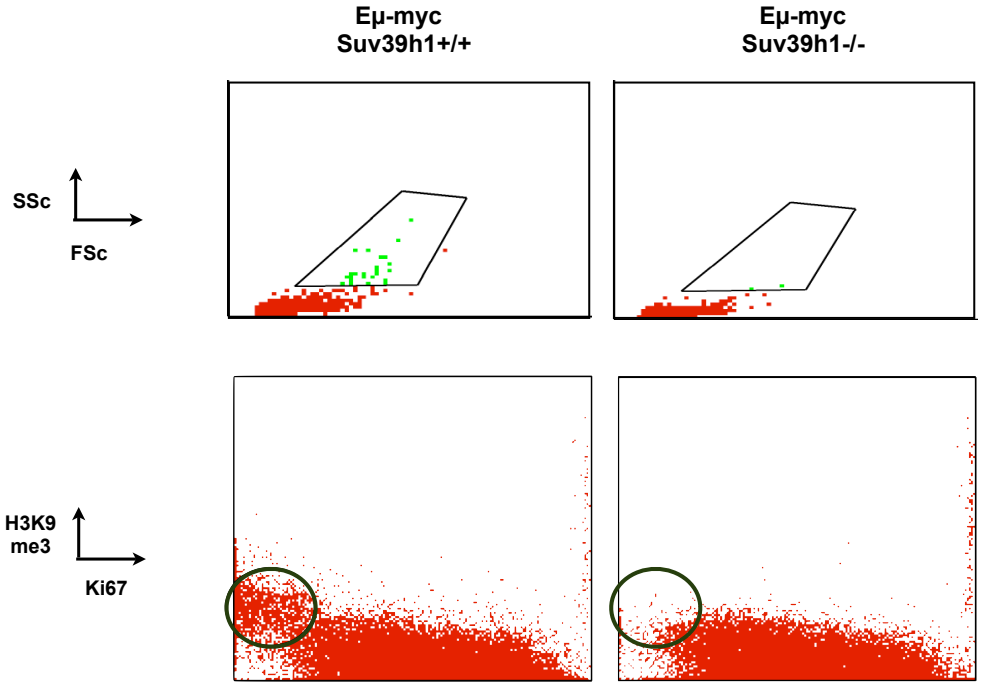

Figure 3.15: Suv39h1 deficient lymphomas show defects in senescence machinery. Freshly explanted lymphoma cells were subjcted to the flow cytometric analysis. TOP: Side scatter/ forward scatter distribution was analysed on flow cytometer, and revealed a sub-population of larger and granule rich cells only in Eμ-myc (n=5) lymphomas, depicted in green and marked with an arrow. This sub-population was absent in Eμ-myc Suv39h1$^{-/-}$ (n=4) lymphomas, as marked with an arrow. BOTTOM: Two-color flow cytometry of lymphoma cells for the cell cycle marker (Ki67) and senescence marker (H3K9me3). Cells located in the dark green circle are considered to belong to the senescent population [As negative controls for the Ki67 staining 20 Gy γ-irradiated NIH 3T3 cells were used].

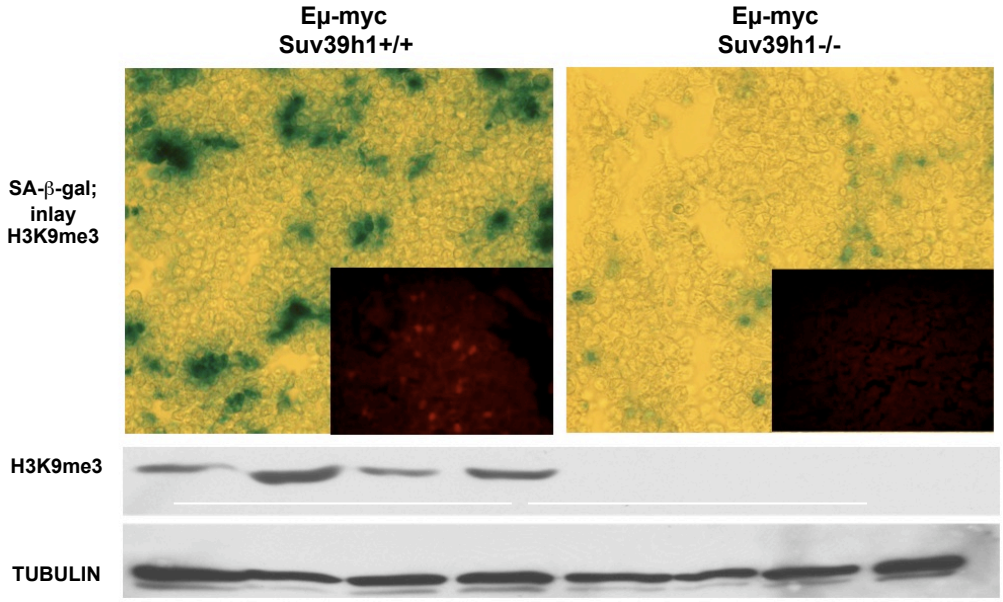

Figure 3.16: Suv39h1 deficient lymphomas are lacking senescent phenotype. TOP: Senescence associatedβ-galactosidase (SAβ-gal) *in situ*. Sections of cryopreserved lymph nodes were stained for the endogenous SA β-gal activity *in situ*. Eμ-myc control lymphomas (n=24) were compared to Suv39h1$^{-/-}$ lymphomas (n=11). Inlay represents an immunofluorescent staining for the H3K9me3 marker *in situ* (tested on sections from formalin fixed, paraffin embeded tissues) [as a negative control for the SA β-gal staining Eμ-myc p53$^{-/-}$ lymph nodes (n=3) were used]. BOTTOM: Western blot analysis of histone H3 lysine 9 tri-methylation (H3K9me3) status with respective tubulin as a loading control in Eμ-myc (n=4) and Eμ-myc, Suv39h1$^{-/-}$ (n=4) lymphomas.

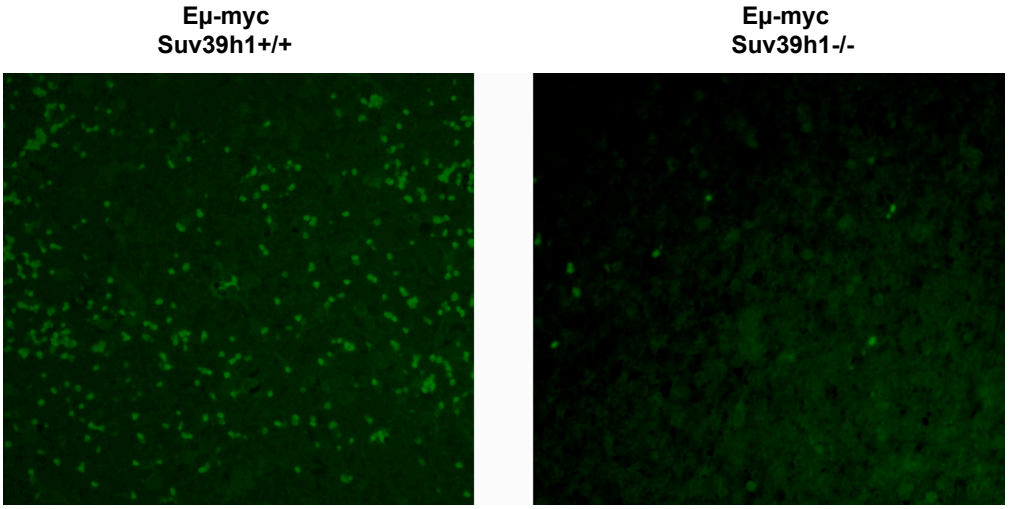

Figure 3.17: Suv39h1 deficient lymphomas are lacking in heterochromatin bound HP1γ positive areas. Sections from the formalin fixed and parafin-embeded lymph nodes were stained for the HP1γ marker *in situ*. Control lymphomas (n=3), were compared to Suv39h1 $^{-/-}$ lymphomas (n=3).

To investigate the possibility of senescence in lymphoma cells negative for Ki67 marker *in situ*, double staining approach was used to stain for the proliferation marker BrdU and senescence marker SA β-galactosidase *in situ*. Those two markers are expected to be mutually exclusive, since BrdU will not incorporate in arrested cells and SA β-galactosidase was reported to be active only in senescent cells.

Here we show that the lower proliferation rates, or lower numbers of cells stained positive for the cell cycle marker observed in Eμ-myc lymphomas (62,867 $\pm$ 3,927% versus 82,100 $\pm$ 3,816% observed in Eμ-myc Suv39h1$^{-/-}$ lymphomas; P=0,0037) are a consequence of cells' ability to enter oncogene induced senescence, as shown by the SA β-galactosidase positive staining, present only in control lymphomas ((Figure 3.18, done in collaboration with C. Loddenkemper *et al*).

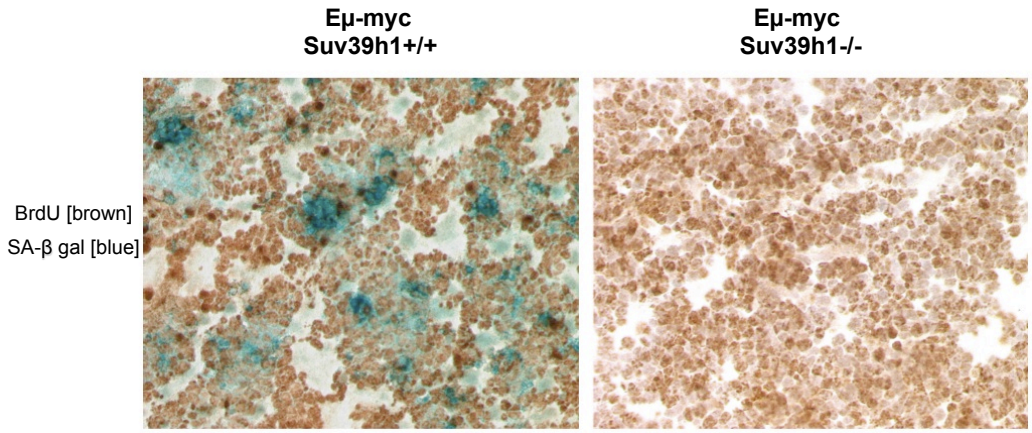

Figure 3.18: Suv39h1 proficient lymphomas lose their cells from the proliferation to senescence. Sections of cryopreserved of Eμ-myc (n=4) and Eμ-myc Suv39h1$^{-/-}$ (n=4) lymph nodes were stained for the endogenous SAβ-gal activity (visualized as blue cells) and subsequently for the BrdU incorporation (visualized as brown cells; done in collaboration with C. Lodenkemper *et al*) *in situ*.

Results obtained in this experiment reveal that the overall lower number of cells in cycle observed in Suv39h1 proficient lymphomas could be due to their loss into senescence.

Concluding from these results: senescence is a "failsafe program" precluding a fraction of cells in the Myc-driven lymphoma from contribution to the further tumor expansion.

Impact of loss of genes implicated in failsafe pathways on senescence machinery

There are several genes known to be involved in the cellular failsafe pathways. Here was tested the impact of loss in 4 genes involved in the maintenance of intact failsafe pathways on senescence *in vivo*. For that purpose B-cell lymphomas arising in different genetic background: Eμ-myc p16$^{INK4a-/-}$ (n=2); Eμ-myc p53 deficient (LOH) (n=3) ; Eμ-myc p19$^{Arf-/-}$ (n=4); Eμ-myc ATM$^{-/-}$ (n=3); and in addition Eμ- myc p16/p19$^{INK4aArf+/-}$ (n=2) were tested [for tumor latencies please see appendices section A.1.1; cryopreserved lymph nodes from Eμ-myc ATM$^{-/-}$ animals were a gift from Dr. M. Reimann; cryopreserved lymph nodes from Eμ-myc p16/p19$^{INK4aArf-/-}$ animals were gift from Mrs. B. Teichman]. Significantly lower SA β-galactosidase positivity was found in Eμ-myc p53 null (1,95 $\pm$ 1,245%; P=0,0107); Eμ-myc p19$^{Arf-/-}$ (2,32 $\pm$ 1,325%; P=0,0008) and Eμ-myc p16/p19$^{INK4aArf-/-}$- (0,71 $\pm$ 0,7%; P $<$ 0.0001) when compared to Eμ-myc lymphomas. Eμ-myc ATM$^{-/-}$ (8,807 $\pm$ 7,465%; P=0,1726) showed not significantly reduced SA β-galactosidase levels when compared to Eμ-myc lymphomas, while Eμ-myc p16$^{INK4a-/-}$ lymphomas have comparable levels of SA β-galactosidase (13,970 $\pm$ 4,483%; P=0,9631) with the Eμ-myc lymphomas (Figure 3.19).

As indicated in here defects in the p16^{INK4a} locus do not disrupt Myc-induced senescence, while defects in p19^{Arf}, as well as the loss of the entire INK4a/Arf locus has a severe impact on the Myc-induced senescence. p53 deficient lymphomas also show strong impairment of the oncogene-induced senescence, which is in accordance with p53s central role in senescence. Lastly, ATM deficient lymphomas show reduced levels of Myc-induced senescence, however there is no complete cessation of senescence in this genotpe. Conclusion from this experiment is that the p53-p19^{Arf} is pathway essential for triggering Myc-induced senescence. p16^{INK4a} seems fully dispensible for senescence induction in a Myc-overexpression setting, while ATM might contribute to the extent of senescence induction. This finding lead to further testing of a specific pathway disruptions in Suv39h1 deficient lymphomas.

Senescence machinery at molecular level

Previous experiments pointed out that Suv39h1 is a mediator of Myc-induced senescence, as well as it was shown that p53 gene and a INK4aArf locus gene product p19^{Arf} are crucial for the induction of Myc-mediated senescence. p19^{Arf} is activated in response to oncogenic Myc, and it transfers Myc signaling to p53, therefore when there is loss of p53 there will be an accumulation of p19^{Arf}.

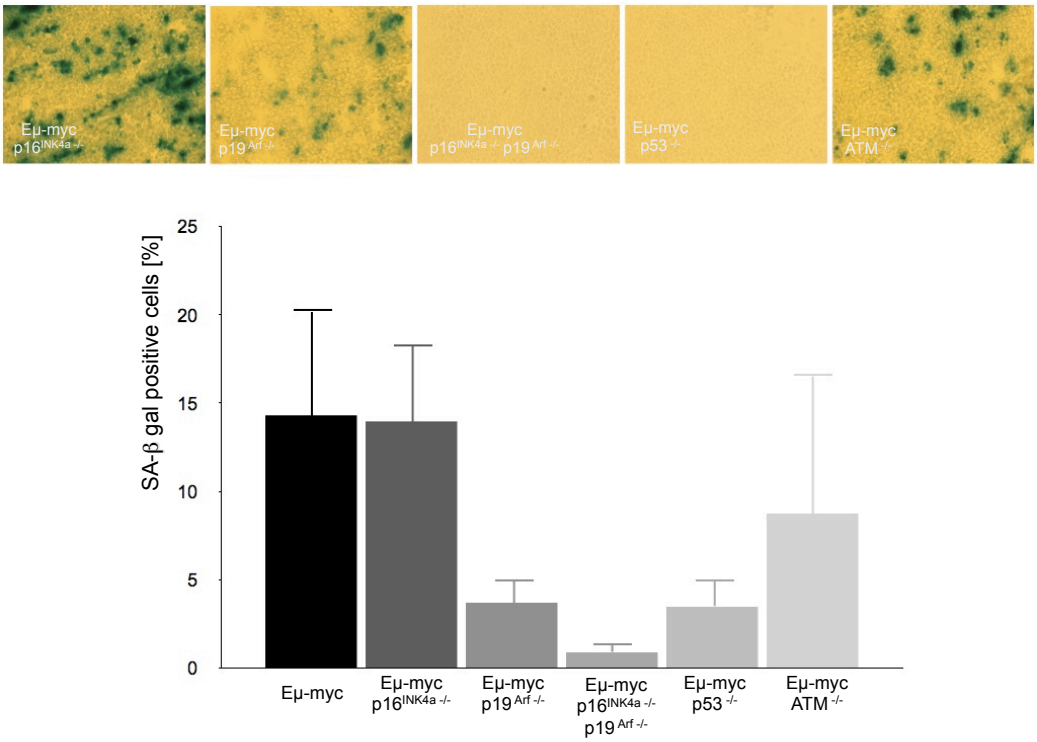

Figure 3.19: Senescence *in vivo* is fully blocked with p53 and INK4aArf gene disruption. TOP: Sections from cryopreserved lymph nodes were stained for the endogenous SA β-gal activity *in situ*. Following lymphoma genotypes were compared: Eμ-myc p16$^{-/-}$ (n=2), Eμ-myc p53$^{-/-}$(n=3), Eμ-myc Arf$^{-/-}$ (n=4); Eμ-myc ATM$^{-/-}$ (n=3), Eμ-myc p16/p19$^{Ink4aArf+/-}$(n=2). BOTTOM: histogram quantification of the staining SA β-gal activity *in situ* staining.

Data from previous research reveal that Suv39h1 deficient lymphomas select against $p19^{Arf}$ expression. Secondly, it was also reported that $p16^{INK4a}$ gene is an important factor in Ras-induced senescence[BLL+05], arguing that the senescence signal is Ras-model is mediated *via* $p16^{INK4a}$ - pRb axis. Therefore, in order to test if $p16^{INK4a}$ - pRb axis are mediating Myc-induced senescence endogenous expression of $p16^{INK4a}$, as well as pRb was tested. In addition we tested for expression levels of 2 cyclin dependent kinase inhibitors $p21^{Cip}$ and $p27^{Kip}$ which are known as mediators between p53 and $p16^{INK4a}$ signaling pathways.

Whole cell protein lysates were isolated from freshly explanted lymph nodes of both genotypes and analysed on Western blot (Figure 3.20).

Sign of an intact senescence machinery is present only in Suv39h1 proficient lymphomas, as seen by presence of hypophosphorylated form of pRb only in case if Suv39h1 is intact. Accumulation of CDK4/6 inhibitor $p16^{INK4a}$ is already reported for Suv39h1 deficient T-cell lymphomas, and could be explained by the inability of $p16^{INK4a}$ to transfer signals further downstream when Suv39h1 is absent. Therefore, this setting will lead to an accumulation of $p16^{INK4a}$.

Myc-induced senescence as a feature of pre-neoplastic lymphomas

Presence of the oncogene-induced senescence features in Suv39h1 proficient manifest lymphomas did not reveal the impact of this mechanism on the kinetics of the lymphoma development. In order to investigate status of Myc-induced senescence in a setting with no outer sign of the disease splenic B-cells of pre-manifest (30 days old) Eμ-myc and Eμ-myc, Suv39h1$^{-/-}$ animals were used. Additionally non transgenic Suv39h1 proficient and deficient B-cells were used for the same analysis.

B-cells were subjected to SA β-galactosidase and H3K9me3 stainings. As shown in figure 3.16, only pre-manifest Eμ-myc B-cells were displaying senescent characteristics (SA β-gal: 21,850 $\pm$ 11,33%; H3K9me3: 13,483 $\pm$ 5,469%), while senescent marks were absent in the pre-manifest Eμ-myc Suv39h1$^{-/-}$ B-cells (SA β-gal: 0,637 $\pm$ 0,44; H3K9me3: 1,68 $\pm$ 1,358%) (P=0,0139 and P=0,0051 respectively). When the non-transgenic genotypes, both wild type B-cells did not display positive senscent staining (SA β-gal: 1,875 $\pm$ 0,516%; H3K9me3: 1,018 $\pm$ 0,186), as well as Suv39h1$^{-/-}$ B-cells (SA β-gal: 0,31 $\pm$ 0,611%; H3K9me3: 0,57 $\pm$ 0,221%; P=0,0322; Figure 3.21).

Results obtained in this experiment indicate that loss of proliferating cells by into senescence is a continuous process, starting as early as the pre-manifest tumor stage, and is induced by the activated oncogene Myc and

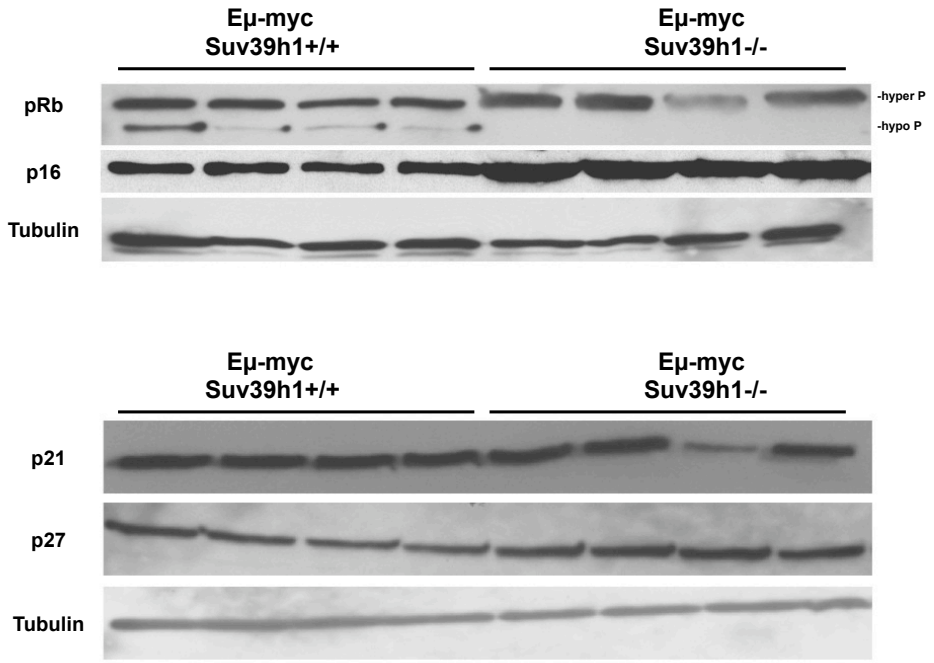

Figure 3.20: Western blot analysis of lymphoma cells isolated from lymph nodes of animals with intact and disrupted Suv39h1 revealed that a fraction of pRb is present in its hypophosphorylated form indicating cell cycle arrest only in Suv39h1 proficient lymphomas. Suv39h1 $^{-/-}$ lymphomas are displaying higher levels of $p16^{INK4a}$ when compared to the control lymphomas. TOP: pRb and $p16^{INK4a}$ status with respective tubulin as a loading control [please note that only in Suv39h1 proficient lymphoma pRb is detectable in hypophosphorylated state, which is characteristic for G1 arrest]. BOTTOM: $p21^{Cip}$ and $p27^{Kip}$ status with respective tubulin as a loading control in Eμ-myc (n=4) and Eμ-myc, Suv39h1$^{-/-}$ (n=4) [please note that $p21^{Cip}$ and $p27^{Kip}$ expression levels do not differ significantly between the 2 genotypes].

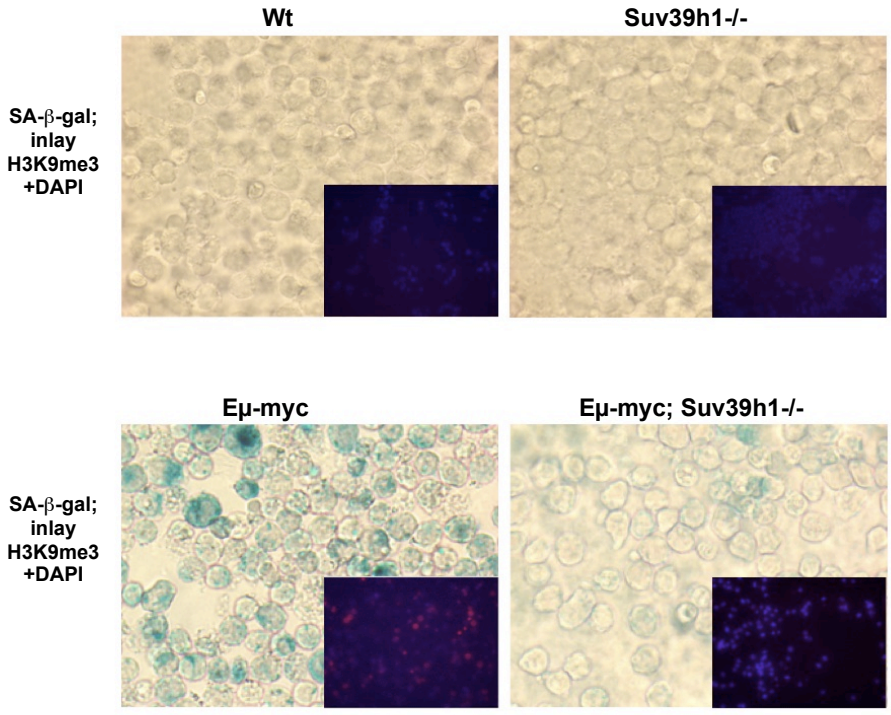

Figure 3.21: Senescence is induced by Myc-overexpression and is occuring as early as in the pre-manifest lymphoma cells. Splenic B-cell cytospins were prepared from wild-type (n=3), Suv39h1$^{-/-}$ (n=3), Eμ-myc (n=3) and Eμ-myc Suv39h1$^{-/-}$ (n=3) 30-day old mice and stained for the endogenous SA β-gal activity and H3K9me3/DAPI [DAPI is used to visualise cells for the subsequent quantification, visualized in blue].

dependent on the presence of intact Suv39h1.

This finding could explain that the lower Ki67 values observed in Suv39h1 proficient setting are the consequence of continuous Myc-induced senescence. As reported previously, immune cells are recruited to the site of senescent cells and clear them from the tissue [XZM+07], therefore finding described in this thesis together with this previous report is exposing Myc-induced senescence as a dynamic process, where exists a constant balance between losing cells into senescence and their elimination from the tissue by the cells of the immune system.

Contribution of bystander cells to the Myc-induced senescence

In order to corroborate previous finding indicating that the ability to undergo senescence is a property of cells with overexpressed Myc, and to further investigate whether Eμ-myc driven B-cells and not bystander cells co-existing in the lymphoma tissue have the ability to undergo senescence, oncogene induced senescence was tested for the bystander cells. In order to test senescence induction in bystander cells a series of transplantation experiments in which Suv39h1 deficient lymphomas would develop in a non-transgenic Suv39h1 proficient background, as well as Suv39h1 proficient lymphomas would develop in Suv39h1 deficient background were conducted.

Fetal liver cells (FLC) from either Eμ-myc; Eμ-myc, Suv39h1$^{+/-}$ or Eμ-myc, Suv39h1 $^{-/-}$ mice were used in order not to use already developed lymphomas with all of the accompanying genetic alterations. These fetal liver cells were transplanted in either wild-type (for Eμ-myc, Suv39h1$^{+/-}$ and Eμ-myc, Suv39h1$^{-/-}$) or Suv39h1$^{-/-}$ (for Eμ-myc) sublethaly irradiated recipients (4 Gy of γ irradiation, single dose). Mice were monitored for the time to tumor onset and *post mortem* lymph nodes were extracted, cryopreserved and stained for the senescence marker SA β-gal (Figure 3.22).

Tumor bystander cells are not undergoing senescence, as shown in figure 3.22, but from the data it could not be concluded if they might have a function in senescence induction.

3.1.4 DNA damage analysis in Myc lymphomas

Recent publications have shown that DNA damage might act as one of the mediators of senescent response. In order to test for the contribution of DNA damage response (DDR) to the mediation of senescence in Myc-lymphoma setting, activation of p53, as a main mediator of the DDR was tested. In order for DDR machinery to properly function p53 has to be activated by checkpoint kinases (ATM/ATR) phosphorylation on the residue

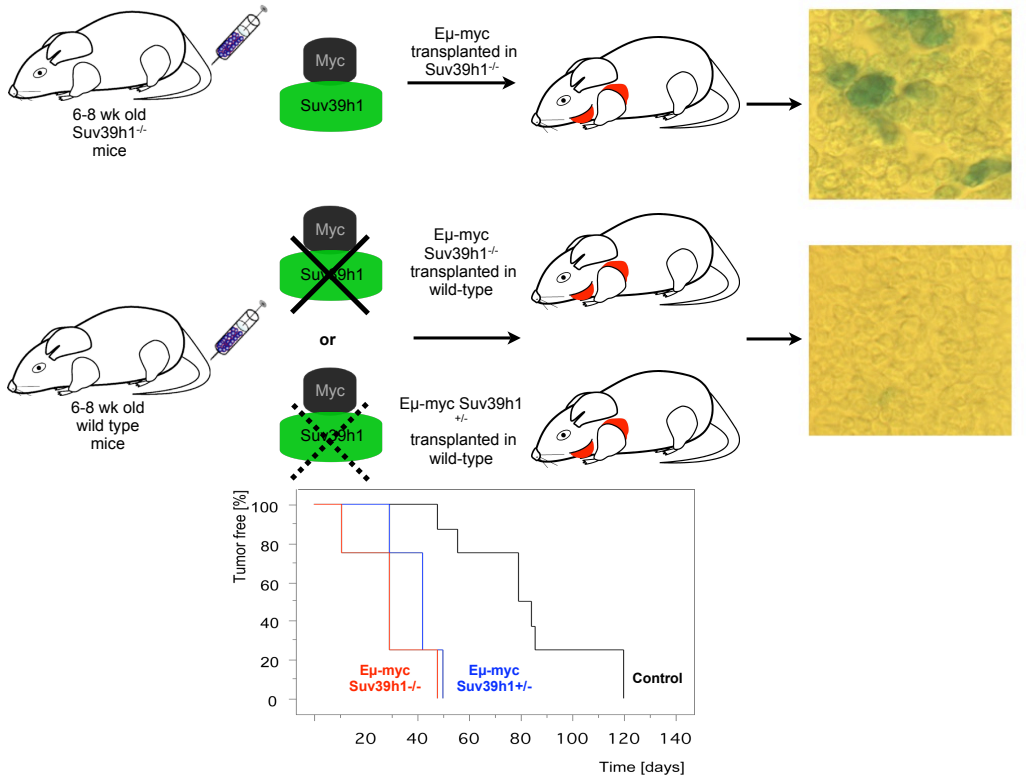

Figure 3.22: Myc-induced senescence is not present in tumor bystander cells. LEFT: Experimental setup. Non transgenic mice were transplanted with fetal liver cells isolated from Eμ-myc; Eμ-myc, Suv39h1$^{+/-}$ and Eμ-myc, Suv39h1$^{-/-}$ fetuses. Transplanted mice were montored for the time to lymphoma onset latencies post fetal liver cell transplantation (as defined by Kaplan-Meier estimator) for Eμ-myc (n=9, black line); Eμ-myc, Suv39h1$^{+/-}$ (n=3, blue line); Eμ-myc, Suv39h1$^{-/-}$ (n=3, red line) lymphomas. RIGHT: Sections of cryopreserved lymph nodes were stained for the endogenous SA β-gal activity *in situ*. Control lymphomas transplanted into the Suv39h1 deficient background (n=9) were compared to Suv39h1 $^{-/-}$ lymphomas transplanted into the wild-type background (n=3).

18(p53S18P). Therefore p53 activation in both Suv39h1 proficient and deficient genotypes was tested by Western blot analysis for the presence and the extent of p53S18P (Figure 3.23).

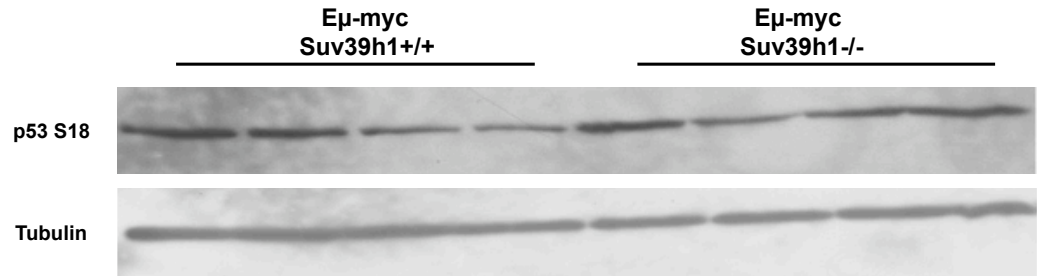

Figure 3.23: Myc-induced DNA damage signaling is intact in Suv39h1 deficient lymphomas. Western blot analysis of lymphoma cells extracted from lymph nodes of animals with intact and disrupted Suv39h1. p53S18P status with respective tubulin as a loading control in Eμ-myc (n=4) and Eμ-myc, Suv39h1$^{-/-}$ (n=4) lymphomas.

Figure 3.23 shows that Myc-induced p53 activation upon stress conditions is not dependent on Suv39h1 status indicating intactness of the DDR machinery.

Myc-evoked oxidative stress and DNA damage response (DDR) machinery

Oxidative stress is one of the mediators of senescence. To investigate the impact of oxidative stress on senescence induction, Eμ-myc mice were continuously exposed to N-Acetylcysteine (NAC; reactive oxygen species scavenger; applied as 0.5% w/v solution in drinking water) starting at birth. It was reported that N-acetylcysteine prevents DNA damage induced by Myc *in vitro* [VWK^{+}02].

No difference in tumor latencies between NAC treated and untreated group of Eμ-myc mice was detected in this experiment. However, when assesed for the senescence marker SA β-gal it was shown that NAC treated mice show a reduction in Myc-induced senescence (SAβ-gal: Eμ-myc + NAC= 7,787 $\pm$ 4,908%; Eμ-myc= 16,608 $\pm$ 9,065%; P= 0,1005). The reduction in reactive oxygen species (ROS) was confirmed by the 2'7'- dichlorofluorescein (DCF) reaction. DCF is commonly used to detect generation of reactive oxygen intermediates. DCF values were measured quantitatively by flow cytometry (Eμ-myc + NAC= 4,061 $\pm$ 1,146%; Eμ-myc= 11,498 $\pm$ 2,081; P= 0,0474), and shown as an immunofluorescent staining (Figure 3.24).

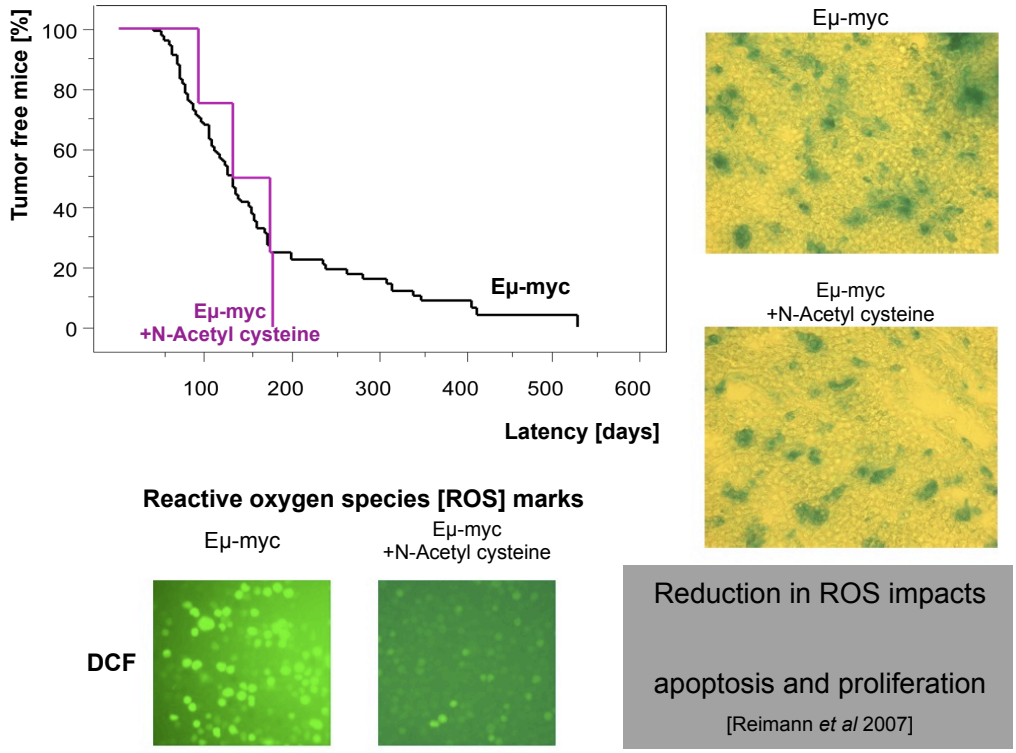

Figure 3.24: Eμ-myc mice with impaired DNA damage response machinery develop tumors with indistinguishable latencies from control mice, and display reduced Myc-induced senescence. TOP Left: Kaplan-Meier "Time-to-tumor onset" latencies of Eμ-myc+NAC (n=4; purple line) and Eμ-myc (n=93; black line). Right: SAβ-gal staining revealed that N-acetylcysteine (NAC) treated mice develop lymphomas with decreased levels of senescence. BOTTOM Left: 2'7'- dichlorofluorescein (DCF) visualisation of the presence of reactive oxygen species (ROS). Right: Reduction in ROS has an impact on proliferation, apoptosis[RLR$^+$07], and as reported in this work also on senescence.

It was previously reported that NAC treated Eμ-myc lymphomas have decreased levels of both proliferation and apoptotic capacity [RLR$^+$07], which could explain no impact on tumor development latencies observed here.

Secondly, as seen here reactive oxygen species (ROS) scavanger NAC was successful in reducing Myc-induced senescence, arguing for an impact of ROS-DDR on senescence mediation.

Remaining question from this approach is: if there would be no reduction in proliferation and apoptosis in the similar approach to the one described above, would an impact of senescence block on tumor latencies *in vivo* be detectable?

Disruption of DNA damage checkpoints in Myc-lymphomas

Additional analysis on the DNA damage-mediated senescence was done by caffeine administration to Eμ-myc mice starting from birth (0.4mg/ml in drinking water supply). Caffeine is compound that cancels ATM/ATR-controlled DNA double strand break checkpoint [DMFC$^+$06], therefore blunting the DDR.

Caffeine administration significantly decreased tumor latencies in Eμ-myc mice undergoing daily caffeine exposure (n=15). Eμ-myc mice developed tumors with the median time of 53 days, significantly earlier than in the non-caffeine treated group (P=0,0003) (Figure 3.25 upper left panel) [see the appendices section A.1.2 for the Kaplan-Meier "Time-to-tumor-onset" plot of wild-type and Eμ-myc caffeine treated mice]. Lymphomas from caffeine treated mice showed reduced staining for SA-β-galactosidase activity (n=8; 6,372 $\pm$ 2,29%; P=0,0002).

Caffeine treated lymphomas also displayed lower frequency of apoptotic cells by TUNEL staining *in situ* (n= 7; 7,44 $\pm$ 3,11%) when compared to the untreated controls (n=3; 17,43 $\pm$ 2,89%; P=0,0015; Figure 3.25).

These results suggest that the DNA damage response (DDR) pathway is playing a role in the mediation of oncogene-induced senescence in Eμ-myc mouse lymphoma model. As shown in the experiment with the caffeine treatment, apoptosis is also important downstream component of the DDR machinery. Implication of both apoptosis and senescence in the DDR in this experiment made it impossible to interpret if the disruption in the senescent machinery could be responsible for the decrease in tumor latencies as observed in figure 3.25. Also, by reducing DNA damage *via* caffeine treatment senescent response was not entirely ablated, suggesting a possibility of an additional mechanism mediating senescent response. This mechanism could collaborate with the DDR signals in mediation of senescence.

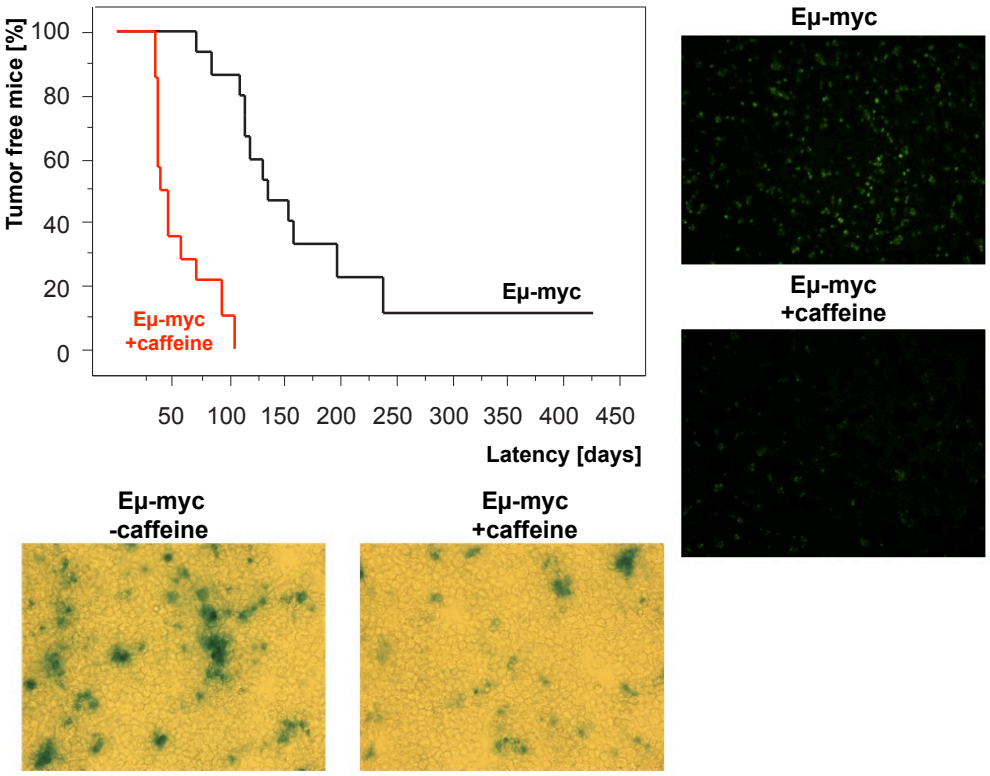

Figure 3.25: Caffeine induced shortening of tumor latencies in Eμ-myc mice. Lymphomas arise as a consequence of impairment in apoptotic and senescent machinery. LEFT: Kaplan-Meier "Time-to-tumor-onset" latencies of Eμ-myc mice with constant water supply of caffeine (n=15, red line) compared to Eμ-myc mice without caffeine (n=15, black line). RIGHT: Lymph nodes from Eμ-myc (n=3) and caffeine treated Eμ-myc mice (n=7) were tested for senescence marker (SA β-gal) and apoptosis marker (TUNEL).

3.1.5 Triggers of Myc-induced senescence

Following observations that DDR is one of the mediators of Myc-induced senescence and that there might be another mediator needed in order to execute senescence. Observing sporadic pattern of senescence positivity in control lymphoma cells posible influence of the tumor architecture and environment was considered as one of triggers of senescence.

Microenvironment as a trigger of Myc-induced senescence

Influence of the tumor microenvironment on senescence induction was tested. Vascularization of tumor contributes to its better growth, but is also keeping cells more oxygenated, sensitizing them to ROS induced DDR, which can potentially lead to induction of senescence. To test for the possible influence of the vascularization, therefore tumor oxygenation, on senescence induction, lymph nodes of Eμ-myc mice were tested for CD31 (blood vessel marker, done in collaboration with C. Lodenkemper *et al*) and SA β-gal *in situ*. In order to analyze obtained data each photomicrograph was divided in 64 equall fields and checked for the relative co-localization of vascularization (CD31) and senescence (SA β-gal) markers (Figure 3.26).

These results demonstrate more frequent occurence of senescence in areas close to the blood vessels [CD31+ SA β-gal+ = 77,0 $\pm$ 11,0%; CD31- SA β-gal+ = 35,0 $\pm$ 17,5%; P=0,0006]. Areas close to blood vessels are better oxygenated areas, results shown in here reveal co-localization of vasculature and senescent cells, which could indicate that the reactive oxygen species (ROS) are playing an important role in Myc-induced senescence. This result indicated that the tumor microenvironment architecture could be used as a prognostic indicator of tumor progression.

In addition when compared blood vessel density in both Eμ-myc and Eμ-myc, Suv39h1$^{-/-}$ lymph node sections, it shows indistinguishable pattern of vessel distribution in both of the genotypes tested. In this experiment a grid composed of 25 fields per photomicrograph was used in order to distinguish between positive and negative CD31 areas [Eμ-myc= 48,10 $\pm$11,1%; Eμ-myc, Suv39h1$^{-/-}$ = 58,20 $\pm$11,0%; P=0,1153] (Figure 3.27).

In conclusion, significantly more senescent cells was found co-localizing with tumor vasculature. Therefore showing that the better oxygenated tumor areas with are more prone of entering Myc-induced senescence.

Secondly, defects in Suv39h1 do not influence distribution or the extent of tumor vascularization, as Suv39h1 deficient lymphomas have a similar vascularization pattern, exposing them to the same level of oxygen and subsequently to the same level of ROS as Suv39h1 proficient lymphomas.

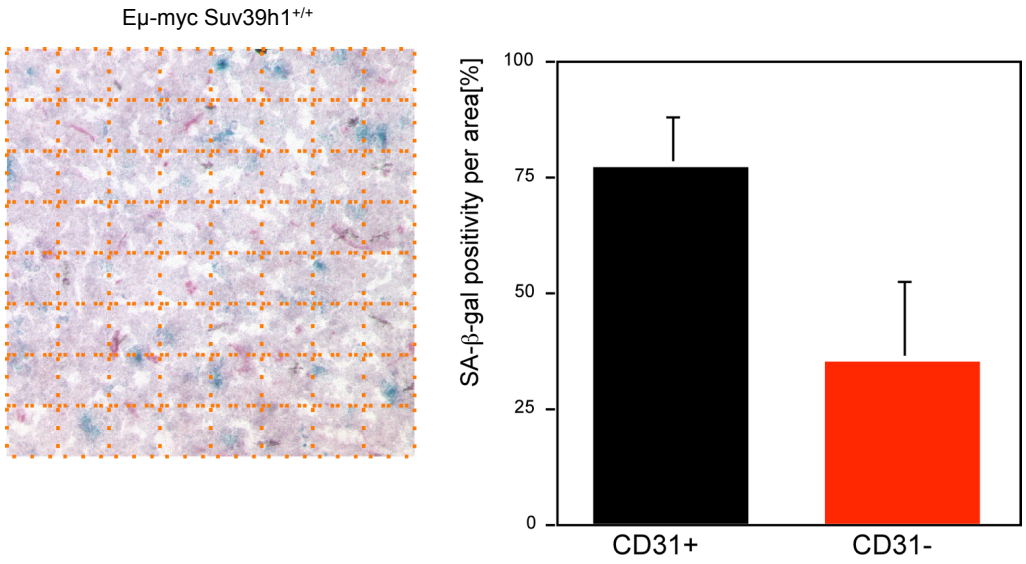

Figure 3.26: More frequent occurence of senescence is detected in areas with well developed vasculature. LEFT: Each photomicrograph is divided by grid into 64 fields (depicted in orange, app.100x 100 μm).To each field could be assigned (based on minimally one positive event in the given field): 1. Negative for SA β-gal;negative for CD31; 2. Negative for SA β-gal, positive for CD31 (purple); 3. Positive for SA β-gal (blue), negative for CD31; 4. Positive for SA β-gal and CD31. Positive SA β-gal areas were quantified and compared with respect of CD31 positivity in Eμ-myc lymphomas. Representative photomicrograph of SA β-gal/ CD31 staining (done in collaboration with C. Loddenkemper *et al*). RIGHT: Histogram of quantification obtained from the approach described on the upper left part of the figure.

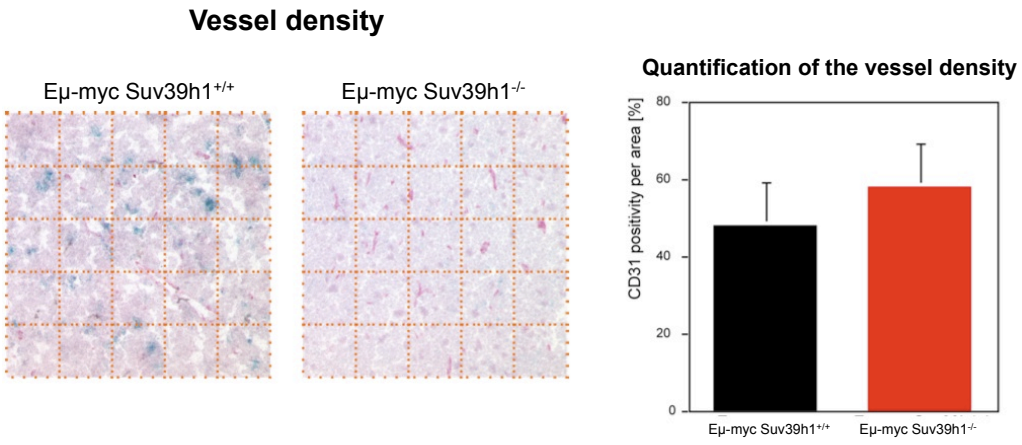

Figure 3.27: Extent of CD31 positive cells is equall in both Suv39h1 proficient and deficient lymphomas. LEFT: Each photomicrograph is divided by grid into 25 fields (depicted in orange; 175x 175 μm). To each field could be assigned (based on minimally one positive event in the given field) 1. Positive for CD31 (purple); 2. Negative for CD31. Positive CD31 areas were quantified and compared with respect to genotypes. Representative photomicrograph of CD31 staining (done in collaboration with C. Loddenkemper *et al*). RIGHT: Histogram of quantification obtained from the approach described on the left.

Genetic signature of Myc-induced senescence

In order to investigate deregulation in other genes affected by Suv39h1 loss in Myc-driven lymphomagenesis RNA isolated from primary Suv39h1 proficient and deficient lymphomas (n=3 for each group) was subjected to the genome-wide transcriptional profiling (cDNA synthesis, labeling, hybridization and statistical analysis was performed by B. Samans *et al*).

The transcript with the strongest differential regulation (beside Suv39h1 transcript which was 14.4 fold downregulated in the Suv39h1 deficient lymphomas) was βIGH3 (Tgfbi or TGFβ-inducible) gene. This gene was previously linked to senescence [DCFR02], and in this experiment it showed a 3.9 fold higher upregulation in Suv39h1 deficient lymphomas compared to the control lymphomas.

Further, following genome-wide transcriptional analysis deregulation in βIGH3 transcript levels was validated on a larger number of samples by a semi quantitative RT-PCR approach (cycle 28 is depicted in Figure 3.28).

Thus, finding of a new gene potentially involved in the Myc-induced senescence is reported in here. Although previously reported Tgfbi upregulated expression as a response to retinoid-induced growth arrest[DCFR02], here is observe upregulation of the same gene in lymphoma setting unable to produce senescent phenotype. This firstly conflicting findings might work in the same direction, as Suv39h1 defects in processing signals from the senescence-related genes positioned upstream in the cascade might be the reason for the accumulation of βIGH3.

Validation of candidate genes involved in senescence

The semi-quantitative RT-PCR analysis were directed towards validating genome-wide expression analysis results revealing deregulated gene expression caused primarily by loss of Suv39h1. Additional primary lymphoma samples were used to validate expression of several transcripts found differentially regulated in previous experiment. These genes were of particular interest since they were involved in transcription initiation, DNA repair, hystone acetylation and insulin signaling among other functions. They included: Taf4B [TAF4b RNA polymerase II, TATA box binding protein (TBP)-associated factor], Mei1 [Meiosis defective 1], Myst 4 [Myst histone acetyltransferase monocytic leukemia 4], Ryk [Receptor tyrosine kinase], Lsp1 [Lymphocyte specific protein] and Cul 2 [Ubiquitin protein ligase binding] (semi-quantitative RT-PCR results can be found in the appendices section A.1.3).

Further work described in this thesis did not focus on elucidating the role

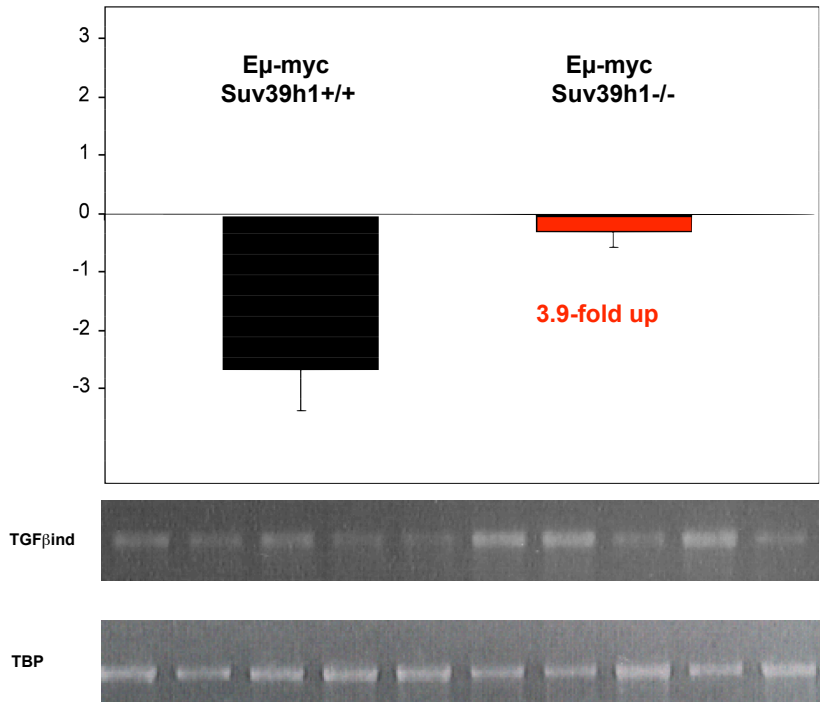

Figure 3.28: Transcript with the highest deregulation in RNA-expression analysis assay is the βIGH3 (TGFβ-inducible) gene. Left: Histogram graph representing results of the gene expression array analysis for TGFβ-inducible gene (3 samples of each genotype were analysed). Right: Validation of gene expression array analysis results for TGFβ-induced (Tgfbi) transcript on freshly isolated lymphoma cells from Eμ-myc (n=5) and Eμ-myc, Suv39h1$^{-/-}$ (n=5) animals, TBP was used as a loading control in a semi-quantitative RT-PCR approach (shown here is PCR-cycle 28).

of previously mentioned genes in senescence-induction. Focus of the research remained on βIGH3 gene and its deregulation. The upstream regulator of βIGH3 gene is TGFβ, therefore the difference observed in the expression of βIGH3 gene might reflect a deregulation in TGFβ signaling.

In order to test this hypothesis semi-quanititative RT-PCR analysis of all three isoforms of TGFβ (TGFβ-1, -2 and -3) was performed. Transcriptional levels of TGFβ-1 were increased in Suv39h1 deficient lymphomas, which was in accordance to the TGFβ function as an upstream trigger of βIGH3 (PCR cycle 33 is depicted in figure 3.29). Levels of TGFβ-2 and TGFβ-3 however remain unchanged in both genotypes [RT-PCRs for TGFβ-2 and TGFβ-3 can be found in the appendices section A.1.3].

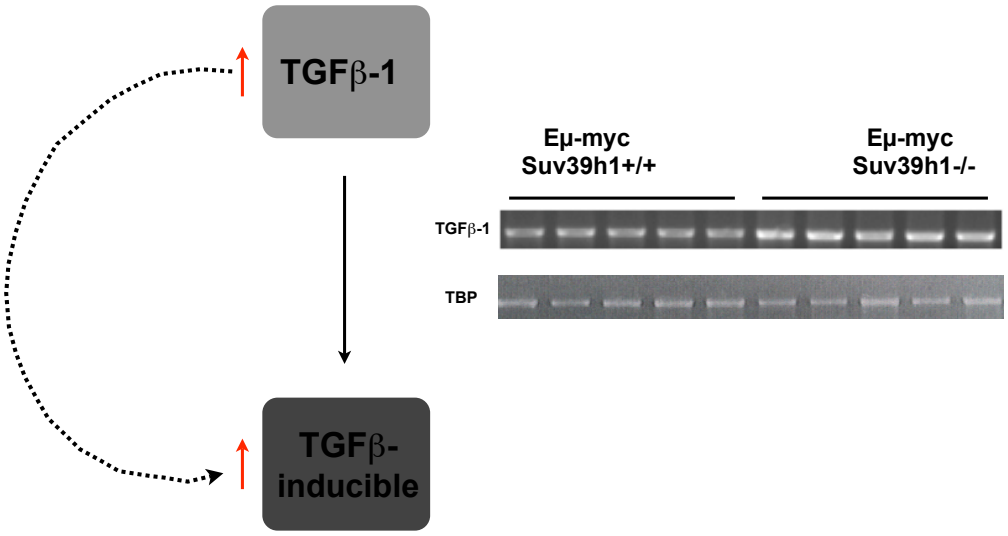

Figure 3.29: TGFβ-1 is an upstream regulator of βIGH3, and shows deregulation in expression depending on Suv39h1 status. LEFT: TGFβ is an upstream regulator of βIGH3, therefore the difference in the expression levels of βIGH3 could reflect differences in levels of TGFβ. RIGHT: TGFβ-1 levels tested by semi-quantitative RT-PCR analysis. TGFβ-1 transcript levels were tested on freshly isolated lymphoma cells from Eμ-myc (n=5) and Eμ-myc Suv39h1$^{-/-}$ (n=5) animals, TBP was used as a loading control.

As seen here, TGFβ-1 is upregulated upon loss of Suv39h1 in Myc-driven lymphomas. Role of TGFβ-1 in tumorigenesis was already reported, and it is complex and often varies depending on the tissue and progression-stage of a certain tumor. Moreover TGFβ-1 mRNA levels might not be the most accurate assessment of the TGFβ-1 levels, therefore protein expression profile of TGFβ-1 was tested in Eμ-myc and Eμ-myc, Suv39h1$^{-/-}$ lymphomas by Western blot analysis. Isolated proteins from the freshly explanted lymph nodes (n=4 for each genotype) were tested, and additionally homogenates of lymph node tissue were tested in ELISA assay for levels of active TGFβ-1 (Figure 3.30).

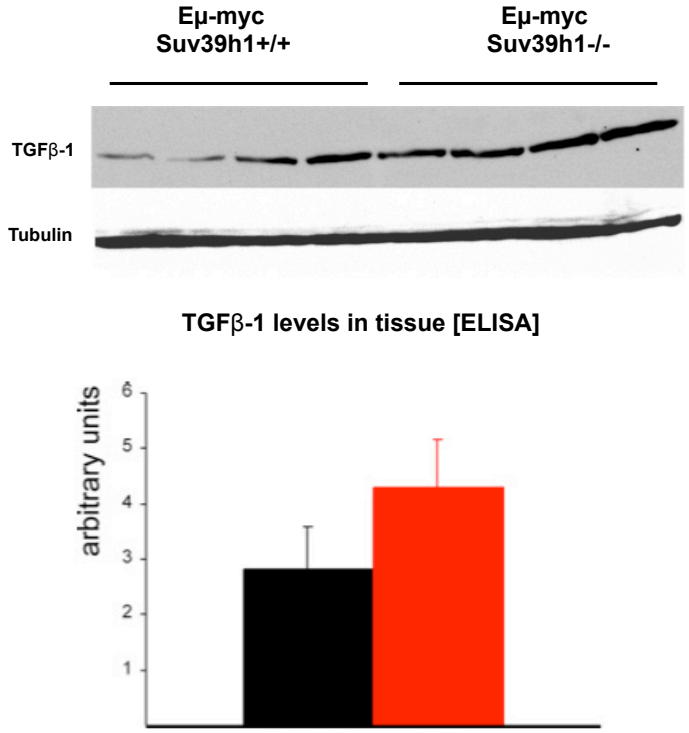

Figure 3.30: Suv39h1 deficient lymphomas display higher expression levels of TGFβ-1 protein. TOP: TGFβ-1 Western blot analysis of Suv39h1 proficient and deficient lymphomas (n=4 for each genotype), tubulin was used as a loading control. BOTTOM: TGFβ-1 levels in the lymph node tissue were tested in commercialy available ELISA assay (n=4 for each genotype).

These findings implicate a possible role of TGFβ-1 as a mediator of Myc-induced senescence. The cellular source of TGFβ-1 in lymph nodes is not known, and it is possible that instead or in addition of lymphoma cells, tumor

bystander cells are secreting TGFβ.

In order to unveil cellular source of TGFβ freshly explanted lymphoma cells were propagated *in vitro*, and after 10 days in culture transcript levels of TGFβ-1 were assessed. Analysis revealed that levels of TGFβ remain higher in Suv39h1 deficient lymphoma cells (Figure 3.31)[see the appendices A.1.3 for the comparison between B-cells of non-transgene origin with the lymphomas, and for the $p15^{INK4b}$ protein expression levels].

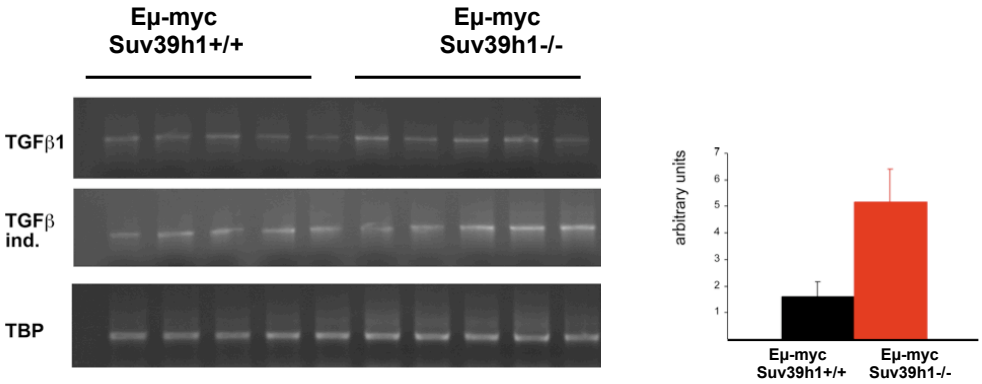

Figure 3.31: Differences in levels of TGFβ-1 expression remain unchanged after *in vitro* culture propagation. LEFT: Eμ-myc (n=5) and Eμ-myc Suv39h1 (n=5) cells were cultured for 10 days and subsequently tested for TGFβ-1 and TGFβ-induced transcript levels, TBP was used as a loading control. RIGHT: Eμ-myc (n=5) and Eμ-myc Suv39h1 (n=5) cells were cultured for 10 days and subsequently cell supernatant was tested for levels of excreted TGFβ-1 by commercially available ELISA assay.

These results suggest that one of the sources of TGFβ-1 in the cell culture are lymphoma cells themselves, however as lymphoma cells are cultured on a layer of feeder cells it can't be excluded that this cells have contributed to the TGFβ secretion profile.

3.1.6 TGFβ-1 gene and its role in senescence

In order to directly analyze potential role for TGFβ-1 in senescence induction *in vitro* Suv39h1 proficient and deficient lymphomas were exposed to the different concentrations of TGFβ-1 (0,10, 100, 1000 pM). This exposure provoked cell death in both control and the Suv39h1 deficient lymphomas in a time and dose dependent manner. In order to prevent cell death by TGFβ-1 apoptotic blocker bcl2 was stably retroviraly introduced into the lymphoma cells, and afterwards lymphomas were subjected to a treatment with different concentrations of TGFβ-1. In the absence of apoptosis it was shown that external admission of TGFβ-1 decreases the proliferative capacity of the control lymphomas. With the highest doses of TGFβ-1 administered in control lymphomas, a complete cessation of proliferation occured, with cells displaying strong senescent features, while Suv39h1 deficient lymphomas remain virtually unaffected (Figure 3.32).

TGFβ-1 induced proliferation block *in vitro* in control lymphomas was accompanied by a strong (dose dependent) senescent phenotype, while senescent cells were virtually undetectable in Suv39h1 deficient setting. Results presented here indicate that TGFβ-1 is able to induce senescent phenotype in control lymphomas (SA β-gal= 31,11 $\pm$ 14,75%; H3K9me3= 36,17 $\pm$ 8,95%) but not in the Suv39h1$^{-/-}$ lymphomas (SA β-gal= 0,12 $\pm$ 0,78%; H3K9me3= 1,5 $\pm$ 0,66%; P $<$ 0,005), arguing it might be the additional mechanism in Myc's induction of senescent response. This finding suggested that TGFβ-1 might have a role in *in vivo* Myc-driven lymphomagenesis.

TGFβ-1 role in senescence induction *in vitro* was tested on two additional genotypes: Eμ-myc p53$^{-/-}$ and Eμ-myc p19$^{Arf-/-}$ (all of those were protected from apoptosis by stable transduction with bcl2 (bcl2 transduction was done in collaboration with Dr. S. Lee; Figure 3.33).

As seen Eμ-myc, p19$^{Arf-/-}$ and Eμ-myc, p53 $^{-/-}$ lymphomas remain resistant to different doses of TGFβ-1, arguing for the essential role of both p19^{Arf} and p53 signaling in maintaining cytokine-mediated senescence.

In addition, it was also shown that TGFβ-1 administration preserves inducibility of previously mentioned target Tgfbi [RT-PCR analysis can be found in the appendices section A.1.3].

Further, to unveil the acute TGFβ-1 response in lymphomas Suv39h1 proficient and deficient cells were exposed for 24 hours to 100 pM of TGFβ-1, and subjected to the genome-wide expression array analysis (cDNA synthesis, labeling, hybridization and statistical analysis was performed by B. Samans *et al*) [see the appendices section A.1.3 for validation of the results obtained in the second set of micro-arrays].

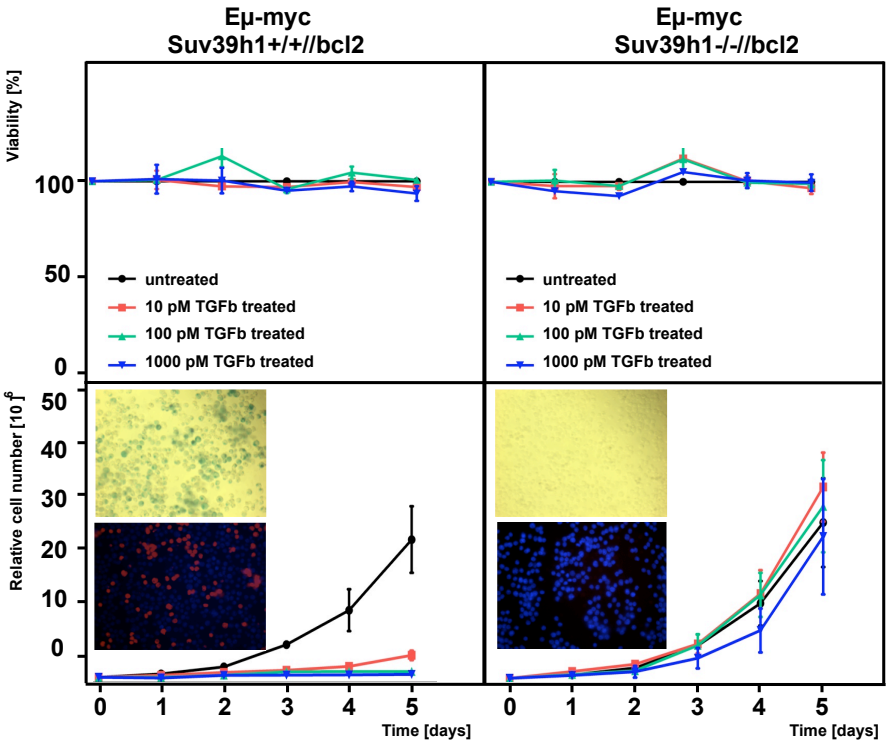

Figure 3.32: TGFβ-1 induces senescence like growth arrest in a dose dependent manner only in Suv39h1 proficient lymphomas. TOP: Relative viability of Eμ-myc (n=4) and Eμ-myc, Suv39h1$^{-/-}$ (n=4) cells exposed to different concentrations of TGFβ-1: 0 pM (black line); 10 pM (red line); 100 pM (green line) and 1000pM (blue line) for 5 days. BOTTOM: Relative growth curves and staining on cytospins of TGFβ-1untreated and 100pM treated cells. Cells were prepared at day 5 *post* treatment and senescent phenotype was tested in Eμ-myc (n=4) and Eμ-myc, Suv39h1$^{-/-}$ (n=4) cells by SA β-gal and H3K9me3 staining (DAPI[blue] is used for total cell number visualisation in H3K9me3[red] staining).

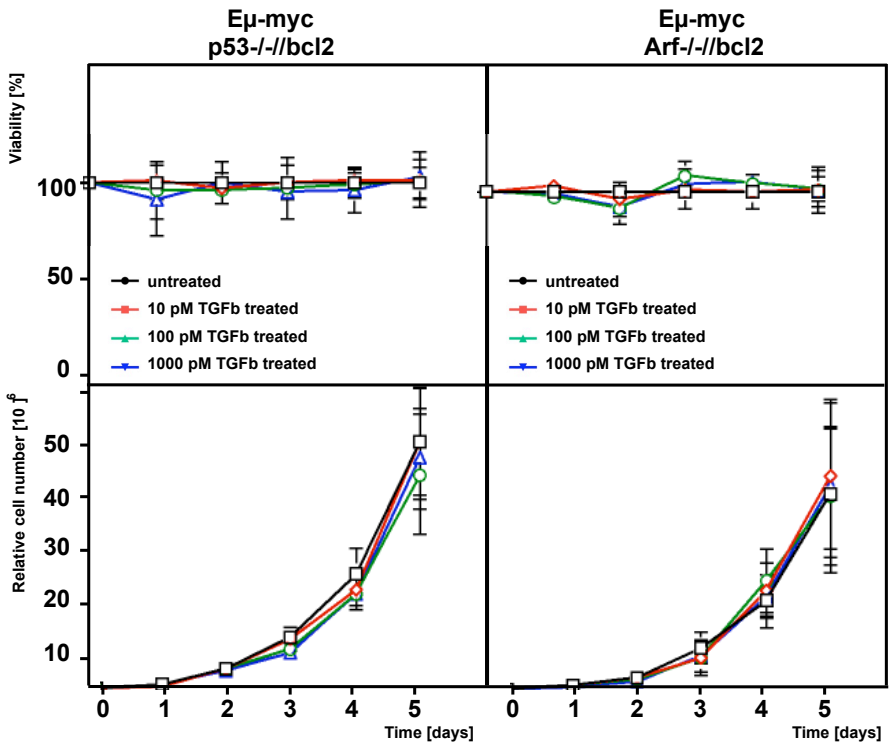

Figure 3.33: TGFβ-1 fails to induce senescence like growth arrest in lymphomas challenged in the p53-p19^{Arf} signalling. Relative viability and relative growth curves of Eμ-myc, p19$^{Arf-/-}$ (n=3) and Eμ-myc, p53$^{-/-}$ (n=3) cells exposed to different concentrations of TGFβ-1 0 pM (black line); 10 pM (red line); 100 pM (green line) and 1000pM (blue line) for 5 days.

Influence of acute Myc and TGFβ-1 induction on senescence execution

In order to test the senescence induction by acute Myc overexpression, mouse embryonic fibroblasts (MEF) were used as experimental platform. Mouse embryonic fibroblasts both proficient and deficient for Suv39h1 were generated (for more details please refer to the method section), and by means of the stable retroviral transduction a 4-hydroxy-tamoxifen (4-OHT)-inducible Myc protein, fused to a modified estrogen receptor component (Myc-ER) was introduced [Western blots of induced Myc can be found in the appendices section A.1.4]. Shown here are cells treated with 100pM of TGFβ-1 with or without Myc activation, cells were tested for senescent markers 5 days post treatment by SA β- gal,H3K9me3 and by protein blot for pRb and p15^{INK4b} (which is a direct target of TGFβ-1, Figure 3.34).

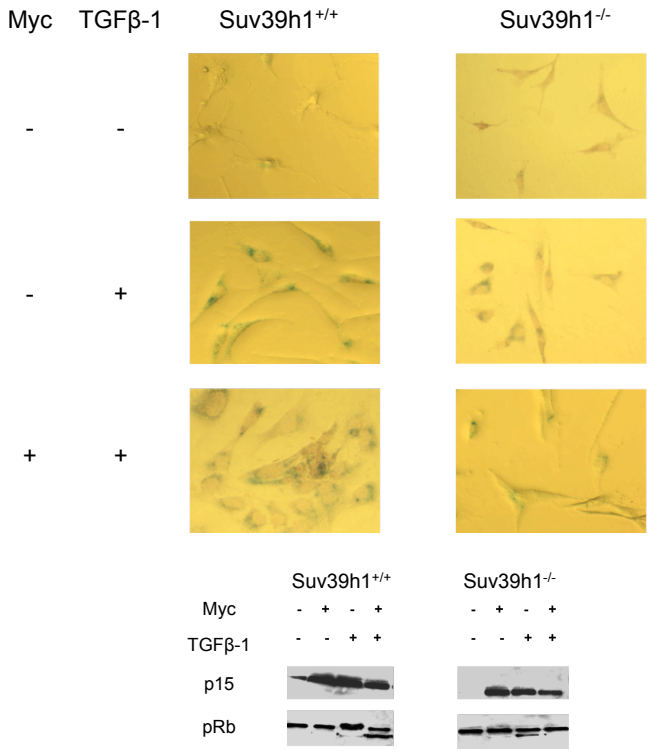

Figure 3.34: Mouse embrionic fibroblasts irrespective of Suv39h1status display senescent phenotype. TOP: Cells from wild-type and Suv39h1$^{-/-}$ background were prepared 5 days post treatment and stained for SA β-gal activity. BOTTOM: Cells from wild-type and Suv39h1$^{-/-}$ background were prepared at day 5 post treatment and analysed for pRb and p15^{INK4b} by Western blot.

In here is shown that activation of Myc by 4-OH-tamoxifen induces senescent phenotype in Suv39h1 proficient MEFs upon exposure to TGFβ-1 as well as in Suv39h1$^{-/-}$ MEFs, as seen by SA β-gal and H3K9me3 staining. MEFs are cellular system in which senescence could be induced even without the presence of functional Suv39h1, as administration of 100 pM TGFβ-1 is able to induce senescence irrespective of the Myc status even in the Suv39h1 deficient MEFs.

This result would argue that Suv39h1 is functioning in a cell/tissue specific manner, and that there are possibly additional histone-methyl transferases (HMTases) able to induce senescent-like arrest, compensating for the Suv39h1 loss. Therefore this system was omitted from further studies presented here.

TGFβ-1 *in vivo* contributes to Myc-induced senescence

The impact of TGFβ-1 signaling on the Myc-driven lymphoma development was tested *in vivo*. For this purpose Eμ-myc mice were exposed daily from the three weeks of age to the drug lisinopril (60 mg/L in the drinking water supply; lisinopril is the angiotensin converting enzyme inhibitor, used primarily to treat hypertension, and was also shown to inhibit TGFβ-1 production [SMN^{+}02]). Mice were monitored for tumor latencies by palpation of peripheral lymph nodes. When animals were at the terminal stage of illness lymph nodes were explanted and subjected to the further analysis (Figure 3.35).

Lisinopril treated mice developed tumors with a median latency of 103 days (compared to the untreated controls P=0,2830; Figure 3.35). When tested for the senescence marker SA β-gal, as well as for the apoptotic marker (TUNEL) lisinopril treated lymphomas have shown reduction in senescence (4.0$\pm$ 1.3%), whereas apoptosis seemed to be unchanged.

To summarize, although treatment with lisinopril did not significantly change time to tumor onset, lymphomas explanted from animals treated with lisinopril showed reduced senescence, without altering the ability of cells to execute spontaneous apoptosis.

TGFβ-1 status in lymphomas with impaired DNA damage response machinery

TGFβ-1 blocker lisinopril decreased intensity of Myc-induced senescence. However, senescence was still detectable, therefore levels of TGFβ-1 protein in animals with and without lisinopril treatment were tested in order to reveal level of the TGFβ-1 reduction. Further, as observed similar senescent reduction phenotype in DDR compromised lymphomas, and previous publi-

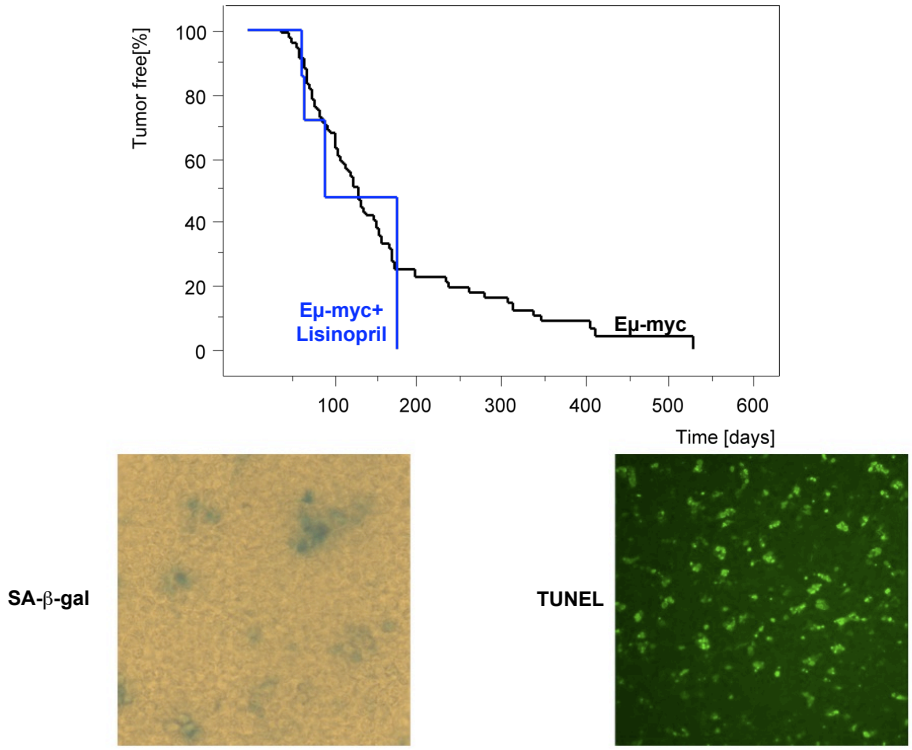

Figure 3.35: Lisinopril treatment reduces senescence, not apoptosis. TOP: Kaplan-Meier "Time-to-tumor-onset" latencies for Eμ-myc+lisinopril (n=7, blue line) and Eμ-myc (n=93, black line). BOTTOM: Top. Sections of cryopreserved lymph nodes from lisinopril treated mice (n=7) were stained for SA β-gal activity. Bottom: Sections of paraffin embedded, formalin fixed lymph nodes from lisinopril treated mice (n=7) were stained for TUNEL activity.

cations have linked TGFβ-1 to induction of ROS, and potential induction of senescence, DDR compromised lymphomas were tested on TGFβ-1 levels as well. Eμ-myc (n=2), as well as Eμ-myc treated with N-Acetylcysteine (n=2), Eμ-myc treated with caffeine (n=2) and Eμ-myc treated with lisinopril (n=2) were tested for the TGFβ-1 expression levels (Figure 3.36).

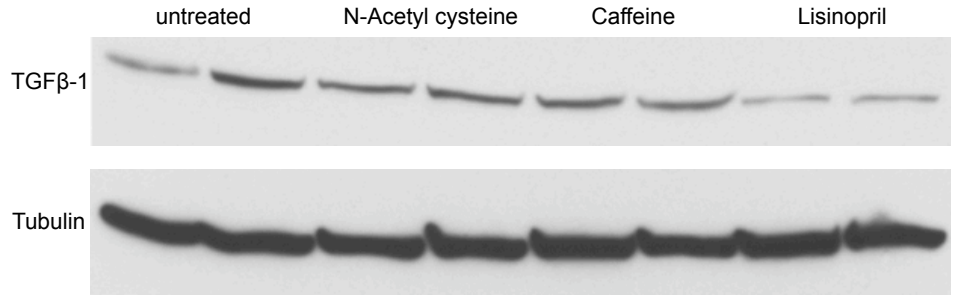

Figure 3.36: TGFβ-1 expression is reduced upon lisinopril treatment and intact under the treatment with agents compromising DDR. Lymph nodes from Eμ-myc mice (n=2) without any additional treatment, Eμ-myc mice treated with N-acetylcysteine (n=2), Eμ-myc mice treated with caffeine (n=2) and Eμ-myc mice treated with lisinopril (n=2) were tested by Westen blot for the TGFβ-1 expression levels. Tubulin was used as a loading control.

As seen here TGFβ-1 levels are not affected by compromised DDR response, arguing that TGFβ-1 mediation could be positioned upstream of the DDR (and for that reason more thorough research on possible DDR malfunctions in lisinopril treated lymphomas would be advisable). However intact spontaneous apoptosis rates in lymph nodes of lisinopril treated mice argue against that. Another possibility is that TGFβ-1 resides in the parallel pathway (for that reason mice treated with both lisinopril as the TGFβ-1 blocker and caffeine or NAC as the DDR blocker should be monitored for the tumor latencies and tested for the complete cessation of senescent phenotype).

Lymphoma microenvironment *in vitro* alters TGFβ-1 expression patterns

As observed earlier in the subsection addressing the tumor microenvironment and senescence, all of the control lymphomas appeared to have multi-focal distribution of senescent cells. Therefore, it was possible that local differences in growth factors as well as oxygen supply might be responsible for the non-homogenous pattern of the senescence positive cells.

To test the possible influence of oxygen tension on the induction of senescence, lymphoma cells were exposed *in vitro* to two different oxygen growth

conditions (21% and 1% of the oxygen, referred as hyperoxia/ normoxia and hypoxia respectively). Please note that 21% of oxygen exceeds levels normally found in tissue, since normal levels of oxygen are approximately 3%, and could reach 1% in not well oxygenated areas of tumor. After 5 days in culture lymphoma cells were tested for TGFβ-1 levels on ELISA assay, and after 10 days in culture RT-PCR analysis was performed and TGFβ-1 transcript was detected in order to see eventual changes caused by hypo- or hyper-oxic conditions (Figure 3.37).

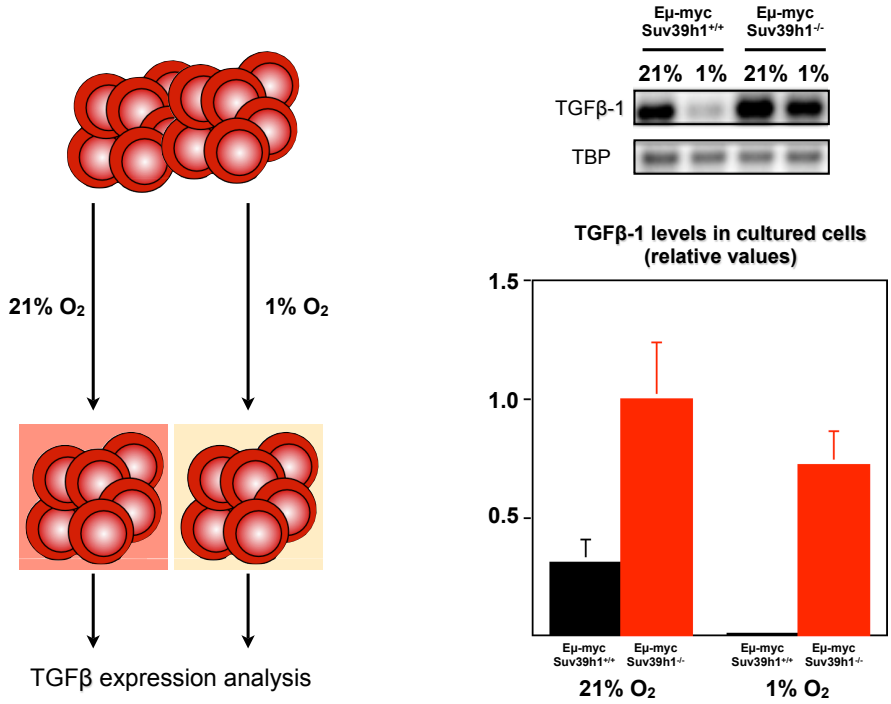

Figure 3.37: TGFβ-1 expression levels change dependent on oxygen conditions in both Suv39h1 proficient and deficient cells. LEFT:Experimental setup: Suv39h1 proficient and deficient lymphoma cells were cultured in 2 different oxygen conditions (21% and 1%). After 10 days in culture RNA was isolated from cells, and tested for TGFβ-1 transcript levels. TOP: Eμ-myc (n=3) and Eμ-myc, Suv39h1 (n=3), TBP was used as a loading control. RIGHT: Eμ-myc (n=3) and Eμ-myc Suv39h1 (n=3) cells were cultured for 5 days days in different oxygen conditions (21% and 1%), and subsequently cell supernatant was tested for levels of excreted TGFβ-1 by commercialy available ELISA assay.

ELISA analysis of lymphoma supernatant revealed higher levels of TGFβ-1 in Suv39h1 deficient cells than in control lymphoma cells. Further, it is shown that TGFβ-1 secretion in both groups (although more pronounced in the control group) is enhanced by higher oxygen levels *in vitro*, arguing that vasculature of tumor could contribute to the TGFβ-1 secretion, as well as to senescence induction.

Concluding, *in vitro* hyperoxic growth conditions can cause an accumulation of TGFβ-1.

3.2 Tumor treatment

One of the main questions concerning tumor treatment is: if cells undergoing treatment have intact machinery that will enable them to execute failsafe programs in a response to conventional chemotherapy. When overexpressed Myc is known to induce a primary apoptotic response, as opposed to Ras/Raf signaling inducing a primarily senescent response [SLM$^+$97]. Previously it was also shown that when treated with anticancer DNA damaging drugs, Myc-driven lymphomas (protected from apoptosis) are able to undergo drug-induced senescence[SWBR$^+$00]. The contribution of senescence to the tumor therapy in a setting where only senescence is specifically genetically terminated was tested.

3.2.1 Suv39h1 deficient lymphoma cells and treatment induced failsafe pathways

Drug-induced apoptosis

Lymphoma cells from different genetic background were tested in their ability to execute drug-induced apoptosis in a response to different concentrations of a DNA-damaging agent [topoisomerase II inhibitor] Adriamycin (ADR) during the course of 24 hours. Viability of cells was assesed by trypan blue dye exclusion. Since ADR is known to induce p53 dependant cell death p53 deficient lymphoma cells were used as a negative control in this setting. Additionally, cells undergone treatment were tested in dual AnnexinV/ Propidium iodide [PI] flow cytometric staining for the determination of apoptotic stage. Annexin V/PI staining is commonly used for distinguishing early to late apoptotic events. PI is the most commonly used dye for DNA content analysis, and also to asses integrity of the plasma membrane, which becomes disrupted in late stages of apoptotic cell death. AnnexinV is detecting relocation of membrane phosphatidylserine (PS) from intra to extracellular surface,

which is an early apoptotic event (Figure 3.38).

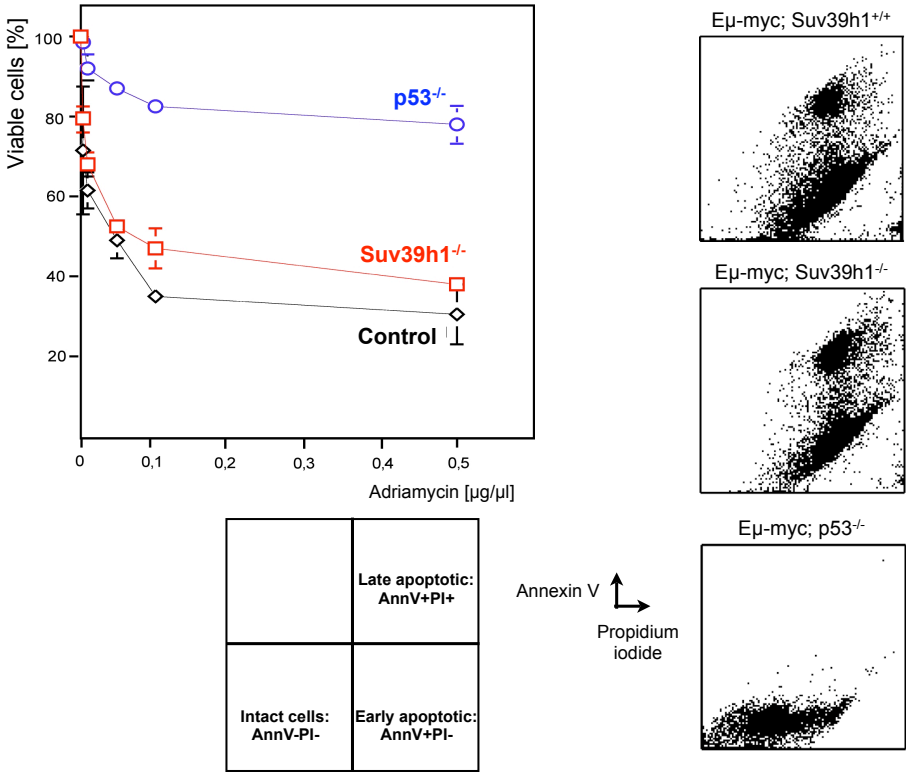

Figure 3.38: Suv39h1 deficient lymphomas are able to undergo drug provoked apoptosis. LEFT. Top: Short term cytotoxicity assay (24 hour exposure to different concentrations of Adriamycin) was assesed in Eμ-myc (black; n=19); Eμ-myc, Suv 39h1 $^{-/-}$ (red; n=12); Eμ-myc, p53 $^{-/-}$ (blue; n=3) (concentrations of Adriamycin were: 0.5μg/μl, 0.1μg/μl, 0.05μg/μl, 0.01μg/μl, 0.005μg/μl). 24 hours post Adriamycin exposure viability was assesed by trypan-blue count. Bottom: Scheme of Annexin V/PI staining: cells can score as intact viable cells (AnnV-/PI-), early apoptostic (AnnV+/PI-) or late apoptotic (AnnV+/PI+). RIGHT: AnnexinV/PI staining of ADR treated lymphoma cells.

As shown in here both Eμ-myc and Eμ-myc, Suv39h1$^{-/-}$ lymphomas retain the ability to execute drug induced apoptosis, leading to further testing on status of Suv39h1 deficient lymphomas in execution of drug-induced senescence.

Drug induced senescence

After observing defects in Myc-induced senescence that Suv39h1 deficient lymphomas are displaying, possibility of Suv39h1 deficient lymphomas displaying similar block of drug-induced senescence in a treatment model was examined. Since there was still no targeted therapeutic aiming only at the senescence machinery, and although senescence is induced by conventional chemotherapy, it is often masked with gross acute apoptotic response, apoptosis was exogenously blocked by stable retroviral transduction with bcl2.

First, apoptotic blocker bcl2 was stably retrovirally introduced into all of the lymphomas tested *in vitro*, then lymphomas were treated with 0.05 μg/ μl ADR, and 7 days post treatment cell cytospin preparations were stained for the senescent marker SA β-gal activity. While Suv39h1 proficient lymphomas displayed their ability to enter senescence upon ADR treatment, Suv39h1 deficient, as well as p53 deficient lymphomas displayed their inability to execute drug-induced senescence (Figure 3.39).

Results shown in here demonstrate inability of Suv39h1 deficient lymphomas to execute senescent arrest in a response to drug therapy. This finding can have important implications in tumor therapy model, which was subsequently tested.

3.2.2 Tumor therapy *in vivo*

In accordance to the observation from section 3.2.1 (i.e. that only control lymphomas retain their ability to enter senescence upon ADR treatment), further analysis was conducted on the impact of Suv39h1 loss on the treatment sensitivity *in vivo*. The disease was recapitulated by transplantation of Suv39h1 proficient and deficient primary lymphomas. 2-3 million of lymphoma cells in 300 μl saline solution suspension was injected into the tail vein of the recipient wild-type mice. Each lymphoma was transplanted into two wild-type syngenic 6-8 weeks old mice, and all of the transplanted lymphomas formed tumors within the range of 20-30 days.

Post transplantation mice were monitored by palpating peripheral lymph nodes every three days, and when lymph nodes were graded as palpable in two consecutive times a single dose (300mg/ kg of body weight) of Cyclophosphamide (CTX) was administered to the mice. Mice were further monitored for the long term treatment outcome. All of the studied lymphomas initially responded to the CTX tretament by regression of tthe palpable lymph nodes, which occured 3-6 days post treatment (Figure 3.40).

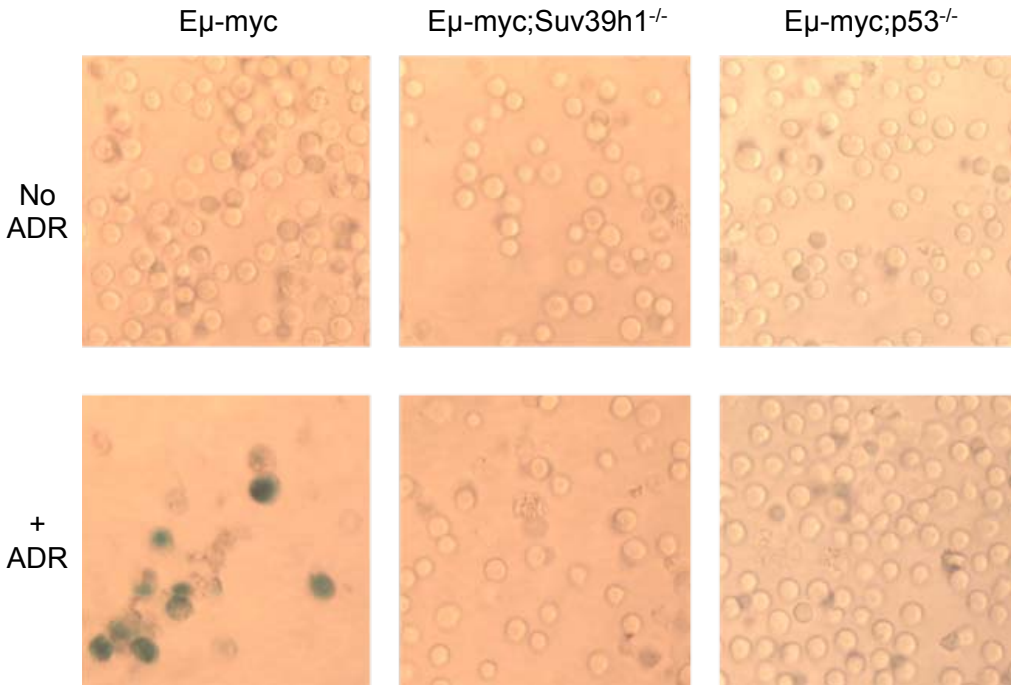

Figure 3.39: Suv39h1 deficient lymphomas fail to senesce upon therapy *in vitro*. Low passage lymphoma cells were retrovirally transduced with a MSCV-bcl2-puro construct, selected with antibiotic for positive clones, and then treated with 0.05μg/μl of Adriamycin for 7 days. Post treatment cell cytospin preparations were stained for the senescence marker SA β-gal in Eμ- myc/bcl2 (n=8), in Eμ-myc,Suv39h1$^{-/-}$/bcl2 (n=6) and in Eμ-myc,p53$^{-/-}$/bcl2 (n=3).

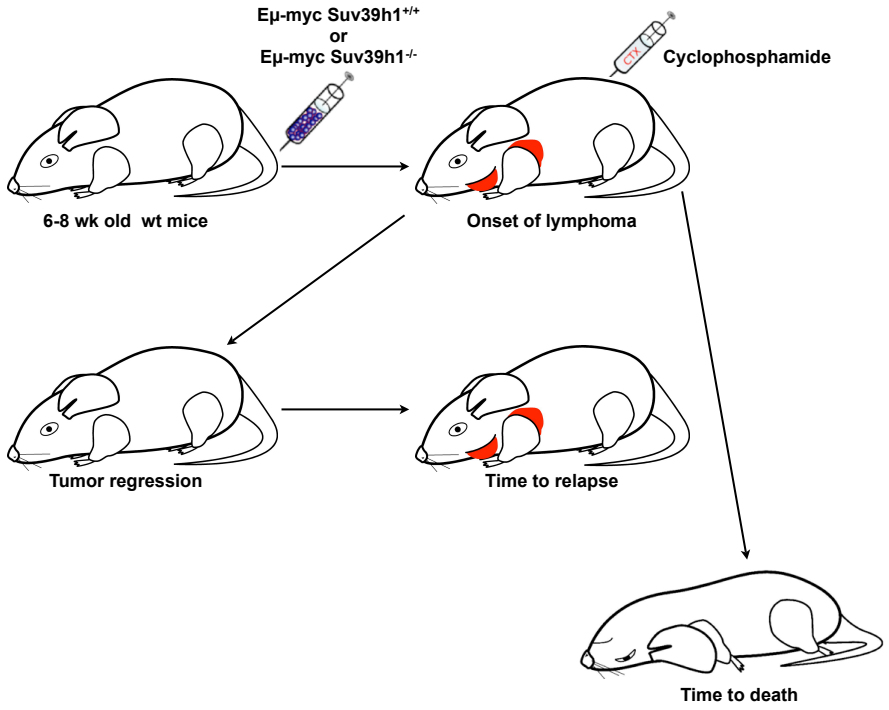

Figure 3.40: Experimental outline for the treatment study. Wild-type mice were transplanted with lymphomas extracted from Eμ-myc, Eμ-myc, Suv39h1$^{+/-}$ and Eμ-myc, Suv39h1$^{-/-}$ mice. Each lymphoma was transplanted into 2 recipient mice. Post transplantation mice were monitored for the onset of the disease by palpation of peripheral lymph nodes. Disease arised in mice 20-30 days post transplantation. At the point of disease occurrence mice were treated with a single dose of Cyclophosphamide and monitored for the time to death or the tumor regression (which occured within 6 days). After mice were graded as tumor free they were monitored for the relapse times for the further 100 days. If mouse at day 100 did not have any visible tumor burden and was not suffering from the severe weight loss it scored as "achieved-long-lasting-remission".

Impaired long term-treatment outcome in Suv39h1$^{-/-}$ lymphomas

After the initial response to the therapy mice were monitored for the 100 days to investigate long-term responses to the therapy. While cohort of control mice achieved long lasting remission in 60% of the cases (15/25), Suv39h1 deficient cohort succumbed to the disease in 80% of the observed cases (13/15) [for the Suv39h1$^{+/-}$ transplantation data, as well as for the bcl2-lymphoma data please check appendices section A.2.1 and A.2.1](Figure 3.41).

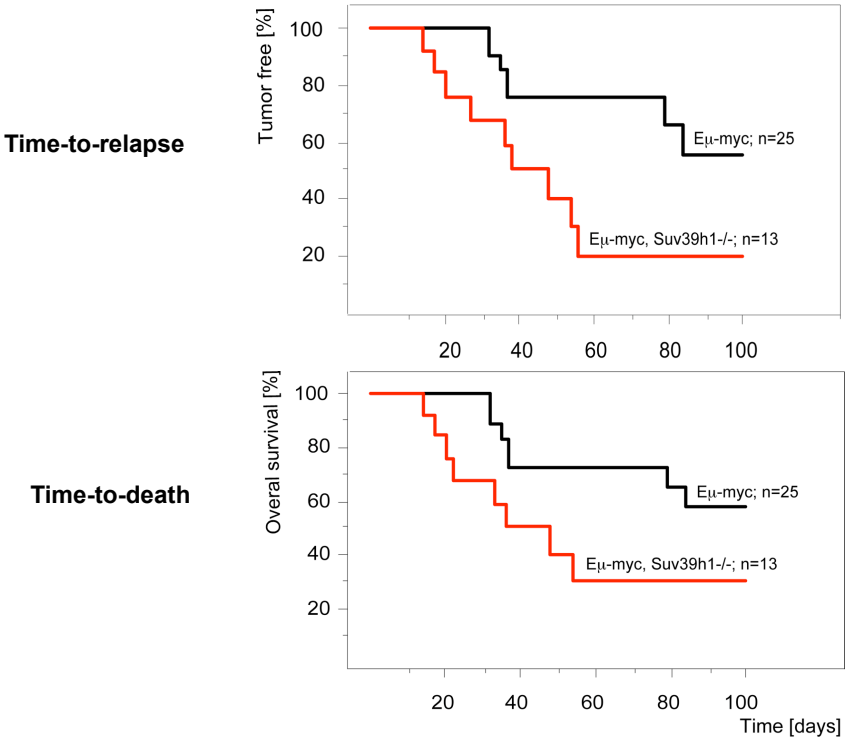

Figure 3.41: Suv39h1$^{-/-}$ lymphomas have inferior long term treatment outcome. TOP: Eμ-myc mice (black line; n=25) and Eμ-myc, Suv39h1$^{-/-}$ mice (red line; n= 15) were monitored for the "Time-to-relapse" latencies (as defined by Kaplan-Meier estimator) post Cyclophosphamide (CTX) treatment. RIGHT: Eμ-myc mice (black line; n=25) and Eμ-myc, Suv39h1$^{-/-}$ mice (red line; n= 15) were monitored for the "Time-to-death" latencies (as defined by Kaplan-Meier estimator) post Cyclophosphamide (CTX) treatment.

Results shown here indicate that animals bearing Suv39h1 deficient lymphomas had faster relapse time as well as reduced overall survival when compared to Eμ-myc mice, indicating that loss of Suv39h1 impairs beneficial long-time response to the therapy.

Correlation between treatment outcome and senescent features of primary lymphomas

As seen previously significant impact of defects in senescent machinery reflect on the long term treatment response. Observing differences in the extent of senescence that each of lymphoma displays, as well as noticing differences in the treatment response of Eμ-myc lymphoma group, a correlation between the two by testing for the extent of senescence (assesed by SA β-gal staining) and comparing it to the long term treatment outcome was attempted to establish here (Figure 3.42) [for the apoptosis data please check appendices A.2.1].

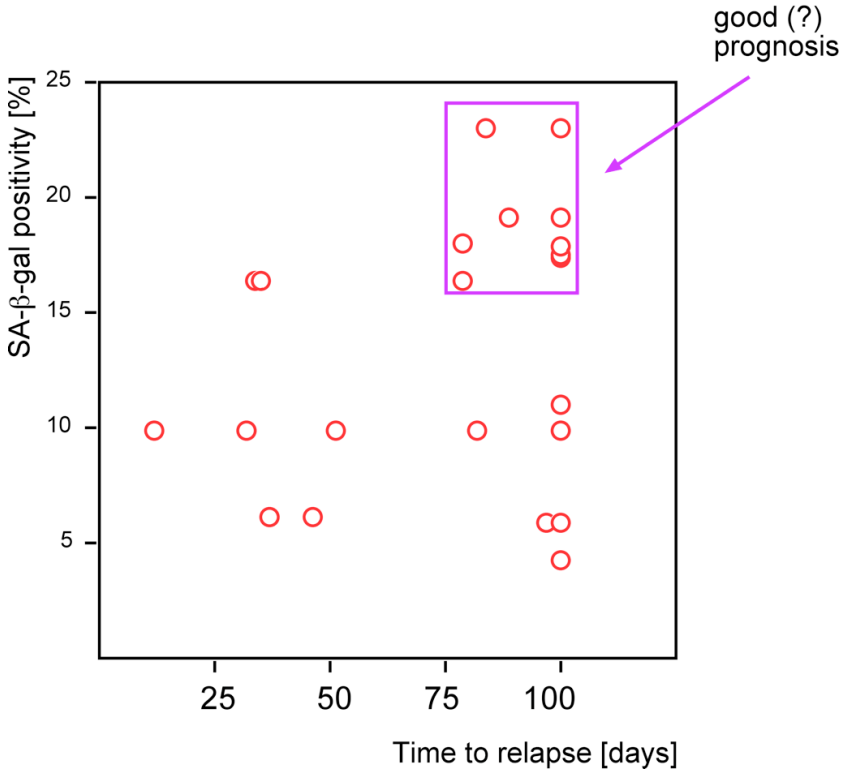

Figure 3.42: Correlation between extent of senescence and response to treatment could potentially be a good prognostic marker. Plot is showing correlation between senescence positivity and the treatment outcome. Group marked as a good prognosis one achieved long term treatment outcome and was highly positive for senescence marker.

Here is observed a moderate dependency between the treatment outcome and the initial senescence positivity of the lymph node. However the association was not tested for the statistic significance, since many of lymphomas

achieved long term treatment outcome, but failed to score high for senescence marker. Therefore SA β-gal should be used together with other senescence markers to further explore this connection.

Chapter 4

Discussion

4.1 Aim and scope of the thesis

The aim of the work presented in this thesis was to investigate the role of Suv39h1 histone methyltransferase in Myc-driven lymphomagenesis *in vivo*, and subsequently to test Suv39h1 contribution to the long term therapy outcome. It was shown in the past decades that most cancers arise as a consequence of insufficient function of cellular failsafe programs. Only recently has research focused on epigenetic alterations as triggers of cancer[FT04]. Epigenetic contribution to the development of cancer is becoming apparent in cases of hypermethylation of promoter regions found in many of the genes in the mammalian genome. These changes are associated with the inappropriate transcriptional silencing of genes and are found as often as disruptions in tumor suppressor genes, they are therefore part of most of the human tumors[JB02]. The epigenetic contribution is further shown by linking changes in post translational histone modifications and development of malignant disease, as is the case presented in this thesis. Lastly, described here is finding of an additional failsafe mechanism mediator, TGFβ, opposing hyperproliferation triggered by Myc-induced signaling and forcing cells to undergo premature proliferative arrest, senescence. Cytokine signaling is a novel concept in the oncogene-induced senescence, and its involvement in senescence induction provides insight into the complexity of senescence regulation.

4.2 Tumor development

4.2.1 Loss of histone methyltransferase Suv39h1 accelerates Myc-driven lymphomagenesis

The Eμ-myc transgenic mouse model is a well established and valuable system to investigate impact of disruptions in apoptotic machinery on B-cell lymphoma development and treatment outcome. Accordingly to previoous reports, as shown in the figure 3.6 all of the mice tested succumbed to B-cell lymphomas. Further, results presented in figure 3.6 of the thesis clearly show that disruption in Suv39h1 gene causes shortened tumor latencies in Eμ-myc. This finding is in accordance to the previous report by Braig *et al* that Suv39h1 histone methyltransferase is a gene with an important role in the execution of the oncogene-induced senescence in Ras-driven tumor setting[BLL$^+$05]. In this model Suv39h1 was identified as a downstream mediator of senescence. Senescence was firstly introduced as an oncogene induced failsafe program in a Ras-overexpressing system[SLM$^+$97], and in the same system it was identified that the Rb-mediated heterochromatin formation is the mechanism leading to transcriptional silencing (senescence)[NNH$^+$03].

However, for oncogenic Myc apoptosis was the first, and until recently the only known failsafe mechanism to prevent uncontrolled proliferation of cells. Therefore results obtained in figure 3.6 reflect critical finding of the work presented in the thesis, that intact Suv39h1 is a prerequisite for longer tumor latencies of Eμ-myc driven lymphomas. Although lymphomas do develop in a setting where Suv39h1 is intact, it became clear that their latencies were about 50 % longer. This finding revealed presence of senescence as a failsafe mechanism in Myc-induced lymphomas. Senescence in this model can be exploited to be investigated as a prognostic indicator as well as to be a basis for a design of a new treatment modalities aiming at the aggressively growing lymphomas.

One of the previous reports revealed that block in the B-cell maturation causes more aggressive phenotype in lymphomas[EWR$^+$99], which could potentially be one of the Suv39h1 mechanism of action. However histology observations in figures 3.2 and 3.3 , as well as results obtained by phenotyping for the B-cell lineage commitment and differentiation in figure 3.4 revealed indistinguishable characteristics in lymphomas arising in both Suv39h1 proficient and deficient animals.

Additional observation in figure 3.6 revealed that the tumor latencies are virtually overlapping for Suv39h1$^{-/-}$ and Suv39h1$^{+/-}$ lymphoma bearing animals. Further examined in figure 3.7 lymphomas arising in Suv39h1

heterozygous background were shown to develop in the cellular environment where the remaining functional Suv39h1 allele is inactivated, which occurs via the random X-chromosome inactivation, therefore making tumors in Suv39h1$^{+/-}$ mice nullyzygous. Process of X-chromosome inactivation, which is normally occurring in female mice should be random, and the cells from the animal, including the B-cells should be in about 50% of the cases Suv39h1 proficient. In the case of Suv39h1 loss tumor cells have an advantage growing in a genetic setting lacking Suv39h1 expression, which is seen by the drastically shortened tumor latencies. This finding, supported by the same pattern of Suv39h1 loss contributing to the shorter survival latencies in the Eμ-N-Ras model[BLL^{+}05] is confirming tumor-suppressive role of Suv39h1 in Myc-lymphoma model.

Concluding from the first part of research presented here intact Suv39h1 gene is important in Myc-driven lymphomagenesis, since disruption in it will lead to significantly faster, however not more aggressive formation of B-cell lymphomas.

4.2.2 Eμ-myc lymphomas enter senescence

Here, for the first time alteration in tumor latencies of lymphomas developing in a Eμ-myc mouse model was linked to the defect in the epigenetic modifications machinery, in particular to the action of Suv39h1 gene. Suv39h1 is a histone methyltransferase, tri-methylating lysine 9 residue on the histone H3 (H3K9me3), and by this methylation it creates docking site for the HP1 proteins, in particular HP1γ, initiating heterochromatin formation. H3K9me3 mark is found to co-localize with senescence associated heterochromatic foci (SAHF) present in senescent cells. Since Suv39h1 is an Rb bound protein, and SAHF are Rb-mediated as well as they map to E2f responsive promoters of the S-phase genes[NNH^{+}03] it was predicted that Suv39h1 is silencing E2f responsive genes. By this silencing Suv39h1 is repressing proliferation, and leading to the cell cycle arrest.

Eμ-myc lymphomas with intact Suv39h1 gene displayed less cells in cycle on account of constant loss of cells into Myc-induced senescence. Lymphoma cells undergone myc-induced senescence displayed all the main characteristic of senescent cells: enlarged size and granularity, tri-methylated mark on histone H3 lysine 9 residue, SA β-gal positivity, as well as accumulation of the HP1γ marks. However, due to technical reasons SAHF are not visible in murine cells, therefore it was not possible to overlay H3K9me3 mark or of HP1γ mark with the DAPI-visualised SAHF regions. Despite this technical difficulties with SAHF visualization, both H3K9me3 and HP1γ marks present usually only in senescent cells were visible only in Suv39h1 proficient

lymphoma cells.

Protein analyses of the Suv39h1 proficient and deficient lymphomas revealed intact senescence machinery only in control lymphomas, as shown by the fraction of hypophosphorylated Rb, as well as by the presence of H3K9me3. This result confirmed that Eμ-myc lymphoma cells are able to enter oncogene-induced senescence program, as observed by histone modifications indicative of chromatin state changes these cells exhibit. Further, Rb signaling is shown to be indispensible for the downstream silencing, as it exists in its "active"/ hypophosphorylated form only when intact Suv39h1 is present.

Senescence was primarily identified as a Ras-inducible program, however since this finding there were reports that senescence can be activated *via* p53 modulation of failsafe machinery pathways. This finding initiated testing on other genetic components of the p53 pathway and their ability to convey signals needed for the senescence induction. Myc-induced senescence was tested on several genes known to be involved in senescence and apoptosis. Results revealed that in the Myc setting $p16^{INK4a}$ is completely dispensable for the senescence induction, as sporadic pattern of senescent cells seems to be unchanged, indirectly confirming previous findings by Krimpenfort *et al* [KQM$^+$01] showing no significant impact of $p16^{INK4a}$ loss on the tumor latencies. However, sporadic senescence pattern was not detectable when genes residing in Arf/p53 pathway were absent, pointing to a crucial role of p53 gene in Myc-induced senescence. Interestingly deletion in ATM, a major DNA damage response mediator did not fully impair senescence induction, directly leading to the idea of a novel mechanism to partially mediate Myc-induced senescence.

Until recently there was a debate whether senescent cells are "end-of-the-tumorigenesis" byproduct, hence being present/accumulated only in the end stage of the tumor, as it was not shown how are senescent cells cleared out of the tissue. Recent finding of Xue *et al* show that tumor cells entering senescence will be removed from the tumor tissue by the immune system. This finding together with our results showing that Myc-induced senescence is a critical tumor suppressive mechanism present as early as in the pre-manifest stage of lymphoma supported the idea of a constant loss/constant production, hence active dynamics of tumor senescent cells[XZM$^+$07].

Taken together, this part of the research has unveiled Myc-induced senescence as an Arf-p53-Suv39h1 dependent program, and unveiled partial dependency upon DNA damage response machinery, as seen by the partial senescence inhibition upon ATM deficiency. Further, oncogene-induced senescence is a dynamic process, starting as early as at the pre-manifest stage of tumor development.

4.2.3 p53 loss in Eμ-myc lymphomas is sufficient to protect from additional Suv39h1 loss

Lymphoma cells with Myc overexpression often exhibit disruptions in apoptotic machinery, caused by loss of tumor suppressor p53 leading to the significantly shortened tumor latencies, displaying more aggressive phenotype[EWR$^+$99]. p53 collaboration with Myc inEμ-myc p53+/- mouse model is well documented through the loss of the additional p53 allele (loss of heterozygosity-LOH)[LHCA86]. Possibility of Suv39h1 defect collaborating with p53 defects were tested in the work presented here. If such a collaboration in the loss of the 2 genes would exist, it would impact tumor latencies in Eμ-myc mice. Results presented in figure 3.12 reveal that tumor latencies are not shortened in Eμ-myc mice with the disruption of p53 and Suv39h1 when compared to the Eμ-myc mice with an intact p53, but disrupted Suv39h1. Further, when lymphomas obtained from the diverse Suv39h1/p53 deficient settings were tested for the intactness of the wild-type p53 allele as well as for the presence of Suv39h1 transcript it was revealed that in the setting with disrupted p53 lymphomas will develop in both Suv39h1 proficient and deficient cells in Eμ-myc, Suv39h1$^{+/-}$ mice. This finding revealed p53 loss as a primary genetic event in Myc-driven lymphomagenesis, which is in line with the current knowledge of p53 being central mediator of both apoptosis and senescence. In this setting losing Suv39h1 expression is becoming redundant, since p53 is co-controlling Myc-induced senescence, and the defects in p53 will therefore be enough to disable both apoptotic and senescent machinery.

This finding is in line with findings of Xue *et al* that p53 activation leads to senescence[XZM$^+$07]. Also, it is shown that p53 action can opt for either apoptosis or senescence; probably much of the decision depends on the tumor cell type. Further, p53 activation in Eμ-myc model is dependent on p19^{Arf}[SMdS$^+$99], finding not observed in many human tumors. Another difference of the mouse system used here is the extraordinary telomere length, which disrupts one of the pathways leading to p53 activation. If p53 pathway is intact is irrespective of Suv39h1 status,however in the case of pre targeted disruptions in both p53 and Suv39h1, p53 will be the first gene to be functionally inactivated, as it mediates both apoptosis and senescence.

4.2.4 Can loss of Suv39h1 be compensated for?

As seen in the Eμ-myc lymphoma mouse model, Suv39h1 is necessary for the mediation of oncogene-induced senescence. However, results obtained using another system: mouse embryo fibroblast (MEF) unveils the possibility of the cell-type specific function of Suv39h1, or a possible compensation by the other

histone methyltransferases, as it was possible to induce senescent-like arrest irrespective of Suv39h1 status. Results obtained in this part of the thesis could question cell-type specific functions of Suv39h1, and could indicate necessity for search of an additional (compensatory) mechanism existing in the mouse embryo fibroblast system.

4.2.5 DDR machinery impacts Myc-induced senescence

DNA damage response (DDR) emerged as an early barrier to the further development of tumor. Outcome of DDR induced signaling can be mapped to apoptosis and senescence, and activated Myc is able to produce DNA damage *in vivo* [VWK$^+$02], directly questioning if a Myc-activation could lead to senescence *via* DNA damage response(DDR). *In vivo* experiments alleviating DDR by either scavenging reactive oxygen species (ROS, by N-Acetylcysteine) or inhibiting kinase (ATM/ATR)-governed DNA double strand break (DSB) checkpoint (by caffeine) revealed reduction, but not the complete absence of sporadic senescence in Eμ-myc lymphomas. Reduction in the senescent phenotype was accompanied either by reduction in apoptosis (as observed in the caffeine treatment approach, in line with its function in degradation of p53 and its nuclear export) or by alterations in apoptosis and proliferation (as described by Reimann *et al* in N- Acetylcysteine approach). Although ablation of senescence *in vivo* by the improperly functioning DDR machinery as a contributing factor to the shortened tumor latencies would be a quite elegant finding, deregulated apoptotic and proliferation machinery in our system prevented resolving the full contribution of DDR to senescence *in vivo* in this model. Persistent Myc-induced DDR is shown to be the upstream mediator of senescence. However, by data shown here it became apparent that DDR is not the only regulator of senescence, as cells are showing reduced sporadic senescence in cases when DDR machinery is blocked.

4.2.6 Cytokine signaling impacts Myc-induced senescence

The gene expression analysis screen was set to identify genes that are deregulated due to the Suv39h1 loss in Myc-lymphomagenesis. TGFβ- induced (Tgfbi or βIGH3) gene was one with the strongest deregulation between Suv39h1 proficient and deficient genotypes. βIGH3 gene was reported to be upregulated upon treatment with differentiation- inducing agents that provoke cellular senescence[DCFR02]. Recent findings show that βIGH3

can also promote metastasis in a colon cancer model[MRR$^+$08]. In Myc-lymphomagenesis model the βIGH3 gene product could be a senescence mediator, acting upstream of Suv39h1. Alternatively, βIGH3 deregulation found as a consequence of Suv39h1 deregulation could serve as an indicator of another mechanism, namely of TGFβ. The identification of TGFβ, a known upstream regulator of βIGH3, as a cytokine displaying higher expression levels when Suv39h1 is ablated, unveiled cytokine-mediated senescence as a component of Myc-induced senescence. Research conducted in this thesis did not reveal the stage in tumor development when TGFβ starts mediating senescence, therefore it is possible that the DNA damage response machinery could serve as a primary mechanism of senescence mediation[VWK$^+$02], later accompanied by TGFβ.

TGFβ is a potent cytokine, with a very complex function, being inducer of the arrest in the late G1 phase of the cell cycle by inhibition of CDKs which phosphorylate pRb and other components [LDL$^+$90],[KOP$^+$93], or a driving force in the tissue growth and morphogenesis in embryo[HMF$^+$87]. TGFβ upregulates p15^{INK4b} and induces cell cycle arrest by directly inhibiting CDK4/6 and by indirectly inactivating cyclin E/ CDK2 *via* the displacement and shuttling of p27^{Kip} from CDK4/6 to cyclin E/CDK2[KOP$^+$93]. Findings of this thesis did not shown that there is a difference in the expression of p15^{INK4b} depending on the Suv39h1 status. However, there was found an increased expression of p16^{INK4a}, proposing an alternative TGFβ-mediated signaling cascade in Eμ-myc induced senescence. Elevated p16^{INK4a} levels in the context of elevated cyclin E levels would also suggest for the impairment in p27^{Kip} function, however p27^{Kip} was tested and its function seems to be intact, arguing again for the alternative mechanism connecting TGFβ signaling to p16^{INK4a}. Further experiments have to be conducted in order to verify this hypothesis. As previously shown, much of TGFβ functions are time and cellular context dependent. As reported in the breast cancer model TGFβ acts at an early stage as a tumor suppressor, changing it's function at more advanced stages of cancerogenesis, where cancer cells are able to bypass primary TGFβ tumor suppressive functions and use it for their own advantage[AFG99],[Gol99]. This could be the case in already end-stage lymphomas of Eμ-myc mice and could explain that p15^{INK4b} is not anymore necessary for the arrest state. If TGFβ can signal through p16^{INK4a} it would still be mediating senescence in a late-stage tumorigenesis.

Experiments conducted here showed if apoptosis is blocked, Suv39h1 proficient cells will arrest in senescence-like mode, while Suv39h1 deficient cells, as well as p19^{Arf} and p53 deficient cells will continue their growth. This experiment established TGFβ's potential in inducing senescence arrest *in vitro*. After cell culture propagation differences in levels of TGFβ expression

remained unchanged in lymphoma cells, indicating that they may be the source of TGFβ.

One of the possible modes of TGFβ production regulated is by the different oxygen conditions cell is exposed to *in vitro*. This finding was supported by the *in vivo* finding of more senescent cells being detected in the proximity of the blood vessels. Although only correlative, these two findings point out that TGFβ could be more concentrated around the well oxygenated areas in tumor. Here should be taken in consideration the fact that HIF-1α , present in the hypoxic areas will be inducing angiogenesis[Sem00], which makes it hard to claim that these areas are all equally well oxygenated. Therefore further set of experiments with substances like pimonidazole ("hypoxia marker") tracking oxygenation *in vivo*[BRD02] should be used to test the correlation of oxygen levels in the areas with high senescence positivity. Also, impact of the TGFβ signaling on DNA damage response (DDR) and possible colocalization with reactive oxygen species (ROS) should be investigated, as ROS are also found to be more abundantly present in well oxygenated areas. *In vivo* treatment with a potential TGFβ-1 blocker revealed reduction in senescent phenotype in Eμ-myc lymphomas, although there was no significant shift in the tumor latencies found. Protein expression levels of TGFβ-1 were tested and it was established that there is only partial reduction as a response to this treatment, which might be the reason of not observing more solid differences in tumor latencies.

Myc-induced, cytokine mediated senescence is a novel concept providing more insight into the at least dual regulation of senescence (cytokine and DNA damage response mediated).

4.3 Tumor treatment

Tumor model used in this thesis is a Burkitt's like B-cell lymphoma. Burkitt's lymphoma is a childhood tumor, characterized by reciprocal translocations between the cMyc gene on chromosome 8 and one of the immunoglobulin (Ig) loci on chromosome 2, 14 and 22[Kle89]. The hallmark of Burkitt's lymphomas is constitutively activated cMyc gene driving tumor growth[HA00]. Further, mutations of p53 were found in more than 30% of Burkitt's lymphomas, additionally p16^{INK4a} is silenced *via* hypermethylation[GBG$^+$91],-[KOM$^+$98]. Tumors developing in Eμ-myc mice also carry mutations in p53 (30%) and INK4a/Arf deletions (20%) [EWR$^+$99]. Lymphomas lacking INK4aArf locus displayed the same characteristics as p53 mutated lymphomas, their latencies were shortened on account of aberrant apoptosis-[SMdS$^+$99].

When aggressively growing Myc lymphomas received standard treatment with cyclophosphamide they entered longer remission periods, and many of them even achieved long lasting remissions, when compared to mice bearing lymphomas with disrupted p53, in a setting with and without external apoptotic block[SL02]. Data presented by Schmitt *et al* had shown that Myc-lymphomas can utilize prognostically valuable program of drug induced senescence only when p53 remains intact. Results in this thesis show that lack of the functional Suv39h1 leads to significantly inferior treatment responses *in vivo*. Although Suv39h1 deficient lymphomas are able to execute drug induced apoptosis they fail to execute drug induced senescence *in vitro* and *in vivo*. Their inability to execute senescence *in vivo* leads animals bearing Suv39h1 deficient lymphomas to relapse shortly after remission is achieved. Their initial response revealed their capability to execute drug induced apoptosis *in vivo*, and their shortened relapse latencies revealed dysfunction in another mechanism that seems to be intact in the Suv39h1 proficient lymphomas, later revealed by the experiment with an apoptosis blocker to be the senescence. However, due to the low number of animals tested in the experiment with the apoptosis block, it would be reasonable to increase the number of animals for reaching the statistical significance. Additionally it was observed that the difference in the extent of the sporadic senescence varies even within the group of Suv39h1 proficient mice, this could be the factor influencing final outcome to the therapy. When extensively tested a weak correlation between senescent phenotype and a relapse latencies occurred. However it should be mentioned that only one of the available markers for senescence was used, and that by broadening the panel of markers for senescence in the future one could possibly make a better estimation then the one observed here. Concluding from the treatment data: senescence disruption by Suv39h1 impairment leads to the significantly shorter relapse times in Eμ-myc mice, resulting in the inferior treatment outcome.

4.4 Future prospects

Myc was identified more than 2 decades ago as the oncogene which is deregulated by Ig translocations in B-cells [DFMG$^+$83], and it was used in mouse models of cancer to mimic Burkitt like B-cell lymphomas found in humans[VH06]. Recently models of sporadic Myc oncogene activation emerged[CRS$^+$08], which recapitulate disease onset in humans more accurately, and would be a valid model to use in the future research. In this thesis efforts have been made to discover an additional factor triggering oncogene-induced senescence. Recent reports have pointed out that the cytokine signaling

plays a central role in both apoptosis and senescence[KMV$^+$08],[AOB$^+$08],-[WSZ$^+$08]. Here is proposed cytokine TGFβ mediation of the senescence induction. Further research on this topic would require series of data revealing the role, mechanism and the regulation of the production of TGFβ in the induction of senescence in lymphoma model. Also, now it is known-[KMV$^+$08],[AOB$^+$08],[WSZ$^+$08] that there are other cytokines eliciting the same senescent response as TGFβ-1 does in Myc-driven lymphomagenesis as tested here. Therefore additional cytokine profiling would reveal if TGFβ is the only deregulated cytokine in this model, or if there are other cytokines contributing to the senescence phenotype observed in the current research. One of the approaches to further specifically dissect TGFβ impact could be treatment of mice at a risk of developing Myc-driven lymphomas with one of the reported TGFβ inhibitors[INC$^+$02],[DBMLR04],[YDT$^+$02]. Also, it would be necessary to expand testing to the pre-manifest stage of the lymphoma development, as TGFβ is reported to have mostly dual action in the tumor development, changing from anti- to pro- tumor survival, therefore comparing pre-manifest stage with a manifest stage of a tumor could provide some clues on how does TGFβ function in this model.

One of the key findings of this thesis was that Myc overexpression is inducing senescence *in vivo*, however induction of senescence in Myc driven lymphomas *in vitro* could not be shown. One of the reasons might be the "cell culture shock", since culture conditions differ greatly from the *in vivo* conditions in which these lymphomas are formed and grown. So far there was only one report of Myc-induced senescence in *in vitro* setting, for human diploid fibroblasts cell model[DRJ$^+$03]. Although this finding indicates that there is such *in vitro* senescence induction, there are no other reports confirming this findings in other cell models. Another conflicting finding, by Wu *et al* [WvRY$^+$07] shows that upon inactivation of Myc in tumors senescence is triggered, this work was dealing with a "oncogene-inactivation-induced-senescence" (OIIS) model, in which upon Myc-inactivation in a different model there is onset of senescence. However, senescence occurred shortly after Myc-inactivation and was present during a period of few days and then was again undetectable, which would indicate that there might be a residual activity of Myc-overexpression induced machinery able to induce senescence. This work was done in another model, and possible differences arising as a consequence of a work in the different cell context should not be excluded.

Although until recently only apoptosis is found to be triggered by Myc's overexpression[LHCA86], senescence became interesting mechanism in a context of Myc action. Presence of Myc induced senescence was shown to exist as early as in the pre-manifest stage [BHK$^+$05], and as shown here is contributing to the anti-proliferative failsafe machinery with the same percentage of

arrested cells as does apoptosis.

Here is shown that the oncogene-induced senescence is dependent on intact Suv39h1 in a Myc-driven lymphoma model, starting to functioning as early as the pre-manifest tumor stages. Also, lymphomas developed in Eμ-myc animals lacking p19^{Arf} or p53 are not displaying any sporadic senescence, which is in line with their tumor development kinetics. This finding underlines necessity of p19^{Arf}-p53 signaling cascade for proper functioning of both failsafe pathways. It would be interesting to further study if these lymphomas are missing H3K9me3 mark in its entirety. It would also be important to find if the cells of pre-manifest lymphomas of p19^{Arf} or p53 deficient animals could induce senescence despite non functional p19^{Arf}-p53 cascade, revealing if there might be another mechanism governing Myc-induced senescence in a stage where tumor is not fully developed.

This another mechanism mediating senescence could be TGFβ related. It is known that TGFβ is able to block endogenous Myc[AM95], however when Myc is under the Eμ promoter TGFβ will not be able to block it, as shown by equal expression levels of Myc protein in both Suv39h1 proficient and deficient lymphomas. Also, It is important to note that TGFβ action on the plethora of the genes deregulated in Myc-driven lymphoma model was not investigated, which would be an interesting set of experiments for the future researcher on this topic. Role of TGFβ in the DNA damage response (DDR) machinery is not fully investigated. Some reports shown that TGFβ silences BRCA1 dependent DDR *via* SMAD3[DKL^{+}05], this provided an insight into DDR regulatory role of TGFβ. This finding has not yet been addressed in a lymphoma mouse model. Compromised DDR machinery (using caffeine or N-Acetylcysteine[NAC] treatment *in vivo*) partially impairs senescent response, however not in its entirety. Attempts to block TGFβ signaling *in vivo* by using drug lisinopril (angiotensin converting enzyme inhibitor[SMN^{+}02]) elicited similar senescence phenotype as treatment with NAC or caffeine aiming to compromise DDR machinery. Reduction in sporadic senescence without significant difference in the tumor onset latencies was observed, which might be due to only about 50 % reduction in TGFβ protein levels. Answer if TGFβ and DDR signaling reside in the same pathway or are 2 independent pathways mediating senescence in Myc-induced lymphomagenesis could be provided by combination of treatments that are blocking both TGFβ and DDR action. This experiment could prove to be hard to conduct as all of the so-far tested compounds also invoke other cellular effects.

It was reported by Knies-Bamforth *et al* [KBFP^{+}04] that widespread Myc expression can induce angiogenesis in hypoxic areas of tumor. The work in this thesis suggests oxygen tension has an impact on the induction of senescence, as seen by co-localization of staining for the blood ves-

sel marker (CD31) with the senescence marker (SA β-gal). In some views hypoxia might be the trigger of senescence[MK06], which is challenged by finding that hyperoxic environment contributes to the increase of reactive oxygen species (ROS), directly triggering the DNA damage, and leading to senescence[ZLSP05]. It was shown by the work from Evan group that interleukin1γ is mediating Myc-dependent angiogenic switch in pancreatic cancer cells[SSR$^+$06]. It was shown that hypoxic stress induces G9a methyltransferase activity, leading to the increased global H3K9me2 patterns[CYD$^+$06], and it would interesting to test impact of hypoxic stress on Suv39h1 activity. It would be interesting to obtain data in the respect to connection of TGFβ and reactive oxygen species (ROS), oxygen tension in lymphomas *in vivo*, since *in vitro* experiments so far were conducted in highly non-physiological conditions. One of the key experiments in respect to TGFβ's role in Myc-driven lymphomagenesis would be *in vivo*, crossing between Eμ-myc and TGFβ knockout animals, unfortunately this is not achievable since TGFβ knockout mice succumb to a wasting syndrome accompanied by a multifocal, mixed inflammatory cell response and tissue necrosis (leading to organ failure) about 20 days after birth[SOK$^+$92]. Conditional knockout of TGFβ-RI could prove to be equally good model for investigating a role of TGFβ in Myc-driven lymphomagenesis[HBK$^+$07]. In this model TGFβ might exert its action on cyclin E, as observed in slight deregulation of cyclin E regulation between Suv39h1 proficient and deficient groups. Discrepancy observed in the p27^{Kip} expression levels in respect to the cyclin E expression levels could also be due to the more direct action of TGFβ on cyclin E[KOP$^+$93]. However, if and why TGFβ has more pronounced impact on Suv39h1 proficient lymphoma molecular machinery should be investigated in the full detail. In the recent view of the cytokine mediated (or enhanced) senescence one could argue that a senescent cell would be able to change proliferation status of its neighboring cells, in this respect full cytokine profile of tumor cells should be investigated.

One of the recent, and very important points of clearance of senescent cells in the tumor system has been shown for the the liver tumor. In this system senescent cells are cleared from the tissue by the immune system[XZM$^+$07], this finding showed that senescence has properties of a dynamic process (as apoptosis). This finding should be tested in lymphoma environment, to confirm if the same clearance by immunological system applies. The question of actual dynamics of clearance of senescent cells as opposed to dynamics of cytokine signaling and impact on the possible arrest could be tested in future.

The second part of the work is focused on the therapy induced senescence as a beneficial program that might enhance better outcome to the tumor ther-

apy. Eμ-myc, Suv39h1 model presented in this thesis is one of the first genetic models *in vivo* dealing with the question of contribution of senescence to the treatment outcome. However, as Suv39h1 function seem not to be impaired in human lymphoma patients it is important to investigate function of other histone methyltransferases (HMTase). Indeed, there are HMTases (like Riz1) found to be mutated in human cancers, mechanistically fitting the epigenetic involvement in the senescence model theory. In the past years an exploding new field of research appeared which is directed towards histone demethylases. Currently there are two models present describing possible mechanisms that cell employs in order to continuously counteract H3K9 HMTase activities, acting both in eu-chromatin and hetero-chromatin. One of these models states that mutations in lysine demethylase will cause a disruption in the heterochromatin status. It has been shown that lysine demethylase hLSD1[SLM$^+$04] is capable of demethylating H3K9[MWY$^+$05], following by demonstration of LSD1's H3K9 demethylase activity *in vivo* [LZV$^+$07]. Of a particular interest in a context of Suv39h1 would be a specific histone K3 (trimethylated lysine) demethylase JMJD2a and JMJD2b (Jumonji domain containing 2a and 2b), since they would be able to counteract actions of Suv39h1 on the histone H3 lysine residues. Recent characterization of a broad spectrum of cancers revealed presence of the chromatin changes in the tumor suppressor or proto-oncogenes, and in turn their deregulated transcription will enhance cancer progression[Est07]. Future biochemical experiments (immunohistochemistry for a diverse range of histone methylases or histone demethylases) on human lymphoma samples might teach us more about involvement of other HMTases or equally important histone demethylases in these processes, and might help to design better strategies for the cancer treatment.

In summary,

The origin of cancer is shaped by the alterations in oncogenes and/or tumor suppressor genes, which can be accomplished amongst other by modifications in the "histone code". This shows complexity of the tumor formation, since main mutation leading to tumorigenesis is often accompanied by additional changes, each of them giving specific selective advantage to the tumor cell. Fate of the tumor cell is dependent on the mutations it accumulated throughout time. Research described in this thesis takes advantage of several features of the tumor suppressor Suv39h1:

1. Suv39h1 loss collaborates efficiently with the Myc overexpression during lymphomagenesis, as shown by the observation that tumors arise in Suv39h1 deficient mice with significantly shorter tumor latencies.

2. Suv39h1 loss elegantly ablates oncogene-induced senescence providing a straightforward model to test impact of drug induced senescence on the long term therapy.

This study underscores the requirement for the active Suv39h1 in senescence pathway when Myc is overexpressed, directly showing that this process is governed by epigenetic alterations. By further analysis it is revealed that senescence in Myc-induced lymphomagenesis requires the cytokine TGFβ signaling pathway as well as the DNA damage pathway.

Concluding, as observed in the treatment studies with the genetic ablation of senescence *in vivo*, this is a potent mechanism of tumor treatment, equally important as apoptosis, and one that can be exploited in the further clinical studies.

Appendix A

Appendices

A.1 Tumor development

A.1.1 Defects of failsafe machinery in Suv39h1 deficient lymphomas

Impact of loss of genes implicated in failsafe pathways on senescence machinery

Eμ-myc mice were crossed to either p19$^{Arf+/-}$ or p16$^{INK4a+/-}$ mice and monitored for tumor latencies by palpation of peripheral lymph nodes every three days. Latencies were plotted as a Kaplan-Meier "Time-to-tumor onset" plot (Figure 58). All of the animals succumbed to B-cell lymphoma; with the time to tumor onset in Eμ-myc, p19$^{Arf-/-}$ (n=6) being 56 days and in Eμ-myc, p19$^{Arf+/-}$ (n=4) being 30 days. Eμ-myc, p16$^{INK4a-/-}$ mice (n=2) succumbed to the lymphoma at median age of 147 days, and Eμ-myc, p16$^{INK4a+/-}$ (n=15) at the median age of 170 days (Figure A.1).

A.1.2 DNA damage analyses in Myc lymphomas

Disruption of DDR checkpoints in Myc-induced lymphomas

Caffeine was administered *via* the water supply to Eμ-myc and the wild-type mice starting from their birth (0.4 mg/ ml). Caffeine administration significantly decreased tumor latencies in the Eμ-myc mice, but did not interfere with the life expectancy of the wild-type mice (n= 3, Figure A.2).

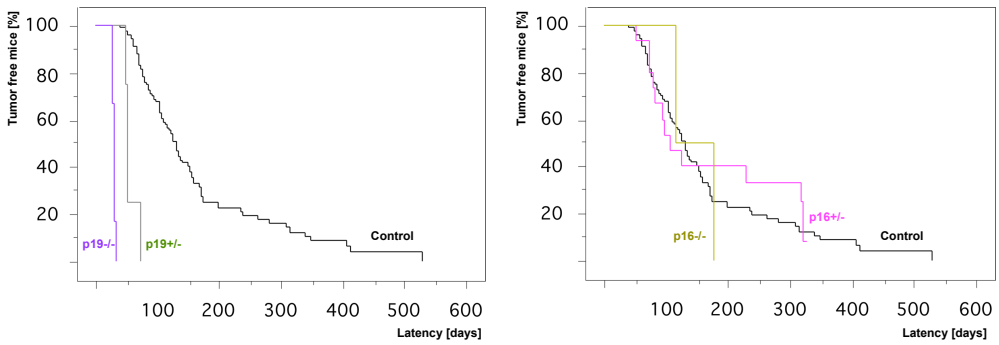

Figure A.1: Defects in p19^{Arf}, but not in p16^{INK4a} accelerate Myc-lymphomagenesis. LEFT: Kaplan-Meier "Time-to-tumor-onset" latencies plot: Eμ-myc, p19$^{Arf-/-}$ (6; magenta line); Eμ-myc, p19$^{Arf+/-}$(n=4; gray line). RIGHT: Kaplan-Meier "Time-to-tumor-onset" latencies plot: Eμ-myc, p16$^{INK4a-/-}$ (n=2; green line); Eμ-myc, p16$^{INK4a+/-}$(n=15; pink line) were compared to Eμ-myc (n=93; black line).

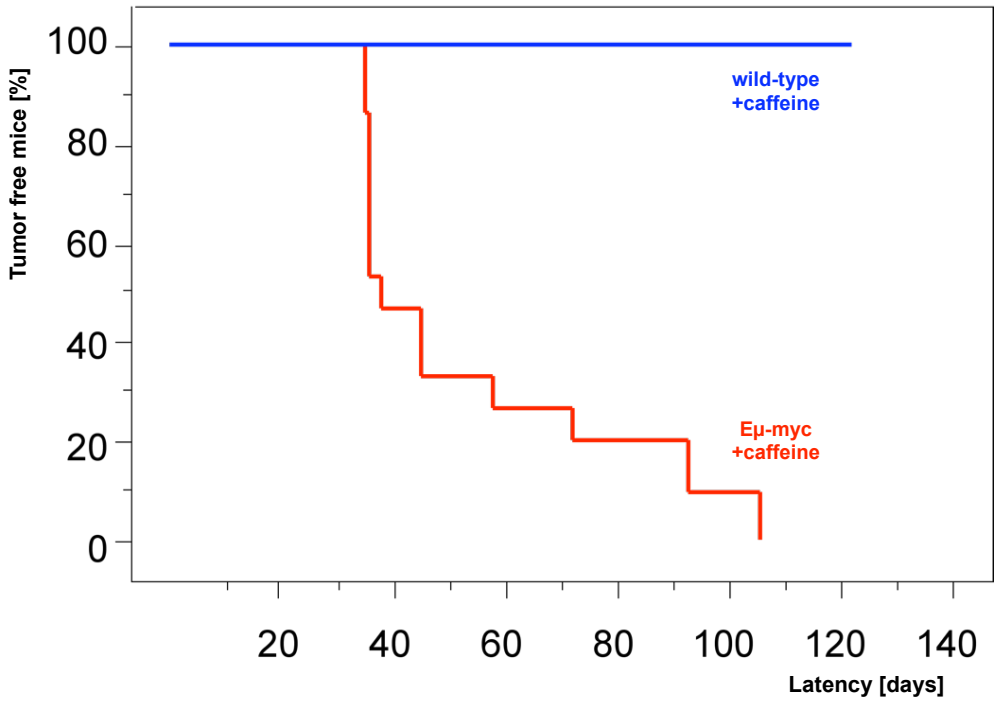

Figure A.2: Kaplan-Meier "Time-to-tumor-onset" latencies in Eμ-myc mice treated with caffeine (n=15, red line) compared to the wild-type mice (n=3, blue line) treated with caffeine.

A.1.3 Triggers of Myc-induced senescence

Validation of candidate genes involved in senescence

Semi-quantitative RT-PCR analyses were directed towards validating previously found deregulated gene expression caused by loss of Suv39h1. In addition to the lymphomas used for the gene-expression analysis more primary lymphoma samples were analyzed for: Taf4B [TAF4b RNA polymerase II, TATA box binding protein (TBP)-associated factor], Mei1 [Meiosis defective 1], Myst 4 [Myst histone acetyltransferase (monocytic leukemia) 4], Ryk [Receptor tyrosine kinase], Lsp1 [Lymphocyte specific protein 1] and Cul 2 [Cullin 2, Ubiquitin protein ligase binding]. Lymphomas were tested before and after propagation *in vitro*, in order to establish source of gene expression (by propagation *in vitro* lymphoma cells outgrow bystander cells, figure A.3).

Levels of TGF β-2 and TGF β-3 transcripts are not differing between the genotypes (Figure A.4).

TGF β-1 gene and its role in senescence

In order to unveil accute response to TGF β-1 signaling in lymphomas Suv39h1 proficient and deficient cells were exposed for 24 hours to 100 pM of TGF β-1 and subjected to the genome-wide expression analysis. Genes found to be differentially expressed were validated by semi-quantitative RT-PCR analysis (Figure A.7).

TGF β-1 induced βIGH3 was also shown (Figure A.8).

A.1.4 Influence of acute Myc and TGFβ-1 induction on senescence execution

In mouse embryo fibroblasts (MEF) with different Suv39h1 status inducible Myc-protein was introduced by means of the stable retroviral transduction [4-hydroxy-tamoxifen (4-OHT)-inducible Myc protein fused to a modified estrogen receptor component (Myc-ER)]. MEFs were tested by Western blot analysis for the Myc-levels post stable transduction (Figure A.9).

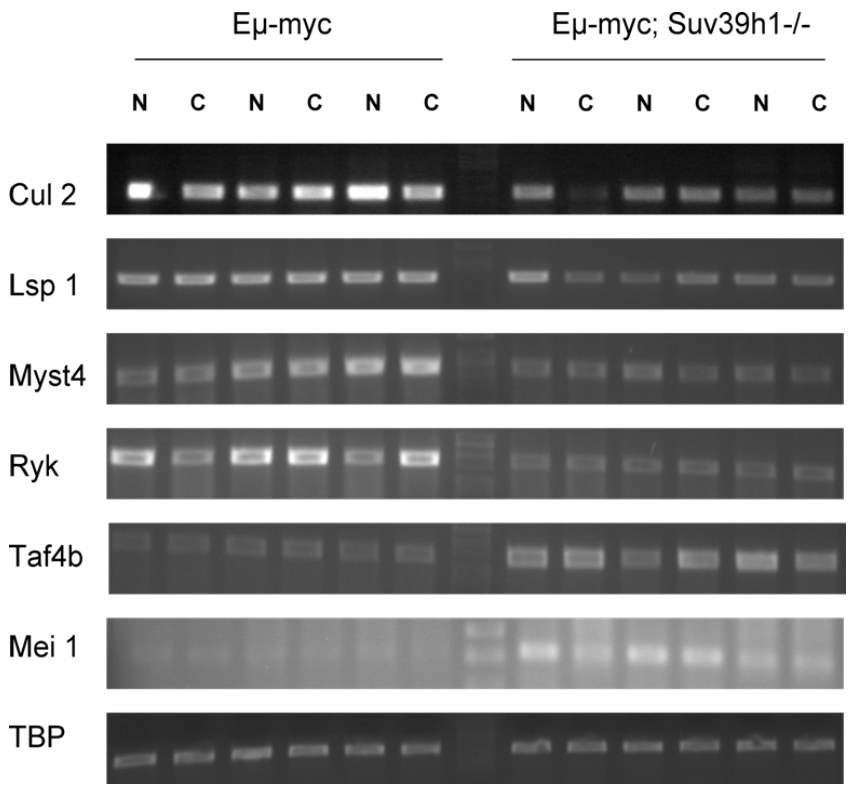

Figure A.3: Validation of microarray results, differentialy regulated genes were tested by RT-PCR analysis. Additional genes were tested on RT-PCR level for the expression of the following genes: Cul2, Lsp 1, Myst4, Ryk, Taf4b and Mei, on freshly isolated lymphoma cells from Eμ-myc (n=3) and Eμ-myc Suv39h1$^{-/-}$ (n=3) (marked as non cultured lymphomas, N) as well as 10 days cultured lymphoma samples (marked as C). TBP was used as a loading control.

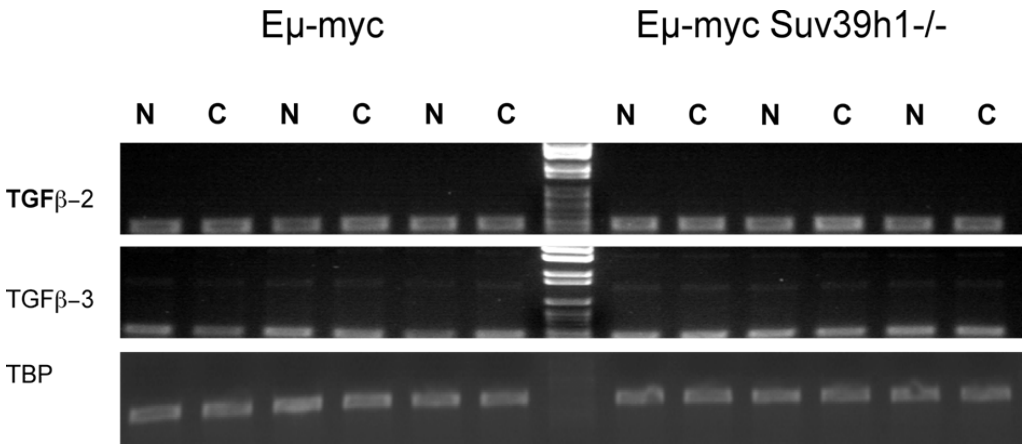

Figure A.4: TGF β-2 and and -3 transcripts remain unchanged in lymphomas with different Suv39h1 status. Expression of the TGFβ-2 and -3 genes was tested by semi-quantitative RT-PCR on freshly isolated lymphoma cells from Eμ-myc (n=3) and Eμ-myc Suv39h1$^{-/-}$ (n=3) (marked as non cultured lymphomas, N) as well as 10 days cultured lymphoma samples (marked as C). TBP was used as a loading control.

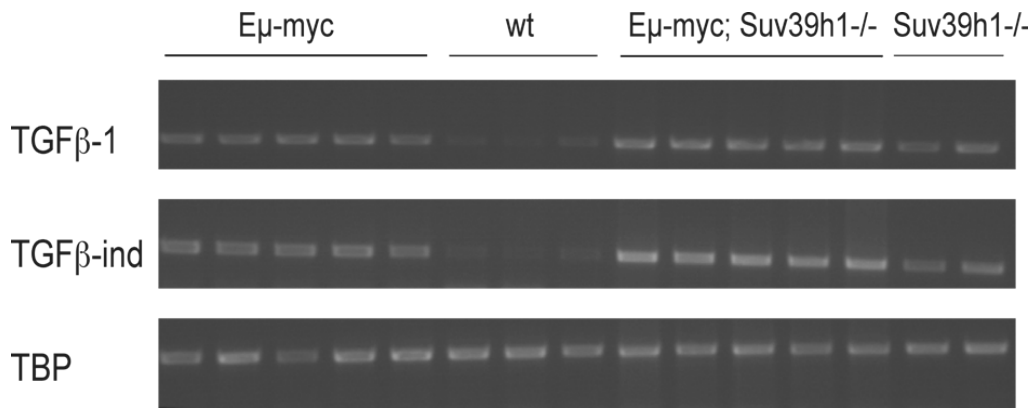

Figure A.5: TGFβ-1 is the upstream regulator of TGFβ-induced (βIGH3), and shows deregulation in expression depending on Suv39h1 status. TGFβ-1 levels were tested by semi-quantitative RT-PCR. TGFβ-1 transcript levels were tested on freshly isolated lymphoma cells from Eμ-myc (n=5) and Eμ-myc Suv39h1$^{-/-}$ (n=5) animals, B-cells from the wild-type animals (n=3) and Suv39h1-/- animals (n=2). TBP was used as a loading control.

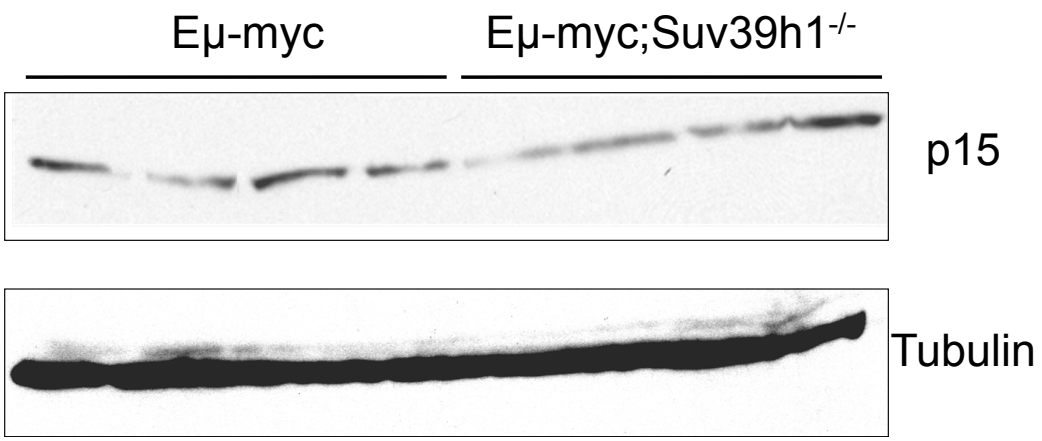

Figure A.6: $p15^{INK4b}$ protein levels do not differ between Suv39h1 proficient and deficient lymphomas. $p15^{INK4b}$ levels were tested by Western blot on freshly isolated lymphoma cells from Eμmyc (n=4) and Eμ-myc Suv39h1$^{-/-}$ (n=4) animals. Tubulin was used as a loading control.

A.2 Tumor treatment

A.2.1 Tumor therapy *in vivo*

Impaired long term-treatment outcome in Suv39h1$^{+/-}$ lymphomas

The disease was recapitulated by transplantation of Suv39h1 proficient and deficient primary lymphomas. 2-3 million of lymphoma cells in 300 μl saline solution suspension was injected into the tail vein of the recipient wild-type mice. Each lymphoma was transplanted into two wild-type 6-8 weeks old mice, and all of the transplanted lymphomas formed tumors within the range of 20-30 days.

Post transplantation mice were monitored by palpating peripheral lymph nodes every three days, and when lymph nodes were graded as palpable in two consecutive times, a single dose (300mg/kg of body weight) of cyclophosphamide (CTX) was administered to the mice. Mice were further monitored for the long term treatment outcome. All of the studied lymphomas initially responded to the CTX tretament by regression of the palpable lymph nodes, which occured three to six days post treatment.

Two Kaplan-Meier plots show "Time-to-death" latencies and "Time-to-tumor-onset" latencies in Eμ-myc, Suv39h1$^{+/-}$ mice (Figure A.10).

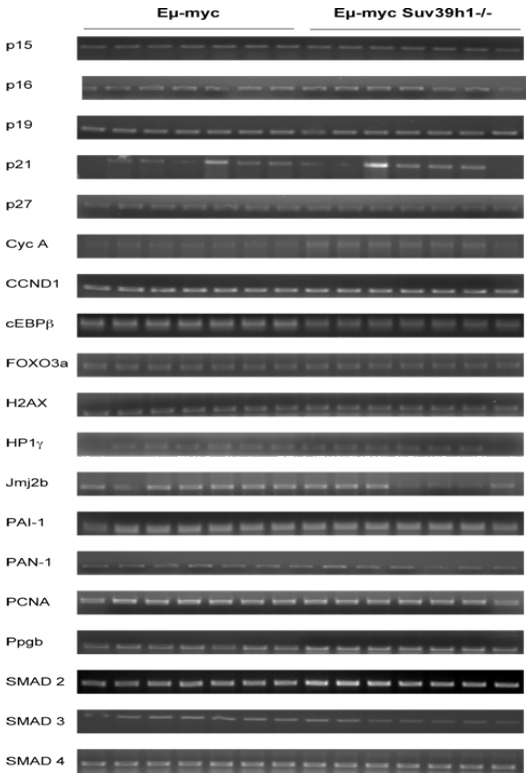

Figure A.7: Semi-quantitative RT-PCR validation of genes found differentially expressed in the second genome-wide expression analysis. Differential expression of genes in the response to TGF β-1 signaling (upon treatment with 100pM of TGFβ-1) was found in TGFβ-1 treated (100pM) lymphoma cells from Eμ-myc (n=7) when compared to Eμ-myc Suv39h1$^{-/-}$ (n=7) animals.

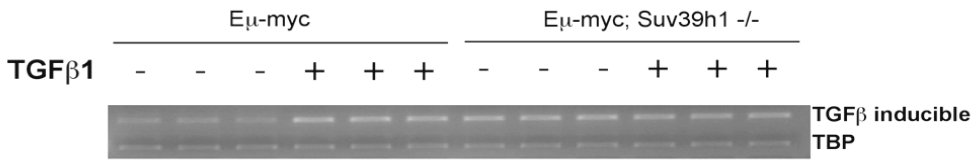

Figure A.8: βIGH3 levels are regulated by TGF β-1. Exogenous addition of TGFβ-1 to lymphoma cells of both Suv39h1 proficient (n=3) and deficient (n=3) background revealed induction of βIGH3 expression in both genotypes. TBP was used as a loading control.

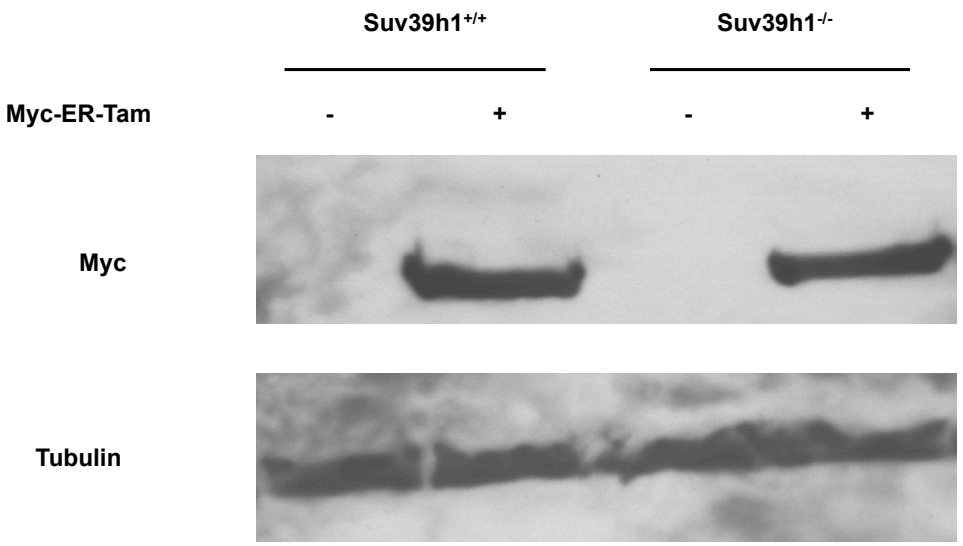

Figure A.9: Analysis of stable transduction by protein expression levels. Expression of Myc was checked in wild-type and Suv39h1 deficient mouse embrionyc fibroblasts (MEFs) post stable retroviral transduction of Myc-ER construct, Eμ-myc (n=2) lymphomas were used as positive controls. Tubulin was used as a loading control.

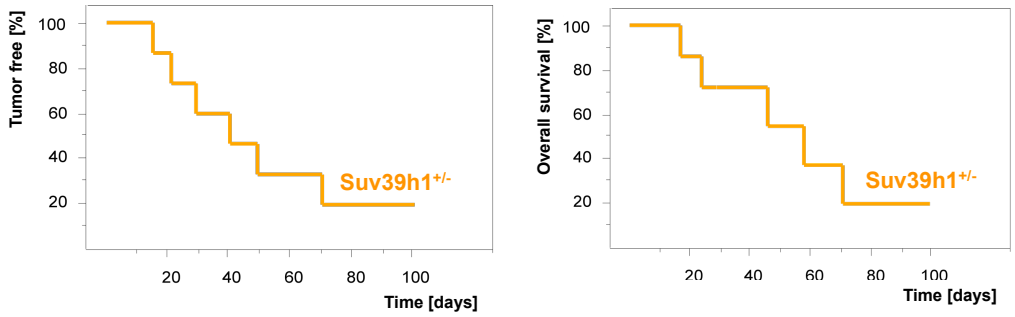

Figure A.10: Animals bearing Suv39h1$^{+/-}$ lymphomas have inferior long term treatment outcome when compared to animals bearing lymphomas with intact Suv39h1. LEFT: Eμ-myc, Suv39h1$^{+/-}$ mice (yellow line; n= 8) were monitored for the "Time-to-relapse" latencies after Cyclophosphamide (CTX) treatment. RIGHT: Eμmyc, Suv39h1$^{+/-}$ mice (yellow line; n= 8) were monitored for the "Time-to-death" latencies post Cyclophosphamide (CTX) treatment.

Impaired long term-treatment outcome in bcl2 protected Suv39h1-/- lymphomas

In the same experimental design as for the primary lymphomas of both genotypes, additionally transplanted lymphomas were stably transduced with the apoptotic blocker bcl2. In this experimental setting senescence was tested as the only intact mechanism upon the therapy. In this experiment each lymphoma was transplanted into the 3 wild-type 6-8 weeks old mice, upon lymphoma formation mice were treated with the single dose of Cyclophosphamide (CTX) and monitored for the 100 days to investigate the long-term response to the therapy (Figure A.11).

Correlation between treatment outcome and induction of spontaneous apoptosis in primary lymphomas

Defects in apoptotic machinery have a tremendous impact on the long term treatment outcome. Therefore to exclude the possibility of apoptotic defects in the original lymphoma pool used for the transplantation studies impacting treatment outcome, both Suv39h1 proficient and deficient lymphomas were tested by TUNEL staining for Myc-induced apoptosis. It was shown that all of the tested lymphomas retained the ability to execute spontaneous apoptosis. However, this result could not be compared to the correlation of senescence and the long-term treatment outcome since paraffin embedded sections were not done for each of lymphoma samples (Figure A.12).

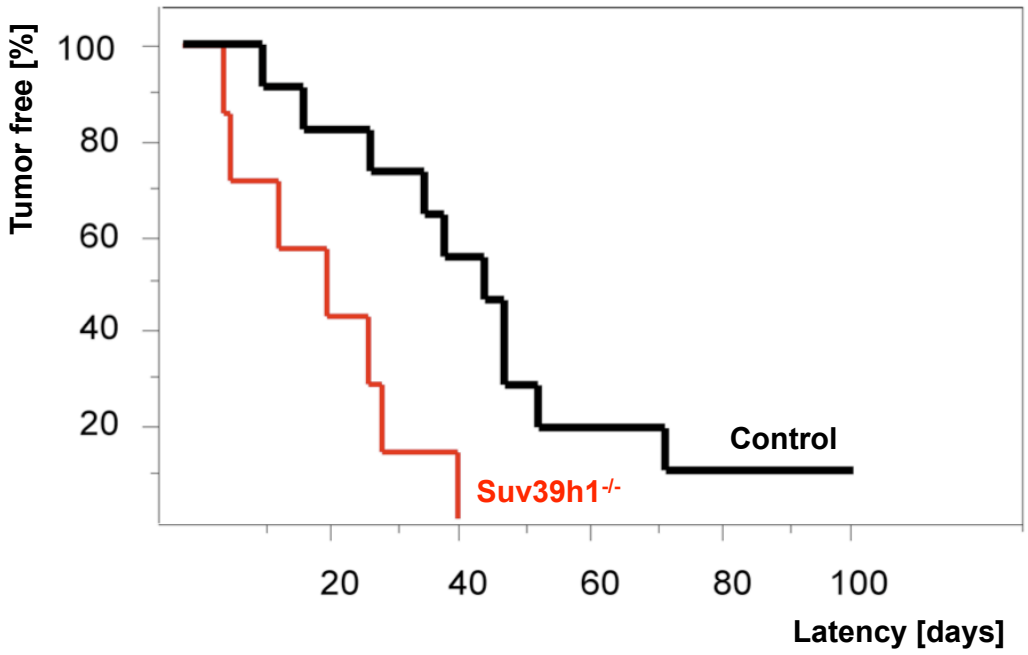

Figure A.11: Drug induced senescence is contributing to the long term treatment outcome when apoptosis is blocked. Eμ-myc/bcl2 (black line, n=11) and Eμ-myc, Suv39h1$^{-/-}$/bcl2 mice (red line; n= 7) were monitored for the "Time-to-death" latencies upon Cyclophosphamide (CTX) treatment.

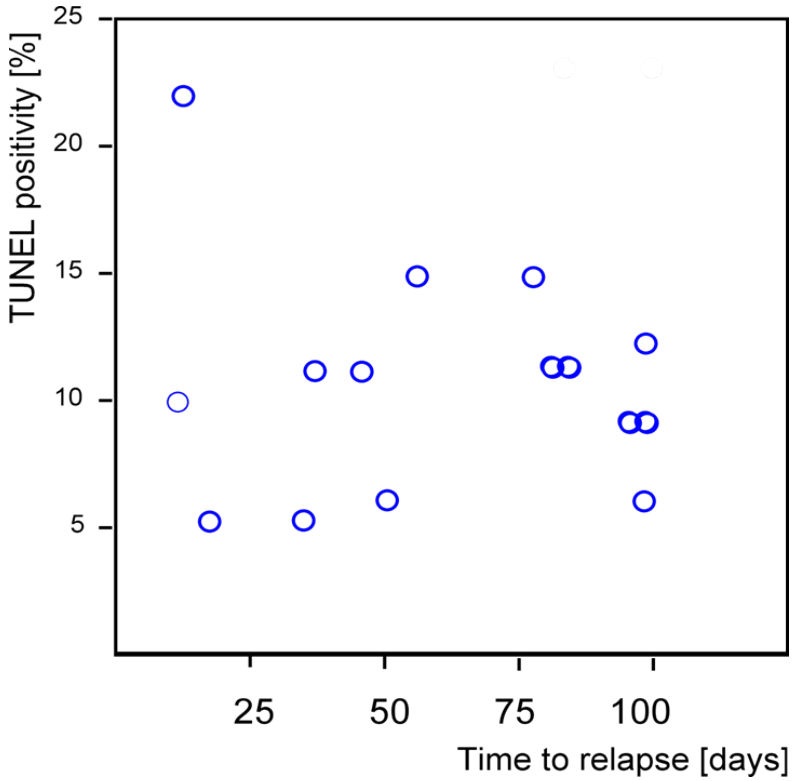

Figure A.12: Correlation between the extent of apoptosis (TUNEL) and the response to the long-term treatment outcome in Suv39h1 proficient mice.

Abbreviations

Abbreviations	Erklärung
ADR	Adriamycin
ARF	Alternative reading frame
Bcl2	B-cell lymphoma 2
βIGH3	TGFβ-inducible gene
BrdU	5-bromo-2'-deoxyuridine
CDK	Cyclin-dependent kinase
CTX	Cyclophosphamide
DNA	Desoxyribonucleic acid
DDR	DNA damage response
Eμ	immunoglobulin heavy chain (IgH) enhancer
FITC	Fluoresceinisothiocyanat
H3K9	Lysine 9 residue on histone H3
H3K9me3	Tri-methylated lysine 9 residue on histone H3
H3S10P	Phosphorylated serine 10 residue on histone H3
HMT	Histone-methyltransferase
HP1	Heterochromatin protein 1
INK4	Inhibitor of CDK4
mRNA	Messenger ribonucleic acid
MSCV	Murine stem cell virus
NAC	N-Acetylcytsteine
NOC	Nocodazole
p53	Tumor protein 53
PI	Propidium iodide
Rb	Retinoblastoma protein
ROS	Reactive oxygen species
RNA	Ribonucleic acid
SA β-gal	Senescence-associated β-galactosidase
Su(var)3-9	Suppressor of variegation 3-9
TGFβ	Transforming growth factorβ
TUNEL	Terminal deoxynucleotidyl transferase dUTP nick end labelling

Acknowledgements

Work described in this thesis was conducted from March 2005 till February 2008 in the lab of Prof. Dr. C. A. Schmitt, Charite Virchow Klinikum/ Max Delbrueck Center for Molecular Medicine (MDC), to whom I want to thank for assigning me to work on the project described in this thesis, laboratory space and reagents provided. I would like to thank to "International PhD Programme" of the MDC/Humboldt University for accepting me in the 2004's selection, and granting me a 3 year scholarship.

Further, I want to thank Dr. A. Uren for all the scientific input, much needed moral support, and his great humour mostly sent through numerous e-mails during the past 4 years, "Me is very thankful". I am greatly indebted to my co-workers: Dr. M. Kilic, you were a wonderful colleague, and even better as a friend. You know that it would not work without you; we will always have our "Vapiano" and "Starbucks" memories. To Asja G, I want to thank for all this wonderful German translations, helpful comments and for an occasional "Cupcake" or"Fussbadcafee" retreats. Thanks to Pascal, Mathias and Anja, I like it even more now when we see each other in casual surroundings. I wish to thank to all of the technicians from the lab for help provided, my biggest thanks is to Mrs. Nadine Burbach. I had great collaborators during my thesis work, Prof. Dr. Christoph Loddenkemper and Mrs. Simone Spieckermann, thank you for great IHC and an excellent company, it was fun doing experiments together with you guys. I wish to thank to my other collaborator, Dr. Samans, whom I only know from our "microarray-on-line encounters".

Big, big thank you to Dr. S. Friedl for all "the" help and beyond, and as Moss would say: "I'm in my happy place...". I wish to thank many of my MDC-based friend: Lizzie for her kindness and Tam-ara for her unkindness which is a kindness itself. CC, Dinko (daj vec jednom zavrsi) and Ole-Bear, thanks for listening and talking (there was always so much to tell). I wish to thank to Mrs. Sibilak and Dr. O. Seumenicht of MDC for their help and friendship, extended further than regular working obligations/ hours. A person to whom I wish to thank for an excellent design of the mouse you

might have enjoyed (if you didn't venture only into reading this last part): Michele Velastri- thank you for the Topolino. I also wish to thank to all of my new coworkers and my very patient new boss for making this year of waiting to pass "like no time".

Now comes the hard part. There are so many people without whose moral support this journey would end up quite soon after it started. Mojim roditeljima, Borjani i Zvonimiru, jer me bezuvijetno podrzavaju, sto proizlazi iz njihove ljubavi, koja je posljedica genetike. Dobila sam vasu najbolju i najgoru osobinu: tvrdoglavost.Mojoj sestri Tihani, koja je bila dovoljno mudra ne napraviti isti izbor poput mene, sto se profesionalnog zivota tice. Sve greske koje cinis sad su dobrodosla skola, nakon tridesete trudi se bit mudra i ne jesti cokoladu. Mojim bakama (Noni i Dadi) i djedovima (Joci i Ernestu), koji su me odgojili kao slobodog covjeka, posebno Dadi, cija su bolest i prerani odlazak utjecali na moj (ne samo profesionalni) zivotni put, medju ostalim i na izbor teme na kojoj sam radila. Ujaku, ujni, Vanji hvala na lijepim vremenima u Beogradu, ova razdvojenost ne djeluje dobro na Balkanskog covjeka.

Mikaelu, bez kojeg bi svakodnevica ove protekle tri godine bila tuzna i teska. U tebi sam nasla osobu koja me razumije, i postuje, koja je isto tako znala potaknuti me da krenem dalje kad mi je bilo dosta svega. Zivjeti s tobom je kao zivjeti s najboljom verzijom same sebe, znaci savrseno.

Birgitta och Rolf tack so mycket for letting me eat and sleep and use your cartridge last Christmas and for many more things as well. One of the next challenges has to be learning Swedish, but you will have to give me some time.

Moja dva "viteza" iz Amsterdama Andrej i Bijelo Medvjed, vjerovali ste kad ja nisam, nikad necu zaboravit sve nase avanture...ludo vrijeme, sad je vrijeme za ozbiljnost (jos malo). To Jaap I wish to thank for his great friendship, and also since he had to put me in his dankwoord (it seems such a long time ago); and most of all for Leontine (your voice always makes me smile). Thank you Paolo, my cook-mate and a future Chef star (if we ever venture into the show).

Thanks all of my other friends here, in the Netherlands and back at home, and the others that I have temporarily lost somewhere in between.

Sad kad sam zavrsila zahvaljivanje ljudima na redu je i moja (jos uvijek sluzbeno) Dona, koja iako ne razumije uvijek sto se to dogadja odabire vjernost i spremna je na nove avanture. Proputovala si uz mene dobar dio Europe, nadam se da ces me se sjetiti u memoarima. Naucila si me da ljubav nikad nije bezuvjetna

I wish to thank to many of my involuntary collaborators: Eμ-myc and Suv39h1 knockout mice-without whom all this work would not be possible.

Da moram sve ovo ponovno proc mislim da bih radje radila sijaset drugih poslova, a opet, ima nesto u biologiji sto fascinira covjeka toliko da je spreman zrtvovati dobar dio sebe za sitni djelic znanja. Radoznalost privremeno pobjedjuje, ali sad je vrijeme da postanemo mudri.

Hvala vam svima!! Thank you all again!!!

Bibliography

[ABW+91] Arents, G; Burlingame, R W; Wang, B C; Love, W E; Moudrianakis, E N: The nucleosomal core histone octamer at 3.1 a resolution: a tripartite protein assembly and a left-handed superhelix. In: *Proc Natl Acad Sci U S A*, volume 88(22):pp. 10148–10152, 1991. ISSN 0027-8424 (Print).

[AFG99] Anbazhagan, R; Fujii, H; Gabrielson, E: Microsatellite instability is uncommon in breast cancer. In: *Clin Cancer Res*, volume 5(4):pp. 839–844, 1999. ISSN 1078-0432 (Print).

[AHP+85] Adams, J M; Harris, A W; Pinkert, C A; Corcoran, L M; Alexander, W S; Cory, S; Palmiter, R D; Brinster, R L: The c-myc oncogene driven by immunoglobulin enhancers induces lymphoid malignancy in transgenic mice. In: *Nature*, volume 318(6046):pp. 533–538, 1985. ISSN 0028-0836 (Print).

[AM95] Alexandrow, M G; Moses, H L: Transforming growth factor beta and cell cycle regulation. In: *Cancer Res*, volume 55(7):pp. 1452–1457, 1995. ISSN 0008-5472 (Print).

[AOB+08] Acosta, Juan C; O'Loghlen, Ana; Banito, Ana; Guijarro, Maria V; Augert, Arnaud; Raguz, Selina; Fumagalli, Marzia; Da Costa, Marco; Brown, Celia; Popov, Nikolay; Takatsu, Yoshihiro; Melamed, Jonathan; d'Adda di Fagagna, Fabrizio; Bernard, David; Hernando, Eva; Gil, Jesus: Chemokine signaling via the cxcr2 receptor reinforces senescence. In: *Cell*, volume 133(6):pp. 1006–1018, 2008. ISSN 1097-4172 (Electronic). doi:10.1016/j.cell.2008.03.038.

[ASA87] Alexander, W S; Schrader, J W; Adams, J M: Expression of the c-myc oncogene under control of an immunoglobulin enhancer in e mu-myc transgenic mice. In: *Mol Cell Biol*, volume 7(4):pp. 1436–1444, 1987. ISSN 0270-7306 (Print).

[BBK+00] Beier, R; Burgin, A; Kiermaier, A; Fero, M; Karsunky, H; Saffrich, R; Moroy, T; Ansorge, W; Roberts, J; Eilers, M: Induction of cyclin e-cdk2 kinase activity, e2f-dependent transcription and cell growth by myc are genetically separable events. In: *EMBO J*, volume 19(21):pp. 5813–5823, 2000. ISSN 0261-4189 (Print). doi:10.1093/emboj/19.21.5813.

[Ben04] Benson, John R: Role of transforming growth factor beta in breast carcinogenesis. In: *Lancet Oncol*, volume 5(4):pp. 229–239, 2004. ISSN 1470-2045 (Print). doi:10.1016/S1470-2045(04)01426-3.

[BHK+05] Bartkova, Jirina; Horejsi, Zuzana; Koed, Karen; Kramer, Alwin; Tort, Frederic; Zieger, Karsten; Guldberg, Per; Sehested, Maxwell; Nesland, Jahn M; Lukas, Claudia; Orntoft, Torben; Lukas, Jiri; Bartek, Jiri: Dna damage response as a candidate anti-cancer barrier in early human tumorigenesis. In: *Nature*, volume 434(7035):pp. 864–870, 2005. ISSN 1476-4687 (Electronic). doi:10.1038/nature03482.

[BK04] Bannister, Andrew J; Kouzarides, Tony: Histone methylation: recognizing the methyl mark. In: *Methods Enzymol*, volume 376:pp. 269–288, 2004. ISSN 0076-6879 (Print). doi:10.1016/S0076-6879(03)76018-2.

[BLL+05] Braig, Melanie; Lee, Soyoung; Loddenkemper, Christoph; Rudolph, Cornelia; Peters, Antoine H F M; Schlegelberger, Brigitte; Stein, Harald; Dorken, Bernd; Jenuwein, Thomas; Schmitt, Clemens A: Oncogene-induced senescence as an initial barrier in lymphoma development. In: *Nature*, volume 436(7051):pp. 660–665, 2005. ISSN 1476-4687 (Electronic). doi:10.1038/nature03841.

[BRD02] Bennewith, Kevin L; Raleigh, James A; Durand, Ralph E: Orally administered pimonidazole to label hypoxic tumor cells. In: *Cancer Res*, volume 62(23):pp. 6827–6830, 2002. ISSN 0008-5472 (Print).

[BRL+06] Bartkova, Jirina; Rezaei, Nousin; Liontos, Michalis; Karakaidos, Panagiotis; Kletsas, Dimitris; Issaeva, Natalia; Vassiliou, Leandros-Vassilios F; Kolettas, Evangelos; Niforou, Katerina; Zoumpourlis, Vassilis C; Takaoka, Munenori; Nakagawa, Hiroshi; Tort, Frederic; Fugger, Kasper; Johansson,

Fredrik; Sehested, Maxwell; Andersen, Claus L; Dyrskjot, Lars; Orntoft, Torben; Lukas, Jiri; Kittas, Christos; Helleday, Thomas; Halazonetis, Thanos D; Bartek, Jiri; Gorgoulis, Vassilis G: Oncogene-induced senescence is part of the tumorigenesis barrier imposed by dna damage checkpoints. In: *Nature*, volume 444(7119):pp. 633–637, 2006. ISSN 1476-4687 (Electronic). doi:10.1038/nature05268.

[BTO+95] Blyth, K; Terry, A; O'Hara, M; Baxter, E W; Campbell, M; Stewart, M; Donehower, L A; Onions, D E; Neil, J C; Cameron, E R: Synergy between a human c-myc transgene and p53 null genotype in murine thymic lymphomas: contrasting effects of homozygous and heterozygous p53 loss. In: *Oncogene*, volume 10(9):pp. 1717–1723, 1995. ISSN 0950-9232 (Print).

[BZP+01] Bannister, A J; Zegerman, P; Partridge, J F; Miska, E A; Thomas, J O; Allshire, R C; Kouzarides, T: Selective recognition of methylated lysine 9 on histone h3 by the hp1 chromo domain. In: *Nature*, volume 410(6824):pp. 120–124, 2001. ISSN 0028-0836 (Print). doi:10.1038/35065138.

[Cam01] Campisi, J: Cellular senescence as a tumor-suppressor mechanism. In: *Trends Cell Biol*, volume 11(11):pp. S27–31, 2001. ISSN 0962-8924 (Print).

[CASC00] Cheung, P; Allis, C D; Sassone-Corsi, P: Signaling to chromatin through histone modifications. In: *Cell*, volume 103(2):pp. 263–271, 2000. ISSN 0092-8674 (Print).

[CBPC04] Chin, David; Boyle, Glen M; Parsons, Peter G; Coman, William B: What is transforming growth factor-beta (tgf-beta)? In: *Br J Plast Surg*, volume 57(3):pp. 215–221, 2004. ISSN 0007-1226 (Print). doi:10.1016/j.bjps.2003.12.012.

[CddF07] Campisi, Judith; d'Adda di Fagagna, Fabrizio: Cellular senescence: when bad things happen to good cells. In: *Nat Rev Mol Cell Biol*, volume 8(9):pp. 729–740, 2007. ISSN 1471-0080 (Electronic). doi:10.1038/nrm2233.

[CFR+95] Chen, Q; Fischer, A; Reagan, J D; Yan, L J; Ames, B N: Oxidative dna damage and senescence of human diploid fibroblast cells. In: *Proc Natl Acad Sci U S A*, volume 92(10):pp. 4337–4341, 1995. ISSN 0027-8424 (Print).

[CHH+00] Chan, T A; Hwang, P M; Hermeking, H; Kinzler, K W; Vogelstein, B: Cooperative effects of genes controlling the g(2)/m checkpoint. In: *Genes Dev*, volume 14(13):pp. 1584–1588, 2000. ISSN 0890-9369 (Print).

[CRS+08] Chesi, Marta; Robbiani, Davide F; Sebag, Michael; Chng, Wee Joo; Affer, Maurizio; Tiedemann, Rodger; Valdez, Riccardo; Palmer, Stephen E; Haas, Stephanie S; Stewart, A Keith; Fonseca, Rafael; Kremer, Richard; Cattoretti, Giorgio; Bergsagel, P Leif: Aid-dependent activation of a myc transgene induces multiple myeloma in a conditional mouse model of post-germinal center malignancies. In: *Cancer Cell*, volume 13(2):pp. 167–180, 2008. ISSN 1535-6108 (Print). doi: 10.1016/j.ccr.2008.01.007.

[CSS+02] Chang, Bey-Dih; Swift, Mari E; Shen, Mei; Fang, Jing; Broude, Eugenia V; Roninson, Igor B: Molecular determinants of terminal growth arrest induced in tumor cells by a chemotherapeutic agent. In: *Proc Natl Acad Sci U S A*, volume 99(1):pp. 389–394, 2002. ISSN 0027-8424 (Print). doi: 10.1073/pnas.012602599.

[CYD+06] Chen, Haobin; Yan, Yan; Davidson, Todd L; Shinkai, Yoichi; Costa, Max: Hypoxic stress induces dimethylated histone h3 lysine 9 through histone methyltransferase g9a in mammalian cells. In: *Cancer Res*, volume 66(18):pp. 9009–9016, 2006. ISSN 0008-5472 (Print). doi:10.1158/0008-5472.CAN-06-0101.

[DBMLR04] DaCosta Byfield, Stacey; Major, Christopher; Laping, Nicholas J; Roberts, Anita B: Sb-505124 is a selective inhibitor of transforming growth factor-beta type i receptors alk4, alk5, and alk7. In: *Mol Pharmacol*, volume 65(3):pp. 744–752, 2004. ISSN 0026-895X (Print). doi:10.1124/mol.65.3.744.

[DCFR02] Dokmanovic, Milos; Chang, Bey-Dih; Fang, Jing; Roninson, Igor B: Retinoid-induced growth arrest of breast carcinoma cells involves co-activation of multiple growth-inhibitory genes. In: *Cancer Biol Ther*, volume 1(1):pp. 24–27, 2002. ISSN 1538-4047 (Print).

[DDGK92] Dang, C V; Dolde, C; Gillison, M L; Kato, G J: Discrimination between related dna sites by a single amino acid residue of myc-related basic-helix-loop-helix proteins. In: *Proc Natl Acad*

Sci U S A, volume 89(2):pp. 599–602, 1992. ISSN 0027-8424 (Print).

[DFMG+83] Dalla-Favera, R; Martinotti, S; Gallo, R C; Erikson, J; Croce, C M: Translocation and rearrangements of the c-myc oncogene locus in human undifferentiated b-cell lymphomas. In: *Science*, volume 219(4587):pp. 963–967, 1983. ISSN 0036-8075 (Print).

[DIAC00] Dimri, G P; Itahana, K; Acosta, M; Campisi, J: Regulation of a senescence checkpoint response by the e2f1 transcription factor and p14(arf) tumor suppressor. In: *Mol Cell Biol*, volume 20(1):pp. 273–285, 2000. ISSN 0270-7306 (Print).

[DKL+05] Dubrovska, Anna; Kanamoto, Takashi; Lomnytska, Marta; Heldin, Carl-Henrik; Volodko, Natalya; Souchelnytskyi, Serhiy: Tgfbeta1/smad3 counteracts brca1-dependent repair of dna damage. In: *Oncogene*, volume 24(14):pp. 2289–2297, 2005. ISSN 0950-9232 (Print). doi:10.1038/sj.onc.1208443.

[DLB+95] Dimri, G P; Lee, X; Basile, G; Acosta, M; Scott, G; Roskelley, C; Medrano, E E; Linskens, M; Rubelj, I; Pereira-Smith, O: A biomarker that identifies senescent human cells in culture and in aging skin in vivo. In: *Proc Natl Acad Sci U S A*, volume 92(20):pp. 9363–9367, 1995. ISSN 0027-8424 (Print).

[DMFC+06] Di Micco, Raffaella; Fumagalli, Marzia; Cicalese, Angelo; Piccinin, Sara; Gasparini, Patrizia; Luise, Chiara; Schurra, Catherine; Garre', Massimiliano; Nuciforo, Paolo Giovanni; Bensimon, Aaron; Maestro, Roberta; Pelicci, Pier Giuseppe; d'Adda di Fagagna, Fabrizio: Oncogene-induced senescence is a dna damage response triggered by dna hyper-replication. In: *Nature*, volume 444(7119):pp. 638–642, 2006. ISSN 1476-4687 (Electronic). doi:10.1038/nature05327.

[DRJ+03] Drayton, Sarah; Rowe, Janice; Jones, Rebecca; Vatcheva, Radost; Cuthbert-Heavens, Darren; Marshall, John; Fried, Mike; Peters, Gordon: Tumor suppressor p16ink4a determines sensitivity of human cells to transformation by cooperating cellular oncogenes. In: *Cancer Cell*, volume 4(4):pp. 301–310, 2003. ISSN 1535-6108 (Print).

[DS99] Davie, J R; Spencer, V A: Control of histone modifications. In: *J Cell Biochem*, volume Suppl 32-33:pp. 141–148, 1999. ISSN 0730-2312 (Print).

[eDTV+93] el Deiry, W S; Tokino, T; Velculescu, V E; Levy, D B; Parsons, R; Trent, J M; Lin, D; Mercer, W E; Kinzler, K W; Vogelstein, B: Waf1, a potential mediator of p53 tumor suppression. In: *Cell*, volume 75(4):pp. 817–825, 1993. ISSN 0092-8674 (Print).

[Eil99] Eilers, M: Control of cell proliferation by myc family genes. In: *Mol Cells*, volume 9(1):pp. 1–6, 1999. ISSN 1016-8478 (Print).

[Est07] Esteller, Manel: Cancer epigenomics: Dna methylomes and histone-modification maps. In: *Nat Rev Genet*, volume 8(4):pp. 286–298, 2007. ISSN 1471-0056 (Print). doi: 10.1038/nrg2005.

[EWG+92] Evan, G I; Wyllie, A H; Gilbert, C S; Littlewood, T D; Land, H; Brooks, M; Waters, C M; Penn, L Z; Hancock, D C: Induction of apoptosis in fibroblasts by c-myc protein. In: *Cell*, volume 69(1):pp. 119–128, 1992. ISSN 0092-8674 (Print).

[EWR+99] Eischen, C M; Weber, J D; Roussel, M F; Sherr, C J; Cleveland, J L: Disruption of the arf-mdm2-p53 tumor suppressor pathway in myc-induced lymphomagenesis. In: *Genes Dev*, volume 13(20):pp. 2658–2669, 1999. ISSN 0890-9369 (Print).

[FB99] Felsher, D W; Bishop, J M: Reversible tumorigenesis by myc in hematopoietic lineages. In: *Mol Cell*, volume 4(2):pp. 199–207, 1999. ISSN 1097-2765 (Print).

[FCHC00] Firestein, R; Cui, X; Huie, P; Cleary, M L: Set domain-dependent regulation of transcriptional silencing and growth control by suv39h1, a mammalian ortholog of drosophila su(var)3-9. In: *Mol Cell Biol*, volume 20(13):pp. 4900–4909, 2000. ISSN 0270-7306 (Print).

[FdSQ+00] Ferbeyre, G; de Stanchina, E; Querido, E; Baptiste, N; Prives, C; Lowe, S W: Pml is induced by oncogenic ras and promotes premature senescence. In: *Genes Dev*, volume 14(16):pp. 2015–2027, 2000. ISSN 0890-9369 (Print).

[FT04] Feinberg, Andrew P; Tycko, Benjamin: The history of cancer epigenetics. In: *Nat Rev Cancer*, volume 4(2):pp. 143–153, 2004. ISSN 1474-175X (Print). doi:10.1038/nrc1279.

[GBBP07] Giordano, Antonio; Bellacchio, Emanuele; Bagella, Luigi; Paggi, Marco G: Interaction between the cdk2/cyclin a complex and a small molecule derived from the prb2/p130 spacer domain: a theoretical model. In: *Cell Cycle*, volume 6(21):pp. 2591–2593, 2007. ISSN 1551-4005 (Electronic).

[GBG+91] Gaidano, G; Ballerini, P; Gong, J Z; Inghirami, G; Neri, A; Newcomb, E W; Magrath, I T; Knowles, D M; Dalla-Favera, R: p53 mutations in human lymphoid malignancies: association with burkitt lymphoma and chronic lymphocytic leukemia. In: *Proc Natl Acad Sci U S A*, volume 88(12):pp. 5413–5417, 1991. ISSN 0027-8424 (Print).

[Gol99] Gold, L I: The role for transforming growth factor-beta (tgf-beta) in human cancer. In: *Crit Rev Oncog*, volume 10(4):pp. 303–360, 1999. ISSN 0893-9675 (Print).

[HA00] Hecht, J L; Aster, J C: Molecular biology of burkitt's lymphoma. In: *J Clin Oncol*, volume 18(21):pp. 3707–3721, 2000. ISSN 0732-183X (Print).

[HAW+93] Harper, J W; Adami, G R; Wei, N; Keyomarsi, K; Elledge, S J: The p21 cdk-interacting protein cip1 is a potent inhibitor of g1 cyclin-dependent kinases. In: *Cell*, volume 75(4):pp. 805–816, 1993. ISSN 0092-8674 (Print).

[HAY65] HAYFLICK, L: The limited in vitro lifetime of human diploid cell strains. In: *Exp Cell Res*, volume 37:pp. 614–636, 1965. ISSN 0014-4827 (Print).

[HBK+07] Honjo, Yasuyuki; Bian, Yansong; Kawakami, Koji; Molinolo, Alfredo; Longenecker, Glenn; Boppana, Ramanamurthy; Larsson, Jonas; Karlsson, Stefan; Gutkind, J Silvio; Puri, Raj K; Kulkarni, Ashok B: Tgf-beta receptor i conditional knockout mice develop spontaneous squamous cell carcinoma. In: *Cell Cycle*, volume 6(11):pp. 1360–1366, 2007. ISSN 1551-4005 (Electronic).

[HM61] HAYFLICK, L; MOORHEAD, P S: The serial cultivation of human diploid cell strains. In: *Exp Cell Res*, volume 25:pp. 585–621, 1961. ISSN 0014-4827 (Print).

[HMF+87] Heine, U; Munoz, E F; Flanders, K C; Ellingsworth, L R; Lam, H Y; Thompson, N L; Roberts, A B; Sporn, M B: Role

of transforming growth factor-beta in the development of the mouse embryo. In: *J Cell Biol*, volume 105(6 Pt 2):pp. 2861–2876, 1987. ISSN 0021-9525 (Print).

[HMT+06] Habu, Yoshiki; Mathieu, Olivier; Tariq, Muhammad; Probst, Aline V; Smathajitt, Chotika; Zhu, Tong; Paszkowski, Jerzy: Epigenetic regulation of transcription in intermediate heterochromatin. In: *EMBO Rep*, volume 7(12):pp. 1279–1284, 2006. ISSN 1469-221X (Print). doi:10.1038/sj.embor.7400835.

[HSW+93] Harvey, M; Sands, A T; Weiss, R S; Hegi, M E; Wiseman, R W; Pantazis, P; Giovanella, B C; Tainsky, M A; Bradley, A; Donehower, L A: In vitro growth characteristics of embryo fibroblasts isolated from p53-deficient mice. In: *Oncogene*, volume 8(9):pp. 2457–2467, 1993. ISSN 0950-9232 (Print).

[HW00] Hanahan, D; Weinberg, R A: The hallmarks of cancer. In: *Cell*, volume 100(1):pp. 57–70, 2000. ISSN 0092-8674 (Print).

[HWB+02] Herold, Steffi; Wanzel, Michael; Beuger, Vincent; Frohme, Carsten; Beul, Dorothee; Hillukkala, Tomi; Syvaoja, Juhani; Saluz, Hans-Peter; Haenel, Frank; Eilers, Martin: Negative regulation of the mammalian uv response by myc through association with miz-1. In: *Mol Cell*, volume 10(3):pp. 509–521, 2002. ISSN 1097-2765 (Print).

[IKKM06] Iiyama, Mitsuko; Kakihana, Kazuhiko; Kurosu, Tetsuya; Miura, Osamu: Reactive oxygen species generated by hematopoietic cytokines play roles in activation of receptor-mediated signaling and in cell cycle progression. In: *Cell Signal*, volume 18(2):pp. 174–182, 2006. ISSN 0898-6568 (Print). doi:10.1016/j.cellsig.2005.04.002.

[INC+02] Inman, Gareth J; Nicolas, Francisco J; Callahan, James F; Harling, John D; Gaster, Laramie M; Reith, Alastair D; Laping, Nicholas J; Hill, Caroline S: Sb-431542 is a potent and specific inhibitor of transforming growth factor-beta superfamily type i activin receptor-like kinase (alk) receptors alk4, alk5, and alk7. In: *Mol Pharmacol*, volume 62(1):pp. 65–74, 2002. ISSN 0026-895X (Print).

[Ito07] Ito, Takashi: Role of histone modification in chromatin dynamics. In: *J Biochem*, volume 141(5):pp. 609–614, 2007. ISSN 0021-924X (Print). doi:10.1093/jb/mvm091.

[JA01] Jenuwein, T; Allis, C D: Translating the histone code. In: *Science*, volume 293(5532):pp. 1074–1080, 2001. ISSN 0036-8075 (Print). doi:10.1126/science.1063127.

[JB02] Jones, Peter A; Baylin, Stephen B: The fundamental role of epigenetic events in cancer. In: *Nat Rev Genet*, volume 3(6):pp. 415–428, 2002. ISSN 1471-0056 (Print). doi:10.1038/nrg816.

[JB04] Jonkers, Jos; Berns, Anton: Oncogene addiction: sometimes a temporary slavery. In: *Cancer Cell*, volume 6(6):pp. 535–538, 2004. ISSN 1535-6108 (Print). doi:10.1016/j.ccr.2004.12.002.

[JGO99] Juven-Gershon, T; Oren, M: Mdm2: the ups and downs. In: *Mol Med*, volume 5(2):pp. 71–83, 1999. ISSN 1076-1551 (Print).

[JKM+99] Jacobs, J J; Kieboom, K; Marino, S; DePinho, R A; van Lohuizen, M: The oncogene and polycomb-group gene bmi-1 regulates cell proliferation and senescence through the ink4a locus. In: *Nature*, volume 397(6715):pp. 164–168, 1999. ISSN 0028-0836 (Print). doi:10.1038/16476.

[JLDR98] Jenuwein, T; Laible, G; Dorn, R; Reuter, G: Set domain proteins modulate chromatin domains in eu- and heterochromatin. In: *Cell Mol Life Sci*, volume 54(1):pp. 80–93, 1998. ISSN 1420-682X (Print).

[JPS06] Jackson, James G; Pereira-Smith, Olivia M: p53 is preferentially recruited to the promoters of growth arrest genes p21 and gadd45 during replicative senescence of normal human fibroblasts. In: *Cancer Res*, volume 66(17):pp. 8356–8360, 2006. ISSN 1538-7445 (Electronic). doi:10.1158/0008-5472.CAN-06-1752.

[JRW+94] Jacks, T; Remington, L; Williams, B O; Schmitt, E M; Halachmi, S; Bronson, R T; Weinberg, R A: Tumor spectrum analysis in p53-mutant mice. In: *Curr Biol*, volume 4(1):pp. 1–7, 1994. ISSN 0960-9822 (Print).

[KBFP+04] Knies-Bamforth, Ulrike E; Fox, Stephen B; Poulsom, Richard; Evan, Gerard I; Harris, Adrian L: c-myc interacts with hypoxia to induce angiogenesis in vivo by a vascular endothelial growth factor-dependent mechanism. In: *Cancer Res*, vol-

ume 64(18):pp. 6563–6570, 2004. ISSN 0008-5472 (Print). doi: 10.1158/0008-5472.CAN-03-3176.

[KK85] Klein, G; Klein, E: Evolution of tumours and the impact of molecular oncology. In: *Nature*, volume 315(6016):pp. 190–195, 1985. ISSN 0028-0836 (Print).

[Kle89] Klein, G: Multiple phenotypic consequences of the ig/myc translocation in b-cell-derived tumors. In: *Genes Chromosomes Cancer*, volume 1(1):pp. 3–8, 1989. ISSN 1045-2257 (Print).

[KMI+98] Kurokawa, M; Mitani, K; Irie, K; Matsuyama, T; Takahashi, T; Chiba, S; Yazaki, Y; Matsumoto, K; Hirai, H: The oncoprotein evi-1 represses tgf-beta signalling by inhibiting smad3. In: *Nature*, volume 394(6688):pp. 92–96, 1998. ISSN 0028-0836 (Print). doi:10.1038/27945.

[KMV+08] Kuilman, Thomas; Michaloglou, Chrysiis; Vredeveld, Liesbeth C W; Douma, Sirith; van Doorn, Remco; Desmet, Christophe J; Aarden, Lucien A; Mooi, Wolter J; Peeper, Daniel S: Oncogene-induced senescence relayed by an interleukin-dependent inflammatory network. In: *Cell*, volume 133(6):pp. 1019–1031, 2008. ISSN 1097-4172 (Electronic). doi: 10.1016/j.cell.2008.03.039.

[KOM+98] Klangby, U; Okan, I; Magnusson, K P; Wendland, M; Lind, P; Wiman, K G: p16/ink4a and p15/ink4b gene methylation and absence of p16/ink4a mrna and protein expression in burkitt's lymphoma. In: *Blood*, volume 91(5):pp. 1680–1687, 1998. ISSN 0006-4971 (Print).

[KOP+93] Koff, A; Ohtsuki, M; Polyak, K; Roberts, J M; Massague, J: Negative regulation of g1 in mammalian cells: inhibition of cyclin e-dependent kinase by tgf-beta. In: *Science*, volume 260(5107):pp. 536–539, 1993. ISSN 0036-8075 (Print).

[Kor74] Kornberg, R D: Chromatin structure: a repeating unit of histones and dna. In: *Science*, volume 184(139):pp. 868–871, 1974. ISSN 0036-8075 (Print).

[Kou07] Kouzarides, Tony: Chromatin modifications and their function. In: *Cell*, volume 128(4):pp. 693–705, 2007. ISSN 0092-8674 (Print). doi:10.1016/j.cell.2007.02.005.

[KQM+01] Krimpenfort, P; Quon, K C; Mooi, W J; Loonstra, A; Berns, A: Loss of p16ink4a confers susceptibility to metastatic melanoma in mice. In: *Nature*, volume 413(6851):pp. 83–86, 2001. ISSN 0028-0836 (Print). doi:10.1038/35092584.

[KT74] Kornberg, R D; Thomas, J O: Chromatin structure; oligomers of the histones. In: *Science*, volume 184(139):pp. 865–868, 1974. ISSN 0036-8075 (Print).

[KZR+97] Kamijo, T; Zindy, F; Roussel, M F; Quelle, D E; Downing, J R; Ashmun, R A; Grosveld, G; Sherr, C J: Tumor suppression at the mouse ink4a locus mediated by the alternative reading frame product p19arf. In: *Cell*, volume 91(5):pp. 649–659, 1997. ISSN 0092-8674 (Print).

[KZRVU+97] Kauffmann-Zeh, A; Rodriguez-Viciana, P; Ulrich, E; Gilbert, C; Coffer, P; Downward, J; Evan, G: Suppression of c-myc-induced apoptosis by ras signalling through pi(3)k and pkb. In: *Nature*, volume 385(6616):pp. 544–548, 1997. ISSN 0028-0836 (Print). doi:10.1038/385544a0.

[Lan95] Land, H: Transformation of primary rat embryo cells. In: *Methods Enzymol*, volume 254:pp. 37–41, 1995. ISSN 0076-6879 (Print).

[LBP04] Lin, Hui-Kuan; Bergmann, Stephan; Pandolfi, Pier Paolo: Cytoplasmic pml function in tgf-beta signalling. In: *Nature*, volume 431(7005):pp. 205–211, 2004. ISSN 1476-4687 (Electronic). doi:10.1038/nature02783.

[LDL+90] Laiho, M; DeCaprio, J A; Ludlow, J W; Livingston, D M; Massague, J: Growth inhibition by tgf-beta linked to suppression of retinoblastoma protein phosphorylation. In: *Cell*, volume 62(1):pp. 175–185, 1990. ISSN 0092-8674 (Print).

[LEJ+99] Lloyd, R V; Erickson, L A; Jin, L; Kulig, E; Qian, X; Cheville, J C; Scheithauer, B W: p27kip1: a multifunctional cyclin-dependent kinase inhibitor with prognostic significance in human cancers. In: *Am J Pathol*, volume 154(2):pp. 313–323, 1999. ISSN 0002-9440 (Print).

[LFI+99] Lee, A C; Fenster, B E; Ito, H; Takeda, K; Bae, N S; Hirai, T; Yu, Z X; Ferrans, V J; Howard, B H; Finkel, T: Ras proteins

induce senescence by altering the intracellular levels of reactive oxygen species. In: *J Biol Chem*, volume 274(12):pp. 7936–7940, 1999. ISSN 0021-9258 (Print).

[LHCA86] Langdon, W Y; Harris, A W; Cory, S; Adams, J M: The c-myc oncogene perturbs b lymphocyte development in e-mu-myc transgenic mice. In: *Cell*, volume 47(1):pp. 11–18, 1986. ISSN 0092-8674 (Print).

[LJ02] Lachner, Monika; Jenuwein, Thomas: The many faces of histone lysine methylation. In: *Curr Opin Cell Biol*, volume 14(3):pp. 286–298, 2002. ISSN 0955-0674 (Print).

[LMR+97] Luger, K; Mader, A W; Richmond, R K; Sargent, D F; Richmond, T J: Crystal structure of the nucleosome core particle at 2.8 a resolution. In: *Nature*, volume 389(6648):pp. 251–260, 1997. ISSN 0028-0836 (Print). doi:10.1038/38444.

[LOJ03] Lachner, Monika; O'Sullivan, Roderick J; Jenuwein, Thomas: An epigenetic road map for histone lysine methylation. In: *J Cell Sci*, volume 116(Pt 11):pp. 2117–2124, 2003. ISSN 0021-9533 (Print). doi:10.1242/jcs.00493.

[LOR+01] Lachner, M; O'Carroll, D; Rea, S; Mechtler, K; Jenuwein, T: Methylation of histone h3 lysine 9 creates a binding site for hp1 proteins. In: *Nature*, volume 410(6824):pp. 116–120, 2001. ISSN 0028-0836 (Print). doi:10.1038/35065132.

[LPA+04] Lee, Jae-Hyuk; Park, Seun-Ja; Abraham, Susan C; Seo, Jae-Sung; Nam, Jong-Hee; Choi, Chan; Juhng, Sang-Woo; Rashid, Asif; Hamilton, Stanley R; Wu, Tsung-Teh: Frequent cpg island methylation in precursor lesions and early gastric adenocarcinomas. In: *Oncogene*, volume 23(26):pp. 4646–4654, 2004. ISSN 0950-9232 (Print). doi:10.1038/sj.onc.1207588.

[LZV+07] Lan, Fei; Zaratiegui, Mikel; Villen, Judit; Vaughn, Matthew W; Verdel, Andre; Huarte, Maite; Shi, Yujiang; Gygi, Steven P; Moazed, Danesh; Martienssen, Robert A; Shi, Yang: S. pombe lsd1 homologs regulate heterochromatin propagation and euchromatic gene transcription. In: *Mol Cell*, volume 26(1):pp. 89–101, 2007. ISSN 1097-2765 (Print). doi:10.1016/j.molcel.2007.02.023.

[MBP92] Marcu, K B; Bossone, S A; Patel, A J: myc function and regulation. In: *Annu Rev Biochem*, volume 61:pp. 809–860, 1992. ISSN 0066-4154 (Print). doi:10.1146/annurev.bi.61.070192.004113.

[MBSE06] Martins, Carla P; Brown-Swigart, Lamorna; Evan, Gerard I: Modeling the therapeutic efficacy of p53 restoration in tumors. In: *Cell*, volume 127(7):pp. 1323–1334, 2006. ISSN 0092-8674 (Print). doi:10.1016/j.cell.2006.12.007.

[MG95] Martin, S J; Green, D R: Protease activation during apoptosis: death by a thousand cuts? In: *Cell*, volume 82(3):pp. 349–352, 1995. ISSN 0092-8674 (Print).

[MGLF07] Mallette, Frederick A; Gaumont-Leclerc, Marie-France; Ferbeyre, Gerardo: The dna damage signaling pathway is a critical mediator of oncogene-induced senescence. In: *Genes Dev*, volume 21(1):pp. 43–48, 2007. ISSN 0890-9369 (Print). doi:10.1101/gad.1487307.

[MJL04] Mason, Douglas X; Jackson, Tonya J; Lin, Athena W: Molecular signature of oncogenic ras-induced senescence. In: *Oncogene*, volume 23(57):pp. 9238–9246, 2004. ISSN 0950-9232 (Print). doi:10.1038/sj.onc.1208172.

[MK06] Maity, Amit; Koumenis, Constantinos: Hif and mif–a nifty way to delay senescence? In: *Genes Dev*, volume 20(24):pp. 3337–3341, 2006. ISSN 0890-9369 (Print). doi:10.1101/gad.1506906.

[MMT+01] Mori, N; Morishita, M; Tsukazaki, T; Giam, C Z; Kumatori, A; Tanaka, Y; Yamamoto, N: Human t-cell leukemia virus type i oncoprotein tax represses smad-dependent transforming growth factor beta signaling through interaction with creb-binding protein/p300. In: *Blood*, volume 97(7):pp. 2137–2144, 2001. ISSN 0006-4971 (Print).

[MRR+08] Ma, Chaoyu; Rong, Yu; Radiloff, Daniel R; Datto, Michael B; Centeno, Barbara; Bao, Shideng; Cheng, Anthony Wai Ming; Lin, Fumin; Jiang, Shibo; Yeatman, Timothy J; Wang, Xiao-Fan: Extracellular matrix protein betaig-h3/tgfbi promotes metastasis of colon cancer by enhancing cell extravasation. In: *Genes Dev*, volume 22(3):pp. 308–321, 2008. ISSN 0890-9369 (Print). doi:10.1101/gad.1632008.

[MWY+05] Metzger, Eric; Wissmann, Melanie; Yin, Na; Muller, Judith M; Schneider, Robert; Peters, Antoine H F M; Gunther, Thomas; Buettner, Reinhard; Schule, Roland: Lsd1 demethylates repressive histone marks to promote androgen-receptor-dependent transcription. In: *Nature*, volume 437(7057):pp. 436–439, 2005. ISSN 1476-4687 (Electronic). doi:10.1038/nature04020.

[NCLW+88] Ngan, B Y; Chen-Levy, Z; Weiss, L M; Warnke, R A; Cleary, M L: Expression in non-hodgkin's lymphoma of the bcl-2 protein associated with the t(14;18) chromosomal translocation. In: *N Engl J Med*, volume 318(25):pp. 1638–1644, 1988. ISSN 0028-4793 (Print).

[NNH+03] Narita, Masashi; Nunez, Sabrina; Heard, Edith; Narita, Masako; Lin, Athena W; Hearn, Stephen A; Spector, David L; Hannon, Gregory J; Lowe, Scott W: Rb-mediated heterochromatin formation and silencing of e2f target genes during cellular senescence. In: *Cell*, volume 113(6):pp. 703–716, 2003. ISSN 0092-8674 (Print).

[NNV+94] Noda, A; Ning, Y; Venable, S F; Pereira-Smith, O M; Smith, J R: Cloning of senescent cell-derived inhibitors of dna synthesis using an expression screen. In: *Exp Cell Res*, volume 211(1):pp. 90–98, 1994. ISSN 0014-4827 (Print). doi:10.1006/excr.1994.1063.

[NSB+01] Nielsen, S J; Schneider, R; Bauer, U M; Bannister, A J; Morrison, A; O'Carroll, D; Firestein, R; Cleary, M; Jenuwein, T; Herrera, R E; Kouzarides, T: Rb targets histone h3 methylation and hp1 to promoters. In: *Nature*, volume 412(6846):pp. 561–565, 2001. ISSN 0028-0836 (Print). doi:10.1038/35087620.

[NTP99] Nesbit, C E; Tersak, J M; Prochownik, E V: Myc oncogenes and human neoplastic disease. In: *Oncogene*, volume 18(19):pp. 3004–3016, 1999. ISSN 0950-9232 (Print). doi:10.1038/sj.onc.1202746.

[Ore99] Oren, M: Regulation of the p53 tumor suppressor protein. In: *J Biol Chem*, volume 274(51):pp. 36031–36034, 1999. ISSN 0021-9258 (Print).

[OSP+00] O'Carroll, D; Scherthan, H; Peters, A H; Opravil, S; Haynes, A R; Laible, G; Rea, S; Schmid, M; Lebersorger, A; Jerratsch, M; Sattler, L; Mattei, M G; Denny, P; Brown, S D; Schweizer, D; Jenuwein, T: Isolation and characterization of suv39h2, a second histone h3 methyltransferase gene that displays testis-specific expression. In: *Mol Cell Biol*, volume 20(24):pp. 9423–9433, 2000. ISSN 0270-7306 (Print).

[PC94] Pang, J H; Chen, K Y: Global change of gene expression at late g1/s boundary may occur in human imr-90 diploid fibroblasts during senescence. In: *J Cell Physiol*, volume 160(3):pp. 531–538, 1994. ISSN 0021-9541 (Print). doi: 10.1002/jcp.1041600316.

[PCS+00] Pearson, M; Carbone, R; Sebastiani, C; Cioce, M; Fagioli, M; Saito, S; Higashimoto, Y; Appella, E; Minucci, S; Pandolfi, P P; Pelicci, P G: Pml regulates p53 acetylation and premature senescence induced by oncogenic ras. In: *Nature*, volume 406(6792):pp. 207–210, 2000. ISSN 0028-0836 (Print). doi: 10.1038/35018127.

[PK71] Paik, W K; Kim, S: Protein methylation. In: *Science*, volume 174(5):pp. 114–119, 1971. ISSN 0036-8075 (Print).

[PKE02] Pelengaris, Stella; Khan, Michael; Evan, Gerard I: Suppression of myc-induced apoptosis in beta cells exposes multiple oncogenic properties of myc and triggers carcinogenic progression. In: *Cell*, volume 109(3):pp. 321–334, 2002. ISSN 0092-8674 (Print).

[POS+01] Peters, A H; O'Carroll, D; Scherthan, H; Mechtler, K; Sauer, S; Schofer, C; Weipoltshammer, K; Pagani, M; Lachner, M; Kohlmaier, A; Opravil, S; Doyle, M; Sibilia, M; Jenuwein, T: Loss of the suv39h histone methyltransferases impairs mammalian heterochromatin and genome stability. In: *Cell*, volume 107(3):pp. 323–337, 2001. ISSN 0092-8674 (Print).

[RE02] Richards, Eric J; Elgin, Sarah C R: Epigenetic codes for heterochromatin formation and silencing: rounding up the usual suspects. In: *Cell*, volume 108(4):pp. 489–500, 2002. ISSN 0092-8674 (Print).

[REO+00] Rea, S; Eisenhaber, F; O'Carroll, D; Strahl, B D; Sun, Z W; Schmid, M; Opravil, S; Mechtler, K; Ponting, C P; Allis, C D; Jenuwein, T: Regulation of chromatin structure by site-specific histone h3 methyltransferases. In: *Nature*, volume 406(6796):pp. 593–599, 2000. ISSN 0028-0836 (Print). doi: 10.1038/35020506.

[RLR+07] Reimann, Maurice; Loddenkemper, Christoph; Rudolph, Cornelia; Schildhauer, Ines; Teichmann, Bianca; Stein, Harald; Schlegelberger, Brigitte; Dorken, Bernd; Schmitt, Clemens A: The myc-evoked dna damage response accounts for treatment resistance in primary lymphomas in vivo. In: *Blood*, volume 110(8):pp. 2996–3004, 2007. ISSN 0006-4971 (Print). doi: 10.1182/blood-2007-02-075614.

[RS92] Reuter, G; Spierer, P: Position effect variegation and chromatin proteins. In: *Bioessays*, volume 14(9):pp. 605–612, 1992. ISSN 0265-9247 (Print). doi:10.1002/bies.950140907.

[SA00] Strahl, B D; Allis, C D: The language of covalent histone modifications. In: *Nature*, volume 403(6765):pp. 41–45, 2000. ISSN 0028-0836 (Print). doi:10.1038/47412.

[SC90] Seshadri, T; Campisi, J: Repression of c-fos transcription and an altered genetic program in senescent human fibroblasts. In: *Science*, volume 247(4939):pp. 205–209, 1990. ISSN 0036-8075 (Print).

[Sch03] Schmitt, Clemens A: Senescence, apoptosis and therapy–cutting the lifelines of cancer. In: *Nat Rev Cancer*, volume 3(4):pp. 286–295, 2003. ISSN 1474-175X (Print). doi: 10.1038/nrc1044.

[SCW+99] Shelton, D N; Chang, E; Whittier, P S; Choi, D; Funk, W D: Microarray analysis of replicative senescence. In: *Curr Biol*, volume 9(17):pp. 939–945, 1999. ISSN 0960-9822 (Print).

[SDR+91] Stein, G H; Drullinger, L F; Robetorye, R S; Pereira-Smith, O M; Smith, J R: Senescent cells fail to express cdc2, cyca, and cycb in response to mitogen stimulation. In: *Proc Natl Acad Sci U S A*, volume 88(24):pp. 11012–11016, 1991. ISSN 0027-8424 (Print).

[Sed98] Sedivy, J M: Can ends justify the means?: telomeres and the mechanisms of replicative senescence and immortalization in mammalian cells. In: *Proc Natl Acad Sci U S A*, volume 95(16):pp. 9078–9081, 1998. ISSN 0027-8424 (Print).

[Sem00] Semenza, G L: Hif-1: using two hands to flip the angiogenic switch. In: *Cancer Metastasis Rev*, volume 19(1-2):pp. 59–65, 2000. ISSN 0167-7659 (Print).

[Ser97] Serrano, M: The tumor suppressor protein p16ink4a. In: *Exp Cell Res*, volume 237(1):pp. 7–13, 1997. ISSN 0014-4827 (Print). doi:10.1006/excr.1997.3824.

[She96] Sherr, C J: Cancer cell cycles. In: *Science*, volume 274(5293):pp. 1672–1677, 1996. ISSN 0036-8075 (Print).

[SL99] Schmitt, C A; Lowe, S W: Apoptosis and therapy. In: *J Pathol*, volume 187(1):pp. 127–137, 1999. ISSN 0022-3417 (Print). doi:10.1002/(SICI)1096-9896(199901)187:1<127::AID-PATH251>3.0.CO;2-T.

[SL02] Schmitt, Clemens A; Lowe, Scott W: Apoptosis and chemoresistance in transgenic cancer models. In: *J Mol Med*, volume 80(3):pp. 137–146, 2002. ISSN 0946-2716 (Print). doi:10.1007/s00109-001-0293-3.

[SLM+97] Serrano, M; Lin, A W; McCurrach, M E; Beach, D; Lowe, S W: Oncogenic ras provokes premature cell senescence associated with accumulation of p53 and p16ink4a. In: *Cell*, volume 88(5):pp. 593–602, 1997. ISSN 0092-8674 (Print).

[SLM02] Seoane, Joan; Le, Hong-Van; Massague, Joan: Myc suppression of the p21(cip1) cdk inhibitor influences the outcome of the p53 response to dna damage. In: *Nature*, volume 419(6908):pp. 729–734, 2002. ISSN 0028-0836 (Print). doi:10.1038/nature01119.

[SLM+04] Shi, Yujiang; Lan, Fei; Matson, Caitlin; Mulligan, Peter; Whetstine, Johnathan R; Cole, Philip A; Casero, Robert A; Shi, Yang: Histone demethylation mediated by the nuclear amine oxidase homolog lsd1. In: *Cell*, volume 119(7):pp. 941–953, 2004. ISSN 0092-8674 (Print). doi:10.1016/j.cell.2004.12.012.

[SMdS+99] Schmitt, C A; McCurrach, M E; de Stanchina, E; Wallace-Brodeur, R R; Lowe, S W: Ink4a/arf mutations accelerate lymphomagenesis and promote chemoresistance by disabling p53. In: *Genes Dev*, volume 13(20):pp. 2670–2677, 1999. ISSN 0890-9369 (Print).

[SMN+02] Shinosaki, Toshihiro; Miyai, Ikuko; Nomura, Yasuharu; Kobayashi, Tatsuo; Sunagawa, Norio; Kurihara, Hidetake: Mechanisms underlying the ameliorative property of lisinopril in progressive mesangioproliferative nephritis. In: *Nephron*, volume 91(4):pp. 719–729, 2002. ISSN 0028-2766 (Print).

[SOK+92] Shull, M M; Ormsby, I; Kier, A B; Pawlowski, S; Diebold, R J; Yin, M; Allen, R; Sidman, C; Proetzel, G; Calvin, D: Targeted disruption of the mouse transforming growth factor-beta 1 gene results in multifocal inflammatory disease. In: *Nature*, volume 359(6397):pp. 693–699, 1992. ISSN 0028-0836 (Print). doi:10.1038/359693a0.

[SPE+95] Shapiro, G I; Park, J E; Edwards, C D; Mao, L; Merlo, A; Sidransky, D; Ewen, M E; Rollins, B J: Multiple mechanisms of p16ink4a inactivation in non-small cell lung cancer cell lines. In: *Cancer Res*, volume 55(24):pp. 6200–6209, 1995. ISSN 0008-5472 (Print).

[SPK+01] Staller, P; Peukert, K; Kiermaier, A; Seoane, J; Lukas, J; Karsunky, H; Moroy, T; Bartek, J; Massague, J; Hanel, F; Eilers, M: Repression of p15ink4b expression by myc through association with miz-1. In: *Nat Cell Biol*, volume 3(4):pp. 392–399, 2001. ISSN 1465-7392 (Print). doi:10.1038/35070076.

[SSR+06] Shchors, Ksenya; Shchors, Elena; Rostker, Fanya; Lawlor, Elizabeth R; Brown-Swigart, Lamorna; Evan, Gerard I: The myc-dependent angiogenic switch in tumors is mediated by interleukin 1beta. In: *Genes Dev*, volume 20(18):pp. 2527–2538, 2006. ISSN 0890-9369 (Print). doi:10.1101/gad.1455706.

[SWBR+00] Schmitt, C A; Wallace-Brodeur, R R; Rosenthal, C T; McCurrach, M E; Lowe, S W: Dna damage responses and chemosensitivity in the e mu-myc mouse lymphoma model. In: *Cold Spring Harb Symp Quant Biol*, volume 65:pp. 499–510, 2000. ISSN 0091-7451 (Print).

[TL98] Thornberry, N A; Lazebnik, Y: Caspases: enemies within. In: *Science*, volume 281(5381):pp. 1312–1316, 1998. ISSN 0036-8075 (Print).

[tPOJ+02] te Poele, Robert H; Okorokov, Andrei L; Jardine, Lesley; Cummings, Jeffrey; Joel, Simon P: Dna damage is able to induce senescence in tumor cells in vitro and in vivo. In: *Cancer Res*, volume 62(6):pp. 1876–1883, 2002. ISSN 0008-5472 (Print).

[TSPG06] Trougakos, Ioannis P; Saridaki, Aggeliki; Panayotou, George; Gonos, Efstathios S: Identification of differentially expressed proteins in senescent human embryonic fibroblasts. In: *Mech Ageing Dev*, volume 127(1):pp. 88–92, 2006. ISSN 0047-6374 (Print). doi:10.1016/j.mad.2005.08.009.

[Tur00] Turner, B M: Histone acetylation and an epigenetic code. In: *Bioessays*, volume 22(9):pp. 836–845, 2000. ISSN 0265-9247 (Print). doi:10.1002/1521-1878(200009)22:9<836::AID-BIES9>3.0.CO;2-X.

[VH06] Vita, Marina; Henriksson, Marie: The myc oncoprotein as a therapeutic target for human cancer. In: *Semin Cancer Biol*, volume 16(4):pp. 318–330, 2006. ISSN 1044-579X (Print). doi:10.1016/j.semcancer.2006.07.015.

[VLL00] Vogelstein, B; Lane, D; Levine, A J: Surfing the p53 network. In: *Nature*, volume 408(6810):pp. 307–310, 2000. ISSN 0028-0836 (Print). doi:10.1038/35042675.

[VWK+02] Vafa, Omid; Wade, Mark; Kern, Suzanne; Beeche, Michelle; Pandita, Tej K; Hampton, Garret M; Wahl, Geoffrey M: c-myc can induce dna damage, increase reactive oxygen species, and mitigate p53 function: a mechanism for oncogene-induced genetic instability. In: *Mol Cell*, volume 9(5):pp. 1031–1044, 2002. ISSN 1097-2765 (Print).

[Wat93] Waterborg, J H: Dynamic methylation of alfalfa histone h3. In: *J Biol Chem*, volume 268(7):pp. 4918–4921, 1993. ISSN 0021-9258 (Print).

[WBL99] Wallace-Brodeur, R R; Lowe, S W: Clinical implications of p53 mutations. In: *Cell Mol Life Sci*, volume 55(1):pp. 64–75, 1999. ISSN 1420-682X (Print).

[WCMA+03] Wu, Siqin; Cetinkaya, Cihan; Munoz-Alonso, Maria J; von der Lehr, Natalie; Bahram, Fuad; Beuger, Vincent; Eilers, Martin; Leon, Javier; Larsson, Lars-Gunnar: Myc represses differentiation-induced p21cip1 expression via miz-1-dependent interaction with the p21 core promoter. In: *Oncogene*, volume 22(3):pp. 351–360, 2003. ISSN 0950-9232 (Print). doi:10.1038/sj.onc.1206145.

[WP96] Wolffe, A P; Pruss, D: Deviant nucleosomes: the functional specialization of chromatin. In: *Trends Genet*, volume 12(2):pp. 58–62, 1996. ISSN 0168-9525 (Print).

[WSTR89] Wustmann, G; Szidonya, J; Taubert, H; Reuter, G: The genetics of position-effect variegation modifying loci in drosophila melanogaster. In: *Mol Gen Genet*, volume 217(2-3):pp. 520–527, 1989. ISSN 0026-8925 (Print).

[WSZ+08] Wajapeyee, Narendra; Serra, Ryan W; Zhu, Xiaochun; Mahalingam, Meera; Green, Michael R: Oncogenic braf induces senescence and apoptosis through pathways mediated by the secreted protein igfbp7. In: *Cell*, volume 132(3):pp. 363–374, 2008. ISSN 1097-4172 (Electronic). doi:10.1016/j.cell.2007.12.032.

[WvRY+07] Wu, Chi-Hwa; van Riggelen, Jan; Yetil, Alper; Fan, Alice C; Bachireddy, Pavan; Felsher, Dean W: Cellular senescence is an important mechanism of tumor regression upon c-myc inactivation. In: *Proc Natl Acad Sci U S A*, volume 104(32):pp. 13028–13033, 2007. ISSN 0027-8424 (Print). doi:10.1073/pnas.0701953104.

[XZM+07] Xue, Wen; Zender, Lars; Miething, Cornelius; Dickins, Ross A; Hernando, Eva; Krizhanovsky, Valery; Cordon-Cardo, Carlos; Lowe, Scott W: Senescence and tumour clearance is triggered by p53 restoration in murine liver carcinomas. In: *Nature*, volume 445(7128):pp. 656–660, 2007. ISSN 1476-4687 (Electronic). doi:10.1038/nature05529.

[YDT+02] Yang, Yu-An; Dukhanina, Oksana; Tang, Binwu; Mamura, Mizuko; Letterio, John J; MacGregor, Jennifer; Patel, Sejal C; Khozin, Shahram; Liu, Zi-Yao; Green, Jeffrey; Anver, Miriam R; Merlino, Glenn; Wakefield, Lalage M: Lifetime exposure to a soluble tgf-beta antagonist protects mice against

metastasis without adverse side effects. In: *J Clin Invest*, volume 109(12):pp. 1607–1615, 2002. ISSN 0021-9738 (Print). doi:10.1172/JCI15333.

[YKK+04] Yoon, In Kyung; Kim, Hyun Kyoung; Kim, Yu Kyoung; Song, In-Hwan; Kim, Wankee; Kim, Seongyong; Baek, Suk-Hwan; Kim, Jung Hye; Kim, Jae-Ryong: Exploration of replicative senescence-associated genes in human dermal fibroblasts by cdna microarray technology. In: *Exp Gerontol*, volume 39(9):pp. 1369–1378, 2004. ISSN 0531-5565 (Print). doi:10.1016/j.exger.2004.07.002.

[YSW+01] Yang, W; Shen, J; Wu, M; Arsura, M; FitzGerald, M; Suldan, Z; Kim, D W; Hofmann, C S; Pianetti, S; Romieu-Mourez, R; Freedman, L P; Sonenshein, G E: Repression of transcription of the p27(kip1) cyclin-dependent kinase inhibitor gene by c-myc. In: *Oncogene*, volume 20(14):pp. 1688–1702, 2001. ISSN 0950-9232 (Print). doi:10.1038/sj.onc.1204245.

[ZER+98] Zindy, F; Eischen, C M; Randle, D H; Kamijo, T; Cleveland, J L; Sherr, C J; Roussel, M F: Myc signaling via the arf tumor suppressor regulates p53-dependent apoptosis and immortalization. In: *Genes Dev*, volume 12(15):pp. 2424–2433, 1998. ISSN 0890-9369 (Print).

[ZLSP05] Zhang, Xiaoling; Li, June; Sejas, Daniel P; Pang, Qishen: The atm/p53/p21 pathway influences cell fate decision between apoptosis and senescence in reoxygenated hematopoietic progenitor cells. In: *J Biol Chem*, volume 280(20):pp. 19635–19640, 2005. ISSN 0021-9258 (Print). doi:10.1074/jbc.M502262200.

List of Figures

List of Tables

Selbständigkeitserklärung

Hiermit erkläre ich ehrenwoertlich, dass ich die Diessertation "Role of Histone H3 Lysine 9 Methylation in Apoptosis and Senescence-related Cellular Failsafe Programs in a MYC-driven Lymphoma Model" selbständig angefertigt und keine anderen als die von mir angegebenen quellen und Hilfsmittelbenutzt habe.

Ich erkläre ausserdem, dass diese Dissertation weder in gleicher Weise oderer anderer Form bereits in einem anderen Pruefungsverfahren vorgelegen hat.

Ich habe ausser den mit dem Zulassungsgesuch urkundlich vorgelegten Graden keine weiteren akademischen Grade erworben od zu erwerben versucht.

Berlin, den 17.07.2008